Tillering in spring wheat:
a 3D virtual plant modelling study

Tillering in spring wheat:
a 3D virtual plant modelling study

Jochem B. Evers

Abstract

This thesis presents a 3D virtual plant modelling study to tillering (lateral branching) in spring wheat (*Triticum aestivum* L.). Tillering in wheat is influenced by light properties. Light intensity determines the amount of assimilates available for growth. Availability of assimilates is assumed to regulate the degree of tillering: a reduction in light intensity, or more specifically in the intensity of Photosynthetically Active Radiation (PAR), results in a lower number of tillers produced. Tillering is also affected by the spectral composition of the light (R:FR, the ratio between the intensities of red and far-red light). R:FR declines with depth in the canopy and with development of the canopy, due to the differential reflection and transmission of red and far-red light by the surrounding vegetation. A low R:FR triggers a shade avoidance response of the plants, which includes a reduction in tiller production. R:FR is highly related to the fraction of light intercepted. The relation between canopy architecture, light properties within the canopy, and tillering in spring wheat plants was studied using a 3D virtual plant modelling approach. The virtue of virtual plant models for this analysis is that each element in the architecture of the canopy is given an explicit 3D representation, which enables simulation of processes at the level of individual organs.

The model used, called 'ADELwheat', was calibrated for spring wheat. The model was validated for ground cover and leaf area index, using an independent dataset. Experiments described in this thesis showed that new tillers ceased to appear when the fraction of light intercepted by the canopy exceeds 0.4. That threshold was independent of plant population density, shading, developmental stage of the plants and rank number of the tiller. When tillering ceased, also the red/far-red ratio was fairly similar across population densities and light treatments. Cessation of tillering in ADELwheat was made dependent on thresholds of light properties. A light model ('nested radiosity') was coupled to ADELwheat and was used to calculate both PAR interception and R:FR at the level of the individual organ. The simulation results showed that the virtual plant modelling approach is useful to simulate global effects of local stimuli. The simulated tillering patterns supported the hypothesis that tillering ceases at specific light conditions inside the canopy. The study demonstrated that the virtual plant modelling approach can provide insight into the factors that determine the developmental plasticity of wheat in terms of tillering.

Keywords: wheat, tillering, phytomer, virtual plant, L-system, functional-structural modelling, plant population density, PAR, shading, red/far-red ratio, light scattering

Contents

Chapter 1

General introduction

Setting the scene

Plants respond to their environment. Growth, the rate of increase in mass and volume, is affected by solar radiation, temperature, nutrients, and water. Development, the (irreversible) progression through the life cycle, is primarily controlled by temperature and photoperiod. Growth and development are connected in the sense that substrates for growth need to be available to realise the production of those organs that conditions for plant development allow to be initiated.

During the vegetative phase wheat (*Triticum aestivum* L.) meristems give rise to phytomers. Phytomers are the basic units the plant is composed of, consisting of a node, an internode, a leaf, and an axillary bud. During the vegetative phase of development of gramineous species, buds on phytomers are triggered to grow out and produce 'lateral branches', i.e. tillers. Buds on phytomers of tillers can also be triggered to produce tillers. Therefore, vegetative development, i.e. the production of leaves and tillers, is basically an exponential process. Every exponential process will be slowed down or stopped sooner or later. Wheat plants, and gramineous species in general, show variable degree of tillering (e.g. Bos and Neuteboom, 1998a). At 'some stage' no more new tillers emerge. There are two types of cessation of tillering. (a) The plants switch to the generative phase: buds of the newly formed phytomers start to develop into floral branches while the outgrowth of the 'parent leaf' is suppressed; this is visible from 'double ridges' (floral structures and leaf initials) at the apex (Kirby and Appleyard, 1981). The transition to produce generative structures takes place at approximately the same time in all apical meristems, i.e. the plant shows a determinate pattern of development. (b) Exclusively vegetative tiller buds are initiated, the plant has not become generative, but yet buds stop producing tillers. The current study concerns the second type of cessation of tillering during the vegetative phase.

Arrest of tillering during the vegetative phase has been viewed as being caused by environmental cues, particularly the red/far-red ratio of light that falls on the base of the plant. The alternative view is that tiller production ceases because the amount of substrates becomes limiting to satisfy the needs for outgrowth of more buds. It was the initial hypothesis of this work that a particular type of modelling can help to examine these hypotheses in a quantitative way in the context of a plant canopy. The case will be expanded in the next sections of this chapter, beginning with the modelling approach.

Virtual plant modelling

Experimental studies yield insight into mechanisms of response to the environment or in rates of processes as determined by external or physiological factors. Experimental conditions often differ substantially from field or natural conditions. De Wit *et al*. (1978) stated: 'In our opinion, simulation models, if they are to be useful at all, should form a bridge between reductionists, who analyse processes separated from their physical, chemical or biological background, and generalists who are interested in the performance of whole systems in which individual processes operate in their natural context'. In the context of this thesis a simulation model is a computer program that describes important components of the system of study, specifies their interrelations, and quantifies the rate of change of these components in relation to external factors. Usually, crop growth and development have been represented in process-based models that basically describe development in relation to temperature and derive the increment of dry matter from light interception. The distribution of dry matter over components (e.g. stems, leaves, roots) and the associated increase in leaf area index are usually functions of development. Such models have been instrumental to provide references for potential crop production in given climates and modelling has influenced the agenda of experimental research (van Ittersum *et al.*, 2003).

The study described in this thesis is based on a modelling approach called 'virtual plant modelling' (Room *et al.*, 1996), also referred to as 'functional-structural plant modelling' (Sievänen *et al.*, 2000; Godin and Sinoquet, 2005). It is a type of plant modelling that takes the spatial structure of the plant or canopy explicitly into account. The virtual plant approach is fundamentally different from the more traditional approach of 'process-based modelling'. For research questions which require the spatial structure of the plants to be taken into account, the traditional type of process-based modelling shows important limitations. The level of detail usually does not reach beyond 'layers' of leaves and other plant organs, and is therefore not directly suitable to model processes at the level of the individual organ.

This is where virtual plant modelling comes in. Virtual plant modelling is a modelling approach in which the three-dimensional (3D) structure of the plant is explicitly described. In other words, all the organs a plant is composed of (leaves, internodes, flowers, fruits, etc.) can be represented in 3D. Depending on the necessary level of detail, smaller (sub-)organs can also be represented (petals, stamens, buds, leaflets, etc.). In this way, the geometry (e.g. leaf shape and curvature, branching angles) and the topology (sequence of and connections between organs) of the plants are described in detail. Since the early 1990s,

virtual plant modelling increasingly aroused interest. On the one hand, this is due to the fact that more and more research groups become aware of the advantages of having an explicit 3D description of a plant. On the other hand, this type of modelling is very much dependent on computational power, and it has not been since the 1990s that regular desktop computers have become sufficiently powerful for this purpose. Be that as it may, the increasing interest for 3D modelling suggests that it is a valuable addition to the set of tools researchers have at their disposal to tackle agronomic, ecological, plant morphological and plant physiological problems.

Basic methodology

Various methods to model virtual plants have been developed (de Visser *et al.*, 2002). The most widely used method is the one based on the L-system principles (Lindenmayer, 1968; Prusinkiewicz and Lindenmayer, 1990). L-systems, named after Aristid Lindenmayer (1925 - 1989) who defined the L-system formalism, provide a basically modular approach to modelling. This enables plants and canopies to be described as a collection of modules. The power of L-systems lies in the possibility to describe relatively complex structures based on a limited set of simple 'productions' or rewriting rules. This can be achieved by recognising the repetitive nature of plant structure, as a plant consists of a basic unit (the phytomer) which is repeated a number of times. For example, the phytomer could consist of a node `N`, an internode `I`, a leaf `[L]`, and an apex `A` at the top. (Note: the square brackets `[...]` around a module indicate that the module is a structure that forks off the main shoot, such as a branch or a leaf). A rewriting rule could be:

```
A --> NI[L]A
```

When the starting point (axiom) of the simulation is `A`, after several time steps in which the rule is applied once, the string looks like:

Step 1: `NI[L]A`

Step 2: `NI[L]NI[L]A`

Step 3: `NI[L]NI[L]NI[L]A`

Etc.

Hence, when applying the rewriting rule several times, the string grows, and the description of the virtual plant is expanded in each time step. After extending this simple model with branch apices, few steps of simulation would result in an extensive string composed of several branches with the same repeated basic unit. For example, consider these two rewriting rules (modules are the same as above, plus `B` = flower bud, `R` = flower):

```
A --> I[L][L][A][A]B
B --> R
```

The axiom is `A`; the schematic virtual plant after time steps one, two and three is shown in Fig. 1; the accompanying strings are:

step 1: `I[L][L][A][A]B`

step 2: `I[L][L][I[L][L][A][A]B][I[L][L][A][A]B]R`

step 3: `I[L][L][I[L][L][I[L][L][A][A]B][I[L][L][A][A]B]R]`

`[I[L][L][I[L][L][A][A]B][I[L][L][A][A]B]R]R`

Whether a rewriting rule is applied in a specific time step can be made dependent on, for example, temperature sum or the developmental state of the virtual plant, using a conditional statement in a rewriting rule, e.g.:

```
A : Tsum > 700 --> G
```

Here, the vegetative apex `A` transforms into a generative apex `G` when the temperature sum has exceeded 700 ºCd. Obviously, a separate rule is needed to increase `Tsum` each time step, based on temperature.

The modules can be extended with one or more parameters, yielding so-called parametric L-systems (Prusinkiewicz and Hanan, 1990). These parameters can be used as identifiers, but since they can be updated during the simulation, they can also represent variables, e.g. internode length, or leaf angle:

```
L(n,l,a) --> L(n,l+g,a+c)
```

In this example leaf module `L` has three parameters (`n` = leaf number, `l` = leaf length, `a` = basal angle), two of which are updated (`g` = length increment, `c` = angle change). The values of `g` and `c` can be fixed, or be made dependent on time step, temperature sum, developmental stage, etc.

step 1   step 2   step 3
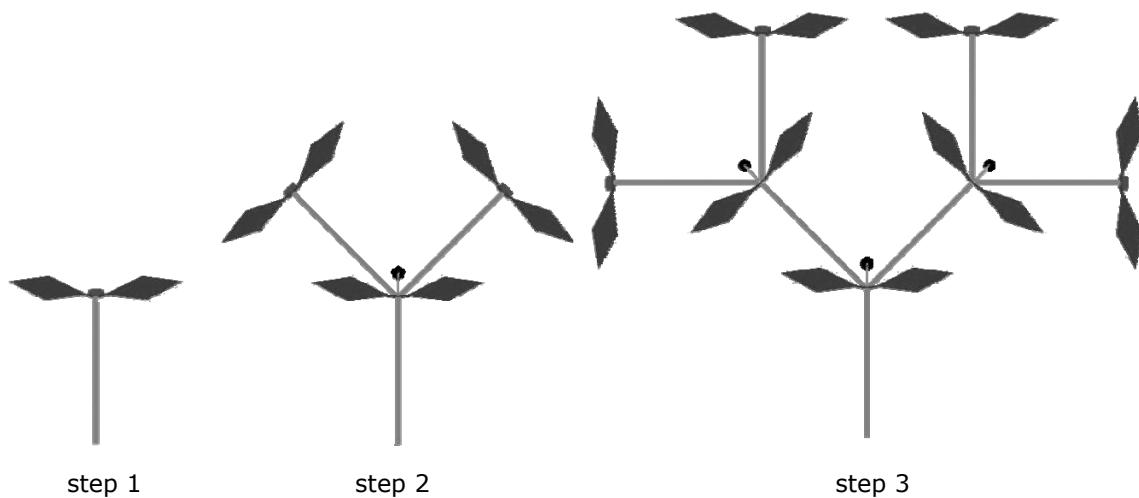
Fig. 1: Schematic visualisation of a virtual plant after three time steps, showing leaves, internodes, flower buds (at the top of each internode) and flowers (small circles on a stalk).

Opportunities and limitations of L-systems

Specific software enables the strings to be visualised. In so-called 'closed' L-systems, as exemplified above, the structure and its development in sequential steps is always the same. Impressively realistic simulations of the development of plants and flowers can be programmed using closed L-systems (for examples see Prusinkiewicz and Lindenmayer (1990), available from the Algorithmic Botany website, www.algorithmicbotany.org). However, such L-systems are of little value as a tool to improve understanding of the system and for testing of hypotheses on its behaviour. Such applications of L-systems became possible with the introduction of 'open L-systems' (Měch and Prusinkiewicz, 1996; Měch, 1997), in which each step in the development of the structure can be made dependent on external driving forces, acting on the structure as a whole, but also on each individual module. For instance, using the open L-systems approach, simulations can be made of plant roots that interact with the soil environment. Also, trees can be simulated of which the orientation of growing branches responds to the amount of light intercepted by each individual leaf; see Měch and Prusinkiewicz (1996) for details on these examples.

Still, the above-mentioned L-systems are mostly descriptive models. The simulated plant structures grow because the rewriting rules make them grow, i.e. there are no underlying mechanisms driving the growth of the virtual plant. Hence, the challenge is to combine the mechanistic basis of process-based models with the 3D architectural description of virtual plant models. Steps in this direction have been taken, by e.g. Fournier and Andrieu (1999) and Drouet and Pagès (2003) both for maize, Hanan and Hearn (2003) for cotton, de Visser *et al.* (2004) for chrysanthemum, and Allen *et al.* (2005) for peach trees. The work described in the current study presents an intermediate form of process integration, using an open L-system. Plant development and subsequent canopy geometry of the virtual plants are descriptive (non-mechanistic), but the branching pattern of the virtual plants is influenced by the light conditions within the canopy. True process integration is on the research agenda, but is outside the scope of this thesis.

A suitable problem to tackle using virtual plant modelling

The modelling study described in this thesis focuses on an extensively studied arable crop, wheat (*Triticum aestivum* L.), and on its tillering behaviour. The morphological development of wheat is a highly co-ordinated process. Very illustrative of this feature is the developmental scheme of Klepper *et al.* (1984), relating the initiation of primordia on the apex as well as the appearance of

different tillers to the number of leaves visible on the main stem. Studies such as those described by Kirby (1990) and Bos and Neuteboom (1998b) also emphasise that the timing of phenological events (initiation and appearance of organs) conform to a specific pattern. These patterns in wheat development make wheat suitable for virtual plant modelling, since they can be caught in straightforward L-system rewriting rules with conditional statements.

The time of appearance of a tiller at a particular position on the plant can be predicted from the stage of development of parent shoots. However, not all tiller buds are activated to grow out. The actual appearance of tillers (timing and frequency of occurrence) is plastic: tillering is influenced by various environmental factors (Tomlinson and O'Connor, 2004). Nitrogen availability is an important factor as it has been shown that nitrogen limitation decreases tiller appearance rate (Longnecker *et al.*, 1993), primarily via an effect on whole plant growth. In addition to nitrogen, temperature and light conditions strongly influence tillering (Bos and Neuteboom, 1998a). Light can affect tillering, and plant development in general, through two of its properties. Both of these properties are dependent on plant population density:

- The effects of Photosynthetically Active Radiation (PAR) intensity. PAR is the part of the light spectrum used by plant tissues for photosynthesis and comprises wavelengths of 400 to 700 nm. PAR intensity within a canopy decreases with depth in the canopy, and with progress of canopy development, and does so at a higher rate when population density is higher. Due to the severely decreased PAR intensity near soil level, tillering is reduced earlier in development of the plant at higher population densities (Simon and Lemaire, 1987). Bos (1999) hypothesised that outgrowth of tiller buds is primarily regulated by the reduction in PAR intensity at the level of the leaf directly associated with the tiller bud (i.e. the parent leaf).

- The effects of the red/far-red ratio (R:FR), i.e. the ratio between the intensities of the red part of the spectrum (ca. 660 nm) and the far-red part of the spectrum (ca. 730 nm). Increase in population density is associated with lower R:FR at the base of the plants as more surrounding vegetation is present to differentially scatter red and far-red light (Holmes and Smith, 1977). Lower R:FR has been related to reduced tillering in barley (*Hordeum vulgare* L.) (Skinner and Simmons, 1993; Davis and Simmons, 1994), dallisgrass (*Paspalum dilatatum* Poir.) (Casal *et al.*, 1986; 1987b), ryegrass species (*Lolium* spp.) (Deregibus *et al.*, 1983; Casal *et al.*, 1985; Casal *et al.*, 1987b; a; Gautier *et al.*, 1999) and wheat (*Triticum aestivum* L.) (Kasperbauer and Karlen, 1986; Casal, 1988), with tillering being expressed

as either number of tillers per plant, (relative) tillering rate, tiller appearance, or site filling (the fraction of possible tiller sites occupied by a tiller). The reduction in tillering mediated by R:FR is part of the shade avoidance response (Franklin and Whitelam, 2005) of gramineous species, which also manifests itself in increased leaf length (Casal *et al.*, 1985), a lower tiller angle (Casal *et al.*, 1990), a higher shoot/root ratio (Kasperbauer and Karlen, 1986) and a change in leaf orientation towards gaps (Maddonni *et al.*, 2002). In this respect, the phenomenon called 'early warning signal' (Casal *et al.*, 1986; Ballaré *et al.*, 1987) is relevant: the early altered assimilate partitioning pattern observed in a young plant that grows among other plants, is a consequence of a drop in R:FR of light that reaches that plant caused by plants in the vicinity, rather than a consequence of a drop in PAR (shading) and the resulting lowered amount of assimilates. In other words: changes in R:FR can act as an early warning signal for future competition, and act long before plants are subjected to shading and the associated decrease in rate of photosynthesis.

Objective of this PhD study, and the steps to be taken
The general objective of the work described in this thesis is to examine tillering behaviour of the wheat plant during the vegetative stages of development, using a virtual plant modelling approach. Several steps were defined to achieve this goal:

a) *Model design:* The first requirement was a virtual plant model of wheat, containing a set of rules that describe wheat development over thermal time. To begin with a head start, this architectural model was based on an existing closed L-system of wheat, called ADELwheat (Fournier *et al.*, 2003). This model was originally written in the freeware L-system program language 'Graphtal' (Streit, 1992). In anticipation of the necessity to link the model to environmental simulation programs (creating an open L-system), it had to be transcoded to the L-system simulation language and simulation program CPFG (Prusinkiewicz *et al.*, 2000; Měch, 2004).

b) *Model parameterisation for spring wheat:* The original ADELwheat model was calibrated for winter wheat (cv. Soisson). In order to represent the spring wheat cultivar Minaret used by Bos (1999) and the growing conditions in Wageningen, the model had to be reparameterised. Simultaneously, the L-system rules of the original ADELwheat could be evaluated, and examined to what extent the rules were generic for wheat, or specific for a cultivar or growing environment. This reparameterisation was based on an outdoor

experiment with spring wheat (cv. Minaret), in which plants were grown at a low population density to allow for abundant tillering. Data on leaf appearance and organ dimensions was gathered by continuous monitoring and by occasional destructive harvests. Geometrical properties of the model were determined by magentic digitisation (e.g. Drouet, 2003), from which data on leaf angle, curvature, and phyllotaxis were derived.

c) *Model validation for different conditions:* To evaluate performance, the reparameterised model had to be validated using an independent dataset, containing data on wheat grown in similar and contrasting growing conditions. For this purpose a second outdoor experiment was done, in which plants were grown at three population densities (of which one was similar to the population density of the parameterisation experiment) and two light regimes (one full light, one shaded). Model performance was evaluated using time course of ground cover fraction and of leaf area index as test output variables. These output variables include effects of all important model characteristics that determine the rate of production of leaf area. In addition to this, a
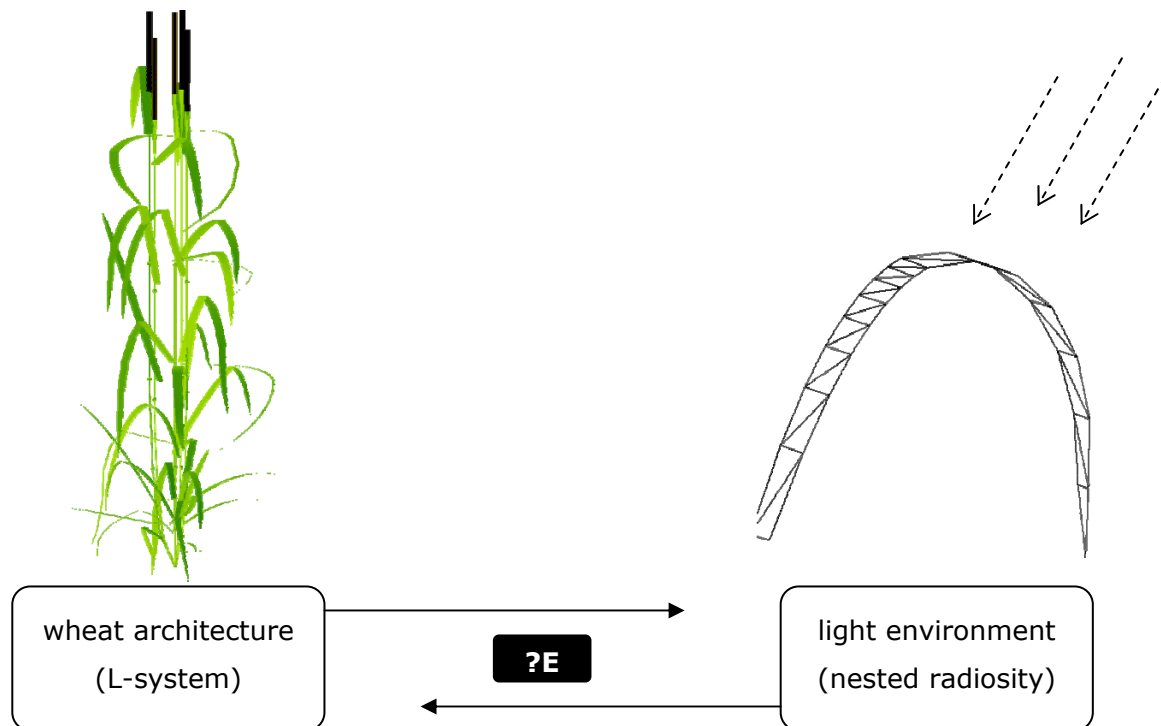
Fig. 2: Schematic representation of the bi-directional flow of information between the wheat L-system (left) and the nested radiosity model (right; the dashed arrows represent incoming light). Each time step, the L-system passes geometrical information on the canopy structure to the nested radiosity model by using the communications module (called ?E), which processes the information and returns data on the light distribution to the L-system, also through ?E.

sensitivity analysis was made, to explore to what extent the model output was sensitive to changes in several important parameters of the model.

d) *Analysis of tillering behaviour:* The same experiment as the one used for model evaluation was used to gain insight into the effects of the light environment inside a wheat canopy on the proportion of appeared tillers and on the timing of tiller appearance. Tillering throughout the experiment was monitored, along with the time course of PAR penetration and R:FR at soil level. From this experiment, hypotheses were derived on frequencies of occurrence of tillers on particular positions in relation to PAR and R:FR.

e) *Interfacing virtual plant model:* To make the virtual plant model of spring wheat simulate PAR interception and R:FR on each individual plant organ, a link had to be established between the virtual plant model and a light interception model ('nested radiosity', Chelle and Andrieu, 1998), creating an open L-system. This could be done by equipping the model with communication modules (called ?E) allowing for bidirectional transfer of data (from the L-system: geometry and module parameters; from the light interception model: PAR, R:FR; Fig. 2). Through the communications module, nested radiosity receives the geometrical status of a canopy of plants, which is described using polygons. The light conditions on these polygons (i.e. absorbed PAR, R:FR of the incoming light) are calculated, and sent back to the L-system, which processes the information (Fig. 2).

f) *Modelling tillering:* The tillering hypotheses had to be incorporated in the virtual plant model, by integrating conditional rules on tiller bud outgrowth in relation to PAR and R:FR. This completes the feedback mechanism in the model: the canopy structure determines the light conditions inside the
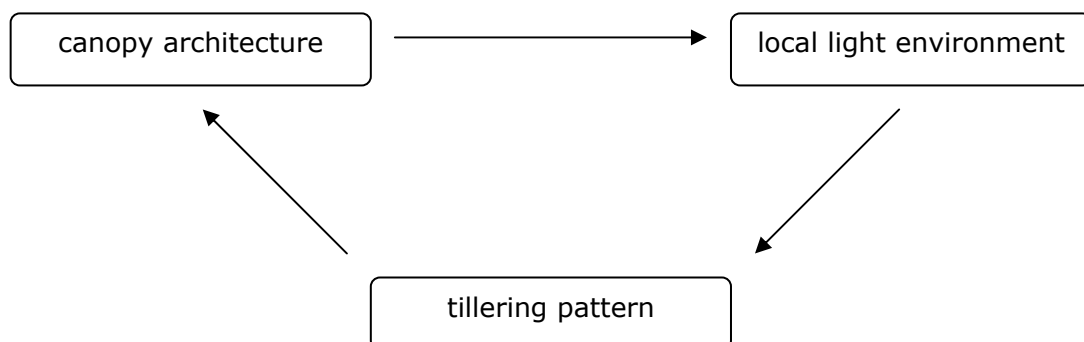
Fig. 3: The feedback mechanism incorporated into the model. The canopy architecture determines the local light environment within the canopy, which affects the tillering pattern of the wheat plants. This, in turn, determines the canopy architecture, completing the circle.

canopy, which influence tillering, which in turn influences the canopy structure (Fig. 3).

These steps are incorporated into the chapters of this thesis in the following way. Chapter 2 contains the model design (a) and parameterisation (b) parts, and chapter 3 presents the model validation (c). Chapter 4 explains the analysis of tillering (d). Finally, chapter 5 treats the interfacing (e) and hypothesis testing (f). A general discussion on the contents of the thesis is presented in chapter 6.

The local nature of the effects of PAR and R:FR, as explained above, makes analysis on the level of the individual organ meaningful. Therefore, a modelling approach that takes individual organs explicitly into account is potentially very useful. This thesis demonstrates the potential of virtual plant modelling to simulate aspects of the developmental plasticity of wheat.

Chapter 2

Towards a generic architectural model of tillering in Gramineae, as exemplified by spring wheat

Jochem Evers

Jan Vos

Christian Fournier

Bruno Andrieu

Michaël Chelle

Paul Struik

Abstract

This chapter presents an architectural model of wheat (*Triticum aestivum* L.), designed to be used for explaining effects of light conditions at the individual leaf level on tillering kinetics. Various model variables, including blade length and curvature, were parameterised for spring wheat, and compared to winter wheat and other Gramineae species.

Thearchitectural model enables simulation of plant properties at the level of individual organs. Parameterisation was based on data derived from an outdoor experiment with spring wheat cv. Minaret.

Final organ dimensions of tillers could be modelled using the concept of relative phytomer numbers (RPN). Various variables in spring wheat showed marked similarities with winter wheat and other species, suggesting possibilities for a general Gramineae architectural model.

Our descriptive model is suitable for our objective, i.e. investigating light effects on tiller behaviour. However, we plan to replace the descriptive modelling solutions by physiological, mechanistic solutions, starting with the localised production and partitioning of assimilates as affected by abiotic growth factors.

Introduction

Functional-structural plant models (FSPM, Sievänen *et al.*, 2000) or virtual plants (Room *et al.*, 1996) allow us to analyse the consequences of changes in the architecture of a plant for the functioning of individual organs, and conversely, the effects of processes at organ level on the development at the plant level. The plant architecture comprises the geometrical and topological organisation of the component plant parts in three dimensions (3D) (Godin, 2000), whereas the adjective 'functional' refers to physiological processes, primarily the production and partitioning of carbon in relation to plant environment, notably radiation.

The current experimental and modelling study focuses on the plastic response of tillering in spring wheat (*Triticum aestivum* L.). Bos (1999) hypothesised that the appearance of a tiller particularly depends on the local light regime experienced by the parent leaf during a certain phase of development of the tiller bud. Whether or not a tiller emerges clearly affects the architecture of the plant, which in turn, affects the light environment of many leaves. Here, the term architecture is extended to represent the shape and orientation in 3D of all organs of a group of individual plants, i.e. a (micro) canopy. The approach taken in this study includes the following steps: (a) the design and parameterisation of an architectural model of (spring) wheat, (b) the coupling of the architectural model to a model that calculates absorption of sunlight for each element of the 3D structure as it develops over time, and (c) the implementation and test of validity of hypotheses on the relation between local light absorption and growth of tillers. The current chapter only addresses the first step, the objectives being (a) to present the general approach to architectural modelling in wheat, (b) to present the experimental procedures to determine model parameter values specific for spring wheat, and (c) to discuss the generality of the parameterisation, primarily by comparison with parameters values obtained for winter wheat cultivar Soisson (Ljutovac, 2002; Fournier *et al.*, 2003).

General approach to architectural modelling of wheat

The current chapter builds on and expands the ADELwheat model, presented earlier (Fournier *et al.*, 2003), which pertained to winter wheat cv. Soisson. A modular approach is taken to model the plant, the phytomer (Fig. 1) being the basic unit. The wheat phytomer consists of an internode, with a tiller bud at the bottom, a node above the internode, a sheath which is inserted on the node, and

a leaf blade (Briske, 1991; Moore and Moser, 1995; Scanlon and Freeling, 1997); the collar marks the transition between sheath and blade. Phytomers are counted in acropetal direction. The main stem (ms) arises from the embryonal axis and produces first order tillers from its axillary buds. Primary tillers give rise to second order tillers, etc. The tillers are denoted according to the phytomer number the tiller emerges from, and after the order of the parent shoot. A tiller and a leaf from which axil the tiller has emerged, are not considered to be part of the same phytomer (Fig. 1). For example, a tiller that emerges from the axil of main stem leaf one is tiller t2, as it is attached to phytomer two of the main stem. A tiller that appears from the prophyll of tiller t2, originates on the first phytomer of that tiller, and is therefore denoted as t2.1. The coleoptile tiller is denoted as t1, as it is the first primary tiller. This notation system is adapted from Klepper *et al*. (1982), the difference being the assignment of successive phytomer numbers to a leaf and the tiller in its axil (n and n+1 respectively) instead of equal ones (both n).

Architectural modelling of wheat needs to quantify (a) the (relative) timing of developmental events, i.e. rates and duration of initiation, appearance and
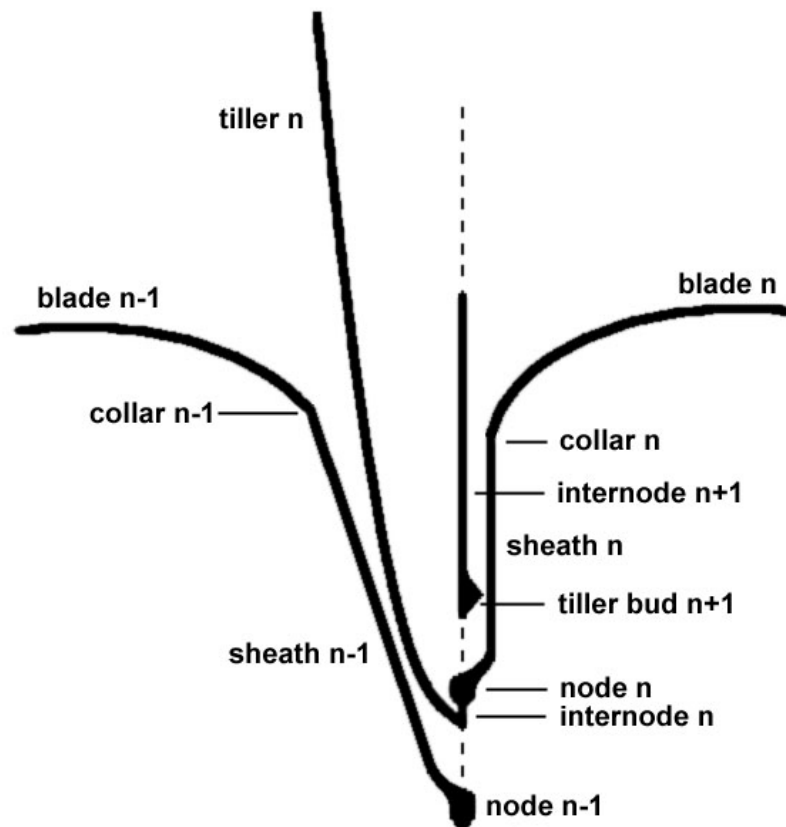

Fig. 1. Schematic representation of phytomers (n-1, n, and n+1) of the wheat plant. Note that tiller n is located in the axil of leaf n-1, as they belong to different phytomers.

24

extension of the components of the phytomers and the relay over time of developmental events, (b) the (final) dimensions of these components, and (c) their geometric properties, e.g. the curvature of leaves in space and azimuth angle between successive leaves as derived from measurement of leaf azimuth.

In the current modelling approach the plastochron, the phyllochron and final leaf number are input parameters of the model. Thermal time ($^{\circ}$Cd) is used to express time related events, assuming the base temperature for development being 0 $^{\circ}$C. Upon initiation at the apex, the components of phytomers start to elongate in sequence. The leaf blade elongates first, immediately followed by the sheath. The last four or five internodes elongate and do so after completion of the sheath. Collar appearance of phytomer n is closely linked to the timing of various phases of phytomer extension in maize and wheat (Fournier and Andrieu, 2000a; Fournier *et al.*, 2004): collar appearance of phytomer n occurs close to the end of sheath extension and the onset of internode elongation of phytomer n, and to the onset of blade elongation of phytomer n+2. The duration of extension of leaf parts and internodes showed little variation regardless of phytomer rank or tiller type. The above-mentioned co-ordination features are incorporated in ADELwheat and allow calculating the timing of blade, sheath and internode extension on a shoot from the time course of collar appearance. They are supposed to be generic for wheat and were not specifically investigated in the present experiment.

The time of appearance of the different orders of tillers is linked to the stage of foliar development, e.g. Haun stage (Haun, 1973), of the main stem (Klepper *et al.*, 1982). For instance, Bos & Neuteboom (1998b) proposed to characterise the difference in foliar development between main stem and tillers with the 'Haun stage delay'. In the current study these delays were also quantified**.** The time between the appearances of two successive tillers is defined as the time expressed in fractional phyllochrons, between the appearance of the first leaf of a tiller or main stem, and the appearance of the first leaf of the next tiller. In the model, two types of this tiller appearance delay (TAD) are distinguished, which differ in the definition of 'next tiller'. In TAD1, the next tiller is the tiller that develops on the same shoot as the considered tiller, but from one phytomer higher. The delay between appearance of t2 and t3 is an example of TAD1, as these tillers emerge from phytomer ranks two and three on the main stem respectively. In TAD2, the next tiller is the first tiller that originates from a phytomer of the tiller in question, with tiller order +1. The delay between appearance of t2 and t2.1 is an example of TAD2.

The inclination of tiller stems is considered to be the same for all tillers; the basal inclination is fixed at 60º, and tillers progressively straighten during development of the first four internodes.

Dimensions of (full-grown) organs and their associations with other plant properties were explored and quantified. In a wheat canopy there are probably not two individual leaves that are exactly the same. However, when modelling, particularly when dealing with individual phytomers in 3D, it is important to simplify the representation of the system to such a degree that it can be parameterised while still simulating the essential features of the system in the real world. Therefore, it is important to recognise similarity rather than differences between properties and to seek for conservative associations between the properties of successively appearing phytomers. Properties of phytomer components, e.g. final leaf length, commonly show a characteristic pattern of change with phytomer number (e.g. Bos and Neuteboom, 1998b; Fournier and Andrieu, 2000b; Lafarge *et al.*, 2002), i.e. the properties of element n+1 are conservatively associated with the properties of element n.

L-systems (Lindenmayer, 1968; Prusinkiewicz, 1999) provide a basically modular approach to modelling, enabling plants and canopies to be described as a collection of modules. In a functional-structural approach, L-systems embed physiology, or are combined with physiological or process-based growth models, e.g. Hanan & Hearn (2003), or exchange data with environmental models. In the current work the wheat architecture is programmed in the plant modelling language CPFG within the L-Studio shell (Prusinkiewicz *et al.*, 2000); ADELwheat was programmed in Graphtal (Streit, 1992). Light absorption per individual leaf element of the 3D structure (beyond the subject of this chapter) can be achieved by interfacing the L-system with the nested radiosity model (Chelle and Andrieu, 1998).

The current chapter presents the concept of modelling the 3D representation of cereal development, which is independent of the programming environment used.

Materials and methods

Experimental setup
To parameterise the model, an experiment was conducted in natural climatic conditions in Wageningen, the Netherlands (51º58′ N), in the period April to June 2003. Spring wheat plants (*Triticum aestivum* L., cv. Minaret) were grown in 70 x

90 cm containers. These contained a soil layer of approximately 35 cm and a 3 cm layer of coarse gravel on the bottom for drainage purposes. The soil was enriched with fertilizer resulting in a nitrogen content of 15 g m^{-2}, which causes no limitation for vegetative development. The seeds were sown at a density of 100 m^{-2}, in a regular grid of 10 x 10 cm. Sowing depth was approximately 5 cm. Weeds, aphids and mildew were controlled by spraying appropriate biocides. The containers were arranged closely together to ensure canopy homogeneity. Part of the plants was used for non-destructive measurements, part for destructive measurements (harvests).

Measurements

Temperature was recorded with shielded thermocouples (type T, TempControl Industrial Electronic Products, Voorburg, NL) every hour (Datataker DT600, Datataker Data Loggers, Cambridgeshire, UK). The thermocouples were placed 6 cm deep in the soil, and within the canopy at 20 cm above the soil surface; air temperature was measured at 1.5 m above soil surface.

Leaf and tiller appearance and length of the appeared part of each leaf of 14 individual plants were monitored every three or four days. These measurements were done on main stems and all primary and higher order tillers. The dimensions of all full-grown organs (blades, sheaths and internodes) were measured destructively on two sampling occasions using separate batches of plants. The first occasion was at maturity of the fifth main stem leaf (n = 12); the second sampling occasion was at maturity of the flag leaves of all shoots (n = 10). Note that leaves were regarded to be full-grown when the ligule had appeared.

Individual plants were digitised using a Polhemus Fastrak magnetic digitiser (Polhemus, Colchester USA). This device records X, Y and Z co-ordinates of objects, relative to a reference point. Using this method, information on midrib curvature and azimuth of leaf blades was gathered (Fig. 2), digitising 5 to 20 points along the midrib depending on the amount of curvature. Digitisation of plants was done on three occasions, as it is not possible to digitise all full-grown leaves at once due to leaf senescence. On the first occasion, 30 plants were digitised when the third main stem leaf was full-grown. On the second occasion 10 plants were digitised, when the eighth main stem leaf was full-grown. At that time, the plants had grown at least five shoots, all of which were digitised. Finally, on the third occasion, full-grown flag leaves of all shoots of six plants were digitised. Plants digitised at the second and third occasion were also among the plants digitised earlier. It was assumed that shape and inclination of leaves
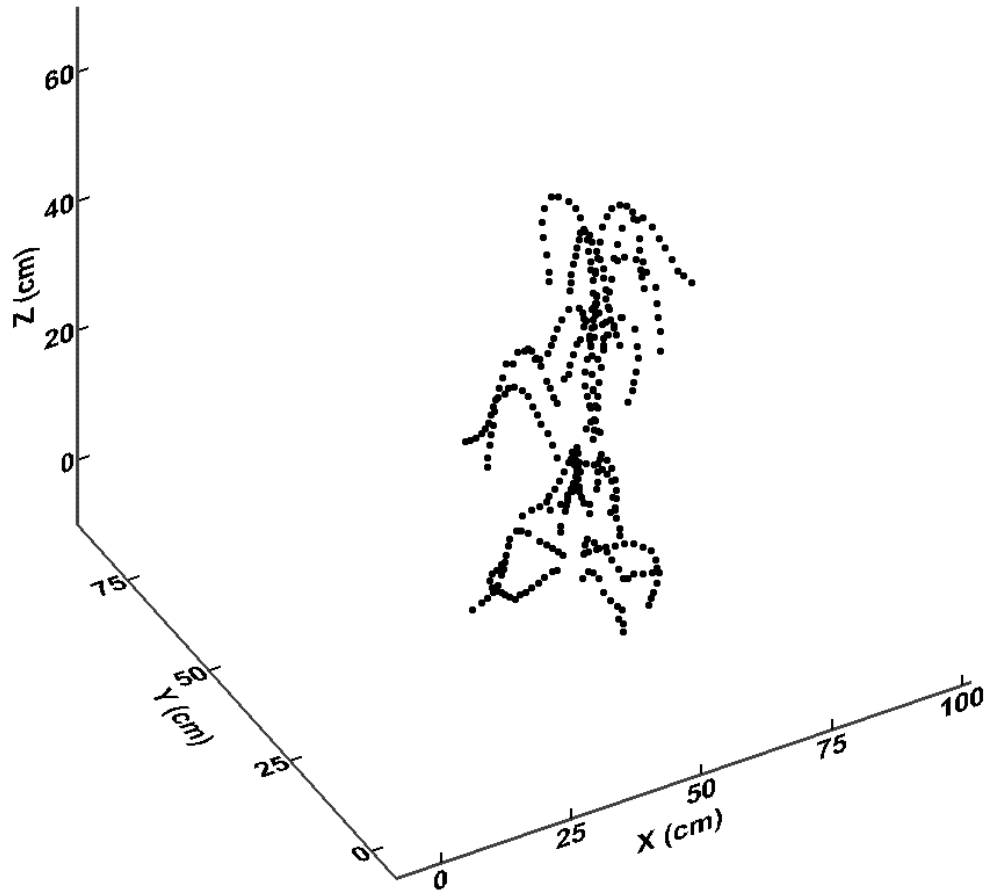
Fig. 2. Visualised 3D scanning data (X, Y and Z co-ordinates expressed in distance (cm) to the scanning reference point) for the leaves of one spring wheat plant in booting stage.

did not change after ligulation. The digitisation database ultimately consisted of geometrical data on 435 full-grown leaves, composed of nearly 10,000 digitised points in total.

Data analysis

Temperature data was converted into thermal time with a resolution of one hour. For the first three weeks after sowing, temperature data from the soil was used as the apex was still under the soil surface; thereafter thermal time data was calculated from the canopy temperature. Digitisation data was analysed using R v1.8.1 (R Development Core Team, 2003). All other data was analysed using Microsoft Excel 2002 (Microsoft Corp., 2002) and SPSS v11.0 (SPSS Inc., 2001). Goodness of fit for the parameterisation functions was analysed by calculating the root mean squared error (RMSE), which is defined as:

$$RMSE = \sqrt{\frac{1}{n} \sum_{i=1}^{N} \left(X_{sim,i} - X_{obs,i} \right)^2}$$

(eq. 1)

where i = sample number, N = total number of measurements, $X_{sim,i}$ = simulated value, and $X_{obs,i}$ = observed value.

Results and discussion

Leaf and tiller appearance

The phyllochron, measured in degree days (ºCd) thermal time between the appearance of two consecutive leaves on the same shoot, showed some variation among the various shoots (Fig. 3). Phyllochron for main stem leaves was 76.2 ºCd (SE 3.71 ºCd). Tiller phyllochron ranged from about 85 to 100 ºCd, when one disregards tillers that appeared very late in the development of the plant (t5, t2.2, and t3.1). One mean value for tiller phyllochron was calculated: 88.0 ºCd (SE 1.95 ºCd). The two mentioned values for main stem and tiller leaves were used in the architectural model. The current ca. 15% difference in phyllochron between main stem and tillers of spring wheat corroborates observations by Bos & Neuteboom (1998a) on this spring wheat cultivar. As found more often (Bos and Neuteboom, 1998a; Hay, 1999), the observed phyllochron of spring wheat is
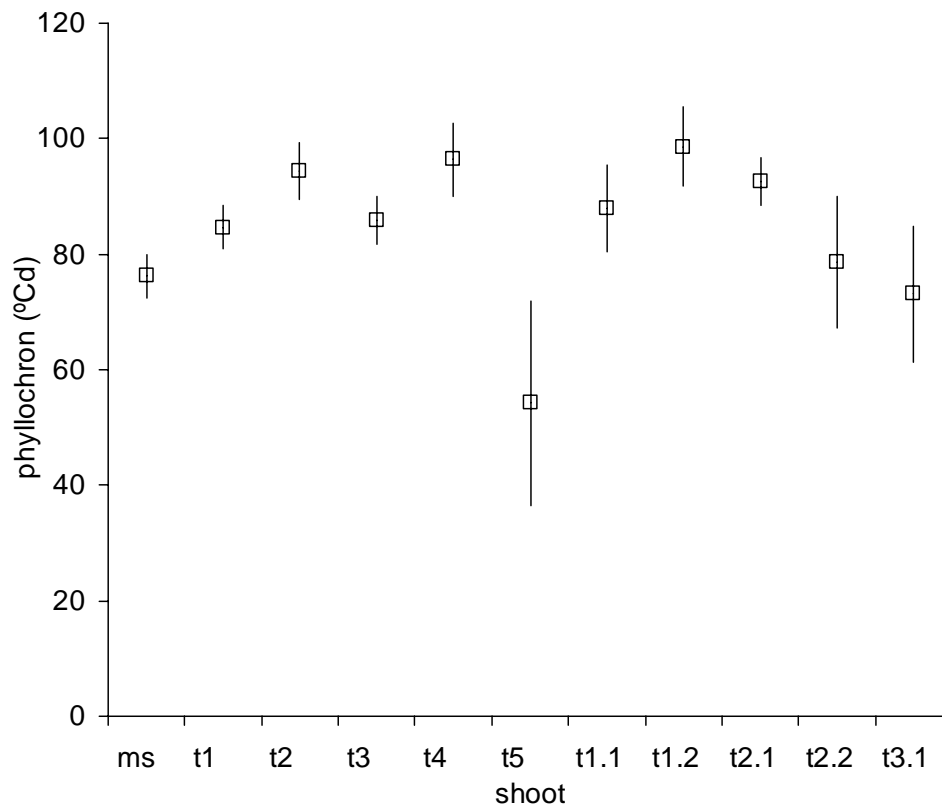

Fig. 3. Average phyllochron (in degree days) for the main stem (ms), primary tillers t1 to t5, and secondary tillers t1.1, t1.2, t2.1, t2.2 and t3.1. Error bars show 2 × SE.

slightly lower than found for winter wheat cv. Soisson.

Effects of photoperiod on phyllochron differ between wheat cultivars (Cao and Moss, 1989; Pararajasingham and Hunt, 1995; Hay, 1999). Therefore, it is clear that phyllochron is a parameter that cannot be regarded as being generic, i.e. it will have to be reparameterised experimentally for cultivar and sowing time. Volk & Bugbee (1991) suggest that the phyllochron can be calculated from daily photosynthetic photon flux density (PPFD, in µmol m^{-2} d^{-1}), irrespective of cultivar and sowing time. However, that approach needs to be tested first before implementation in the current architectural model is warranted.

TAD1 was calculated using data from t2, t3 and t4, as other tillers appeared more erratically, rendering an analysis less meaningful. TAD1 between t2 and t3 was 0.99 (SE = 0.001) phyllochrons; between t3 and t4, TAD1 was 0.70 (SE = 0.13) phyllochrons. For use in the model, one mean value for TAD1 was calculated: 0.84 (SE = 0.07) phyllochrons. For parameterisation of TAD2 data from ms, t1, t2 and t3 was used yielding 1.60 (SE = 0.04) phyllochrons. Note that for the calculation of the TAD values the actual phyllochron of the shoot in question is used and not the average phyllochron across tiller types as calculated in the previous section.

Relative phytomer number

Properties of the components of phytomers show a gradient with phytomer ranks. Gradients of final blade, sheath and internode dimensions along any tiller of cv. Soisson could be regarded as being similar to gradients along the main stem after applying a certain phytomer shift (Fournier *et al.*, 2003). A phytomer shift is basically a certain decimal number of phytomers, characteristic for each tiller, which is added to the actual phytomer rank, obtaining the relative phytomer number (RPN). That concept appeared to apply to spring wheat as well. The phytomer shift was calculated for primary tillers one to four based on the internode length data (Fig. 4) in a two-step fitting process: first, the data points of all tillers were superposed on the main stem data points which was done by shifting the points to the right (indicated by the arrow in Fig. 4a); this was done several times to obtain the best linear fit. The result of the phytomer shift is shown in Fig. 4b. Next, phytomer shift values for each individual tiller type were calculated precisely, by minimising RMSE between the internode length data and the obtained linear model. The resulting shift values are listed in Table 1. The shifts appeared to vary linearly with tiller number ($y = ax + b$, with y being phytomer shift, a the slope, x tiller number, and b the intercept ($R^2 = 0.95$ for $a = 0.703$ (SE = 0.12) and $b = 1.19$ (SE = 0.32), RMSE = 0.18).
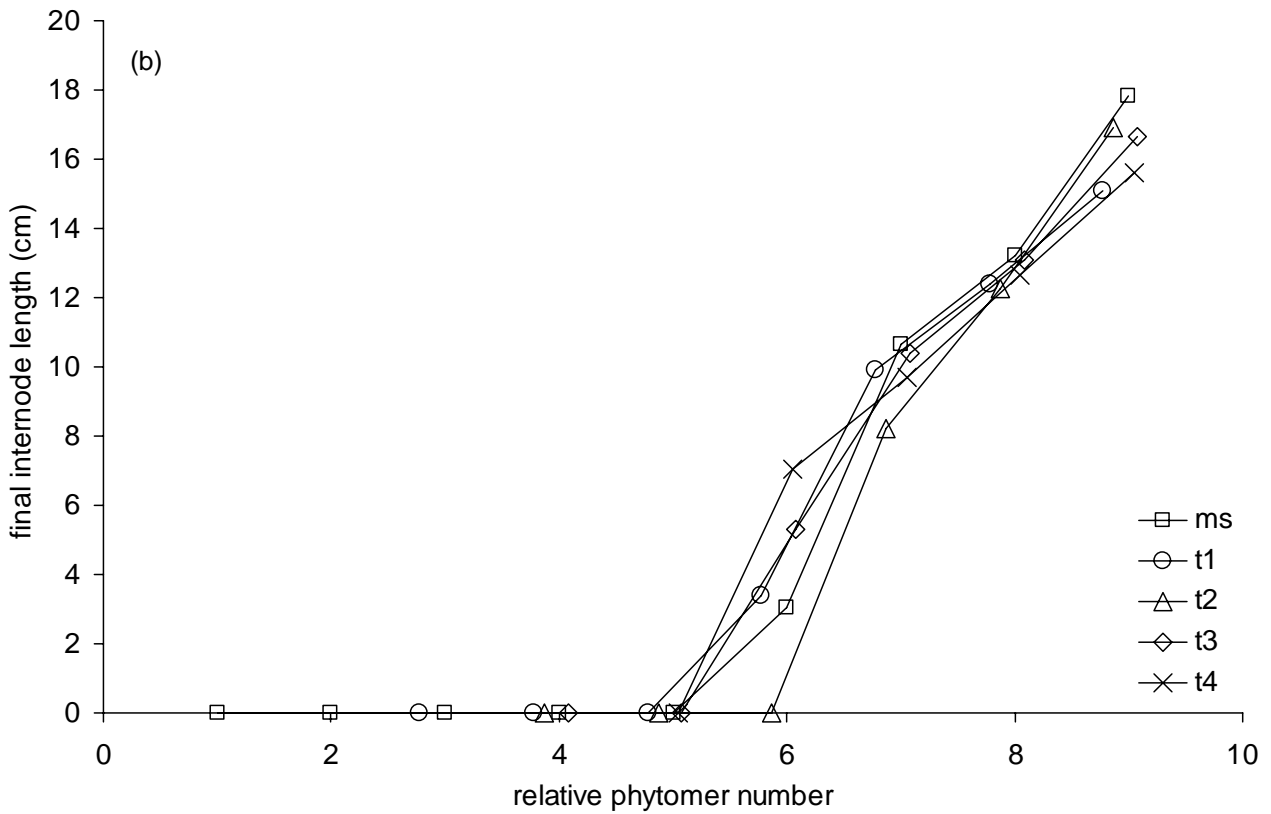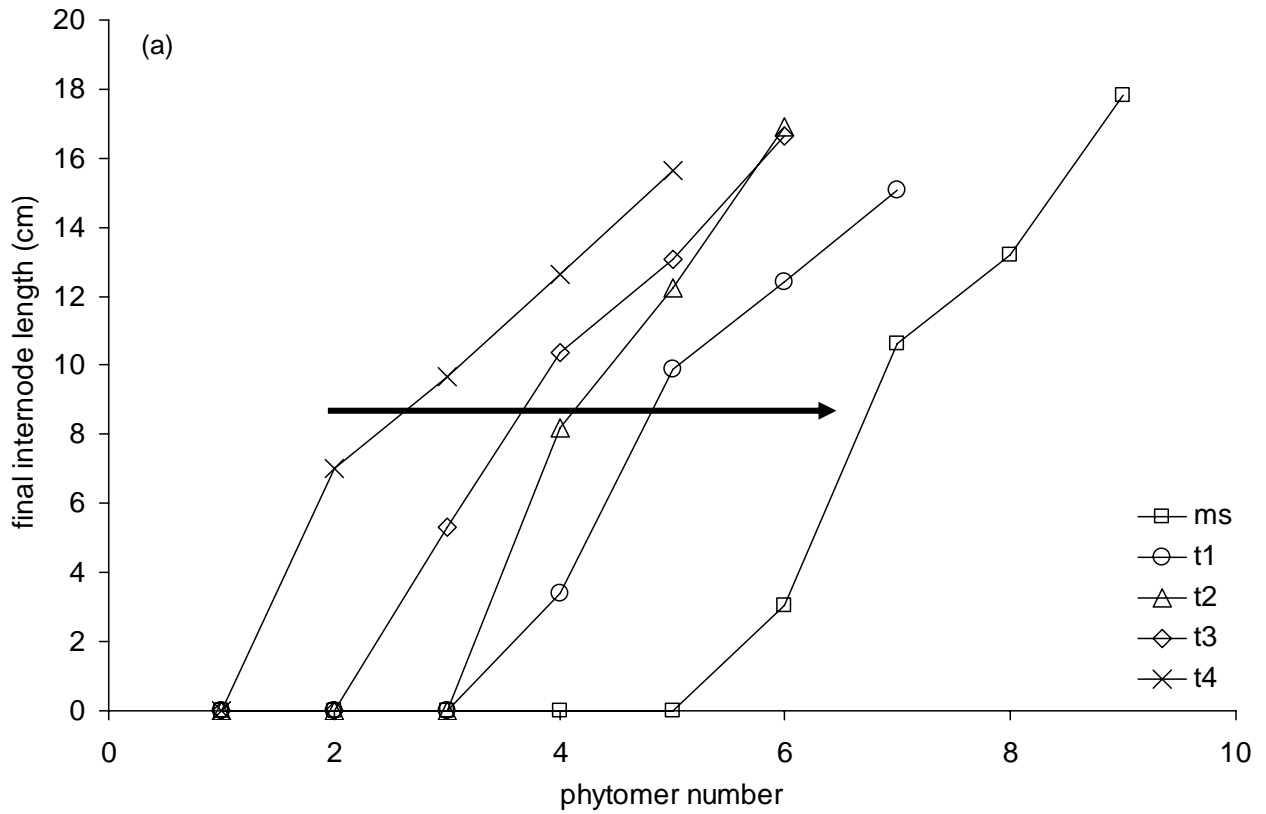
Fig. 4a,b. Final internode length vs. phytomer number for the main stem (ms) and primary tillers t1 to t4. The arrow in Fig. 4a indicates the direction of phytomer shift; Fig. 4b shows the same data after the shifts have been applied (relative phytomer number).

Table 1: Phytomer shifts for primary and secondary tillers. A phytomer shift indicates the amount of fractional phytomer that has to be added to the number of a phytomer in question, to make it resemble the main stem in terms of final organ dimensions.

shoot	phytomer shift
t1	1.78
t2	2.87
t3	3.08
t4	4.05
t1.1	3.85
t1.2	4.28
t2.1	4.13

In the rare case of the presence of t5 or t6, the relation for t1 to t4 is extrapolated to calculate the phytomer shift values. The phytomer shifts were applied to derive single associations between RPN and final blade length and width, sheath length, and also internode length. The same method as described here for primary tillers was used to determine phytomer shifts of secondary tillers (see Table 1).

The virtue of a tiller-specific phytomer shift, outlined above, is that properties of phytomers of the next order of tillers can be derived from the parent shoot. In this way modelling the properties of each tiller independently is avoided. There is another method to reach the same goal, namely the concept of 'summed phytomer number' or 'summed leaf position' (Bos and Neuteboom, 1998b; Tivet *et al.*, 2001; Buck-Sorlin, 2002) in which phytomer ranks on tillers are calculated as the sum of phytomer numbers from the base of the plant to the phytomer in question. For example, in this view phytomer three on tiller t2 would get summed phytomer number five (two phytomers on the main stem plus three phytomers on the primary tiller). It appeared that this concept reflects the similarities between organ dimensions of different tillers well for spring wheat, too. However, phytomer shifts are expressed as fractions and are therefore more precise than the integers of summed phytomer numbers, and for this reason we have chosen to use the former approach in the model.

The current values for phytomer shifts are comparable to those found for Soisson winter wheat grown at two plant population densities. Nevertheless, we suggest calculating the values for each cultivar and population density if the purpose of modelling requires an accurate mimicking of the changes of the 3D structure over time. The summed phytomer number concept, however, can serve as an acceptable and elegant simplification to relate properties of phytomers of order n+1 to those of order n, when detailed measurements are not available.

Final leaf number

The final number of leaves produced on the main stem did not vary much among plants: in 86% of the cases the final leaf number was nine. Final leaf number in wheat depends on genotype, vernalisation, day length, temperature and nitrogen supply (Rawson and Zajac, 1993; Longnecker and Robson, 1994; Hay, 1999; Brooking and Jamieson, 2002). In the current model, the parameter for final main stem leaf number is set to nine. Subsequently, the final leaf number for tillers are calculated by subtracting the phytomer shift for that specific tiller from the main stem final leaf number, and rounding this value to the nearest integer. This parameterisation appears to hold well for all tillers (RMSE = 0.38). A module has been developed (Jamieson *et al.*, 1998) to calculate final leaf number in relation to temperature and photoperiod. That module can be incorporated in the current architectural model, avoiding final leaf number being specified as an input parameter.

Leaf dimensions

Length of the blade of full-grown leaves of all shoots showed a distinct curve when plotted against RPN (Fig. 5). Comparable curves have been found earlier for
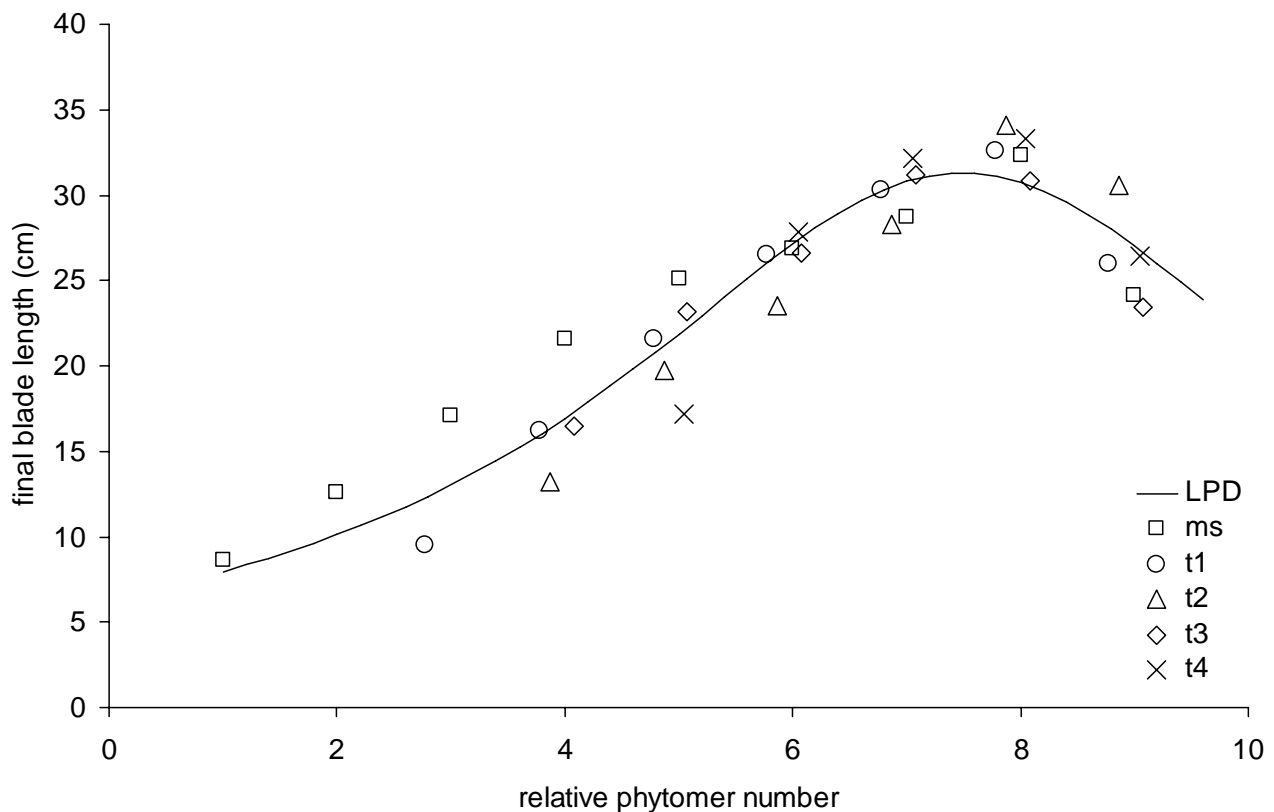

Fig. 5. Final blade length versus relative phytomer number of the main stem (ms) and primary tillers t1 to t4. The curve indicates Lorentz Peak Distribution function fit (LPD).

several spring and winter wheat cultivars (Pararajasingham and Hunt, 1995; Hotsonyame and Hunt, 1997). A non-linear regression based on the Lorentz Peak Distribution function was applied to the data (Buck-Sorlin, 2002):

$$y = y_m / \left[1 + \left(\frac{x - x_0}{b} \right)^2 \right]$$

(eq. 2)

This function has three parameters: y_m, maximum final blade length, b, slope coefficient and x_o, RPN at y_m. This function appeared to fit well ($R^2 = 0.89$ for parameter values $y_m = 31.3$ cm (SE = 0.71 cm), $b = 3.79$ (SE = 0.26) and $x_0 = 7.49$ (SE = 0.13)) to the final blade length data (n = 33), see also Fig. 5. The function appears particularly suitable for RPN values of four and higher; blade length of phytomers two to five of the main stem is underestimated. An alternative approach using a bilinear function, which is used in the winter wheat parameterisation, was explored as well. However, besides the slightly higher RMSE compared to the Lorentz Peak Distribution function (2.48 versus 2.30), this method requires five instead of three parameters and was therefore not used in the spring wheat model.

Spring wheat cv. Minaret and winter wheat cv. Soisson differ distinctly in variability in length of the first full-grown leaf of all shoots. In spring wheat this length varied among shoot types, from about 8 to 18 cm, whereas in winter wheat it was nearly constant at around 9 cm (note that in spring wheat this variation in first leaf length is eliminated when phytomer shifts are applied). Apart from this difference, the general shape of the final blade length versus phytomer rank curves is similar across various gramineous species, e.g. maize (Fournier and Andrieu, 1998), sorghum (Kaitaniemi *et al.*, 1999; Lafarge *et al.*, 2002), barley (Buck-Sorlin, 2002), rice (Tivet *et al.*, 2001) and annual bluegrass (Cattani *et al.*, 2002), although in wheat, the peak of the curve is situated commonly at the penultimate leaf whereas in the other species the decline in final leaf length starts at lower phytomers. Nevertheless, results on wheat final blade length reported by Pararajasingham & Hunt (1995), Hotsonyame & Hunt (1997) and Bos (1999) show a decline in final blade length starting at the top three to four leaves, indicating an effect of photoperiod, nitrogen supply and population density on the shape of the curve. Therefore, the Lorentz Peak Distribution can be regarded as an appropriate function to describe final leaf length distribution along a stem in Gramineae; the precise shape is determined by conditions during development of the plant.

Sheath length of full-grown leaves was parameterised in a way similar to blade length. After applying phytomer shifts, several functions that would likely fit the final sheath length data well were tested: linear, exponential, expo-linear, and logistic. The best approximation (R^2 = 0.95, n = 33) was made by fitting the logistic function:

$$y = \frac{y_m}{1 + e^{a-kx}}$$
(eq. 3)

This distribution function (Fig. 6) showed lowest RMSE (1.20), and contains only three parameters: y_m, asymptote for final sheath length, *a*, lag coefficient and *k*, slope coefficient. The parameter values after fitting were y_m = 21.5 cm (SE = 1.52 cm), *a* = 2.83 (SE = 0.25) and *k* = 0.533 (SE = 0.07).

This parameterisation of sheath length does not imply an underlying mechanism. It has been chosen for its good description of sheath length distribution along the shoot, as there appears to be some variability in the shapes of the curves in various Gramineae. Sheaths on the main stem had a constant length for the first four to five phytomers in the winter cultivar, consistent with earlier observations (Gallagher, 1979), whereas in spring wheat the length
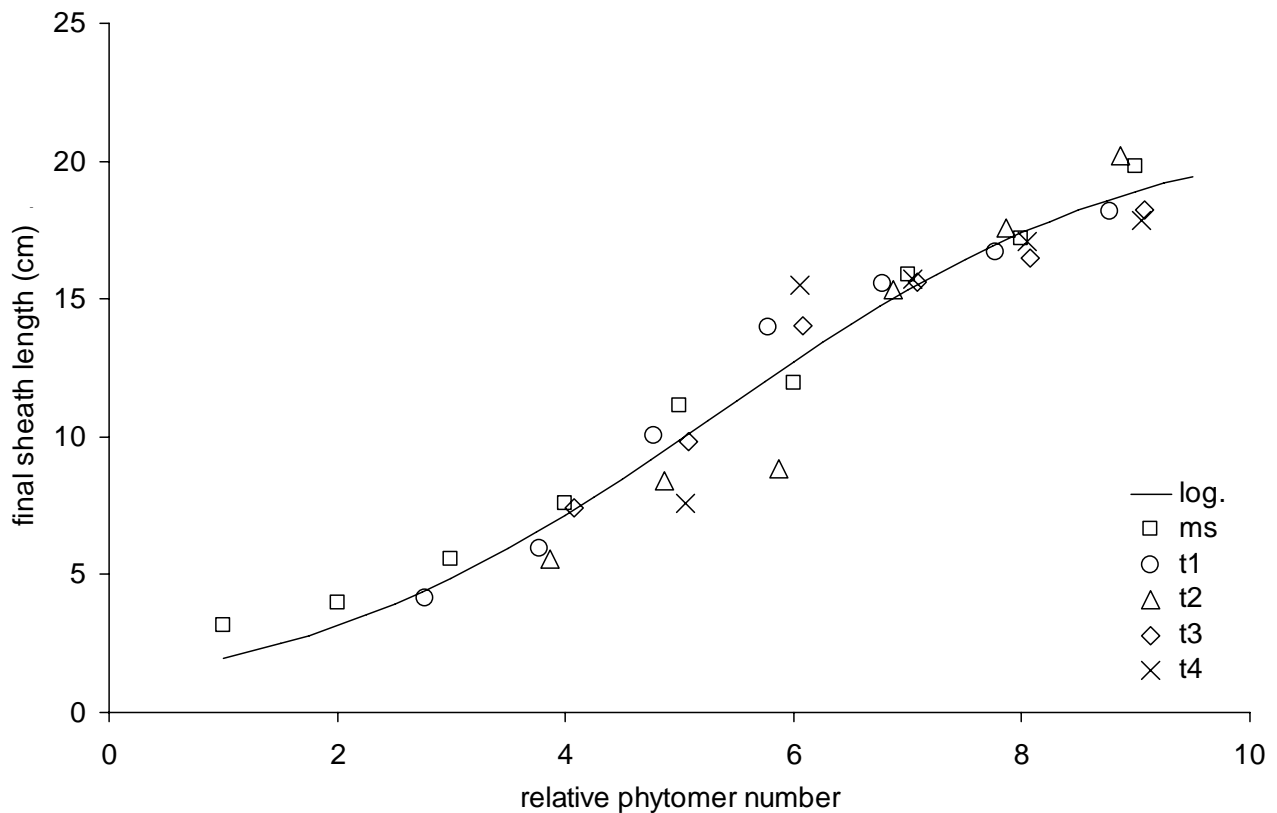

Fig. 6. Final sheath length versus relative phytomer number of the main stem (ms) and primary tillers t1 to t4. The curve indicates the logistic function fit (log.).

initially increased monotonously with phytomer rank. In spring wheat, sheath length started to level off from RPN values of seven and higher, instead of showing continued linear increase with phytomer number like in winter wheat; in maize sheaths length was even observed to decrease from phytomer number seven onwards (Fournier and Andrieu, 1998; 2000b). As a consequence of this variability across species and cultivars, final sheath length versus RPN probably needs reparameterisation for every new species, cultivar and sowing time.

Maximum blade width of full-grown leaves did not yield one single association with RPN, neither in spring wheat nor in winter wheat. However, in spring wheat maximum blade width appeared to correlate well to final sheath length using the linear function $y = ax + b$, with slope $a = 7.8 \ 10^{-2}$ cm cm^{-1} (SE = $0.5 \ 10^{-2}$ cm cm^{-1}) and intercept $b = 0.21$ cm (SE = 0.06 cm) ($R^2 = 0.90$; n = 33), see Fig. 7. This relation is used to model final maximum blade width (RMSE = 0.13), and results in a sigmoid shape of the curve that describes maximum blade width vs. RPN because sheath length was modelled as a logistic function of RPN. A sigmoid shape has been shown by Bos & Neuteboom (1998b) as well, who fitted a similar sigmoid function to model maximum blade width versus summed phytomer number directly. Additionally, Pararajasingham & Hunt (1995) observed
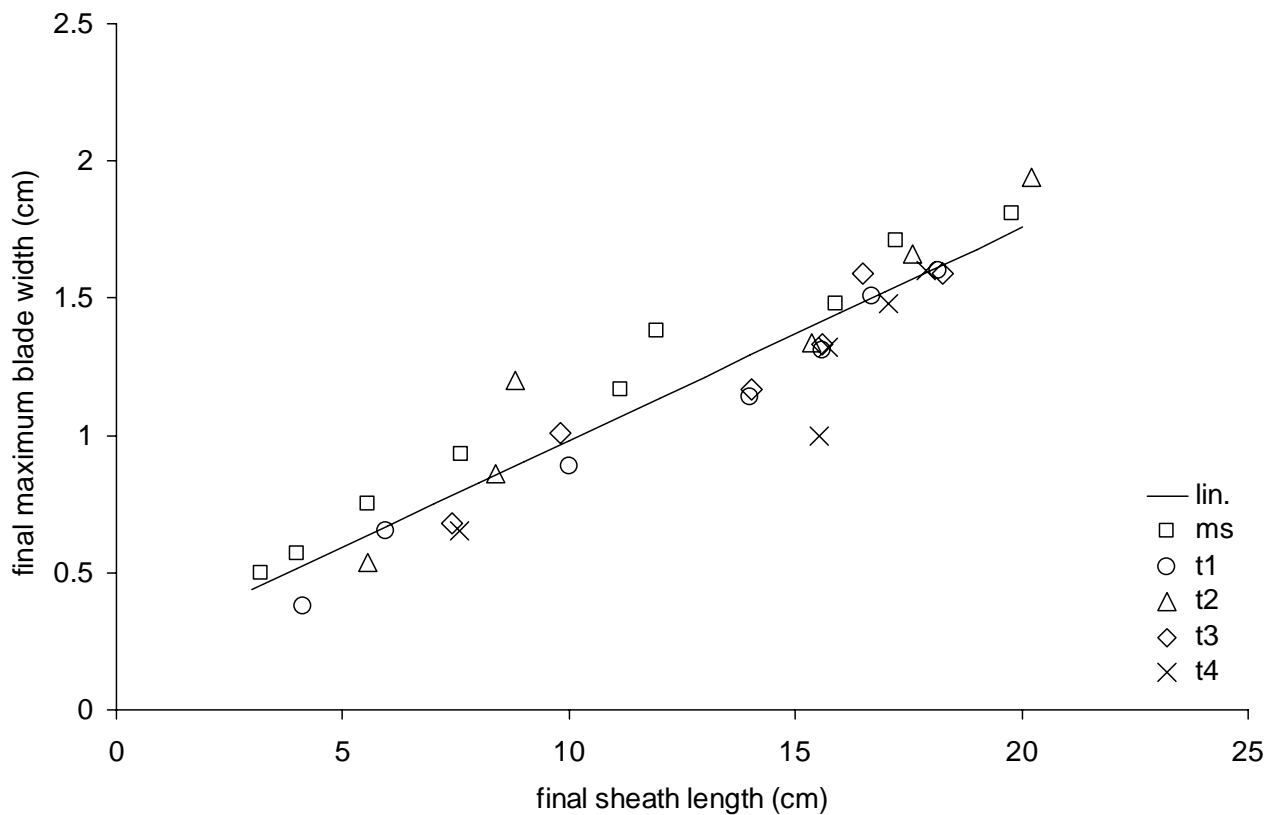

Fig. 7. Final maximum blade width versus final sheath length of the main stem (ms) and primary tillers t1 to t4. The line indicates the linear fit (lin.).

a similar pattern for main stems of several spring and winter wheat cultivars grown at different photoperiods. However, some of the cultivar × photoperiod combinations showed a decrease in maximum blade width at the top three to four phytomers instead of a plateau, whereas other cases could be described using a simple linear function. Similar variability in blade width of main stem leaves has been observed by Hotsonyame & Hunt (1997). This reinforces the view that maximum blade width of Gramineae cannot be modelled solely as a robust function of RPN; more variables such as photoperiod or light intensity (Bos *et al.*, 2000), population density and nitrogen level need to be taken into account. A study on population density effects on leaf area growth in spring wheat (Bos, 1999) showed that increasing population density results in a decrease in maximum blade width for the top four main stem leaves; such a relation can be investigated and incorporated into the model. In the current model maximum blade width is an input parameter in a second order polynomial equation (Prévot *et al.*, 1991), yielding the change in leaf width as a function of the distance to the blade base.

Leaf geometry

Curvature of the blade midrib was modelled using the method proposed for maize (Prévot *et al.*, 1991), and applied to maize (Fournier and Andrieu, 1998) and winter wheat cv. Soisson. The model describes the wheat blade as a combination of an ascending parabolic part, and a descending elliptic part. No twisting of the blade is taken into account; the blade is supposed to be in a plane, bent in the third dimension. Fig. 8 shows a schematic representation of a modelled leaf blade. Parameters Φ_0 and $d\Phi_n$ are angles that define the parabolic part of the curve; Φ_i and Ψ_e define the elliptic part. Besides these, an additional parameter ε is used to define eccentricity of the elliptic part, based on the length of the horizontal and vertical axes d and e respectively; the absolute value of ε is the eccentricity, and its sign is the direction of the ellipse main axis. Furthermore, a parameter P_{cass} was used to define the ratio between length of the parabolic part and length of the blade, to model the transition between parabola and ellipse. Figs. 9a and b show two digitised (dots) and modelled (lines) spring wheat leaf blades. The first example (Fig. 9a) was modelled using only the parabolic part, the second example (Fig. 9b) shows both a parabolic and an elliptic part. Over 94% of the digitised full-grown leaves could be fitted using either only the parabolic function or both the parabolic and elliptic functions; the remaining 6% could not be fitted and were therefore unsuitable for parameter derivation. As a clear distinction could be made between leaves situated near the bottom of the
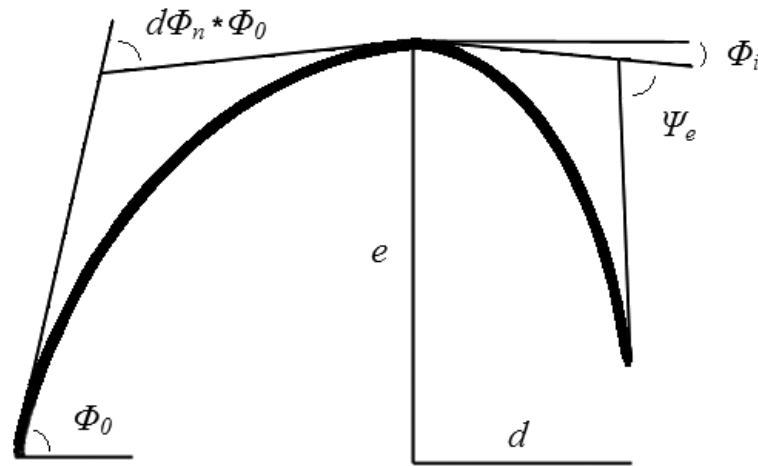
Fig. 8. Model of leaf blade curvature as proposed by Prévot et al. (1991) for maize. Φ_0 and $d\Phi_n$ define angles of the parabola (ascending part); Φ_i and Ψ_e define angles of the ellipse (descending part); d and e are lengths of the horizontal and vertical ellipse axes, respectively.
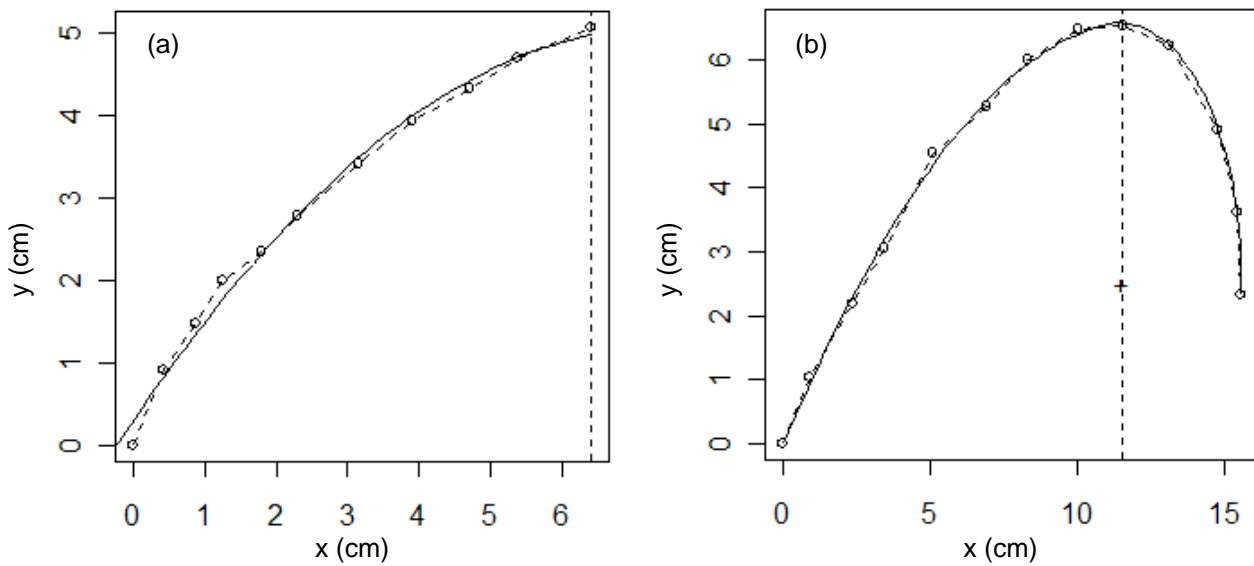
Fig. 9a, b. Two examples of spring wheat leaf blade curvature; the dots represent the digitised points, the lines represent the modelled blade curvature. The x- and y-axis represent distance to the blade 'insertion point', i.e. the point at which the blade is touching the stem. The vertical dashed line indicates the transition between parabola and ellipse, P_{cass}, which is defined as the ratio between length of the ascending part of the blade and length of the entire blade.

plant and the higher leaves, these two groups were parameterised separately. This separation was based on two categories of P_{cass}, as for most of the lower leaves (phytomer numbers six and higher when counting, only for this purpose, from the top downwards) P_{cass} appeared to be close to one, meaning the blade does not have a descending part (Fig. 9a). The parameter values for leaf curvature were entered in a database and their distributions calculated. In the architectural model parameter values for leaf curvature are drawn from these distributions. This stochasticity is implemented to reflect the variation in blade curvature found in the field.

Analogous to midrib curvature, parameterisation of leaf blade azimuth was done using a purely statistical approach based on the digitisation dataset. This was done by analysing the angles between consecutive leaves. Phytomer shifts were applied to the tillers to compare full-grown leaves of comparable RPN. A distinction can be made between angles at RPN ≤ 3 (Fig. 10a), and higher ranks (Fig 10b). For an RPN value of two, the majority of the angles was near +180º and -180º, indicating the tendency towards opposite azimuth. For RPN value of three the angles were more dispersed with few points only between -120º and +60º. For RPN values higher than or equal to five a less regular orientation was observed, with a slight preference for lower angles. Therefore, in the model, two sets of phytomer ranks were distinguished (RPN one to three, and all higher RPN values; note that in the range of RPN values between 3.5 and 5.5 a limited amount of data was available, therefore it is not precisely known at which RPN the limit is located). For both sets the distribution of observed orientation was calculated and in the model values were drawn from these distributions.

The observations that blade azimuth was mainly opposite for the lower phytomers, and more towards a spiral configuration in higher phytomers, agree with observations in winter wheat cv. Soisson, and in maize (Fournier and Andrieu, 1998; Maddonni *et al.*, 2002). In maize, blade azimuth can be altered during development of the plant, as a result of light signalling due to scattering by neighbouring plants (Maddonni *et al.*, 2002). It was shown that the leaves adopted azimuth angles perpendicular to the row structure. If any such response would potentially be present in spring wheat, it would not be manifest in the current experiment, since the wheat plants were sown in a regular grid without any row structure. Any light signalling would then come from all directions and would be neutralised as a consequence. Due to this unaffected development of blade orientation, the obtained parameterisation defined here for spring wheat can be regarded as being general, although the distributions might differ somewhat among cultivars, depending on final leaf number.
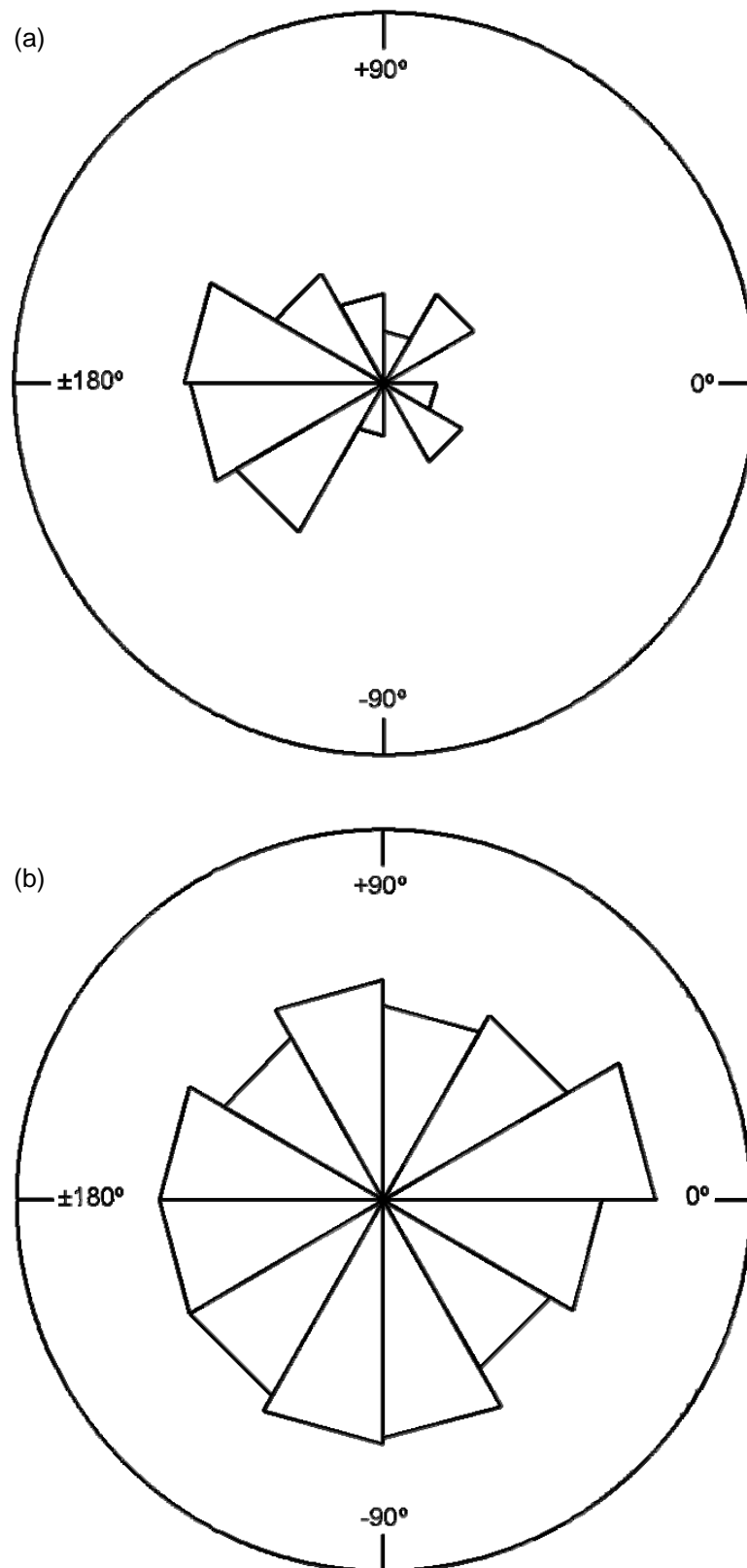
(a)

+90°

±180°

0°

-90°

(b)

+90°

±180°

0°

-90°

Fig. 10a, b. Circular histogram showing the distribution of azimuth angle between consecutive leaves, for RPN values 1-3 (a) and higher than 3 (b). Data from all shoots are shown (n=281).

Internode length

When not elongated, internodes were assigned length zero. Length of elongated full-grown internodes showed a very close relationship with RPN and was approximated by a linear function of the form $y = ax + b$, with slope a = 3.80 cm (SE = 0.23 cm) and intercept b = -17.5 cm (SE = 1.71 cm) (R^2 = 0.94, RMSE = 0.95, n = 33). The RPN of the first elongated internode is defined as $f = 1 - b/a$. This is one plus the x-intercept of the linear model ($-b/a$), since the x-intercept represents the RPN of the last non-elongated internode.

The current value for a is close to the one observed in Soisson, namely 3.42 and 3.58 for 250 and 70 plants m^{-2} respectively. For new applications of the model, final internode length needs recalibration, including the RPN of the first elongated internode (f). In spring wheat cv. Minaret f was 5.59, but higher values were found in winter wheat cv. Soisson, namely 6.19 and 7.37 for 250 and 70 plants m^{-2} respectively. Since the total number of internodes in wheat that elongate is usually four or five, this parameter is likely to depend on the total number of vegetative phytomers initiated which is usually much higher in winter wheat than in spring wheat cultivars. In contrast to wheat, maize shows a distinct decline in internode length with increasing phytomer number from phytomer 9 or 10 onwards (Fournier and Andrieu, 2000a; Birch *et al.*, 2002). Therefore, parameterising this variable for other Gramineae most likely requires redefining the function that describes internode length along the stem.

General discussion and concluding remarks

This chapter describes our efforts to parameterise a three-dimensional architectural model of spring wheat, which will be applied to explain the tillering pattern, as influenced by light conditions at the leaf from the axil of which the tiller may or may not emerge. Two aspects of light will be examined, namely the amount of photosynthetically active radiation received per leaf and the red / far-red ratio of the light received. Such an application requires a detailed 3D description of a wheat canopy, in order to simulate light interception and scattering accurately; see Fig. 11 for an example of a small simulated wheat plot. The model presented in this chapter is highly descriptive in the sense that properties of organs are predetermined, with the exception of two stochastic elements. However, this does not invalidate the model as a tool to test local effects of light on tillering. The application of the model is straightforward as long as experiments to derive model parameters (reported here) and experiments to test model results (to be reported later) are conducted under comparable conditions. In the current experiments we aimed at potential growth conditions

(van Ittersum *et al.*, 2003), i.e. plants grown with ample availability of nutrients and water and in the absence of impact of pests, diseases and weeds. In this context the results of Bos' (1999) sensitivity analysis are relevant: leaf area growth per unit soil surface appeared most sensitive to the number of appearing tillers and less so to leaf length and leaf width. So our modelling study focuses on the most influential component of leaf area growth.

Yet, in the long term it is our intention to develop an architectural model of wheat that can serve as a basis for representation of cultivars other than Minaret. In order to reduce the amount of time and effort needed to correctly parameterise the model, it may be necessary and possible to introduce simplifications. The incorporation of a more general tiller simulation routine based on the concept of summed phytomer numbers (Bos and Neuteboom, 1998b), is an example of such a simplifying concept. Future sensitivity analysis will provide insight in the parameters that critically determine the modelling results. This could lead to fixation of parameter values of which the influence is small, and that could therefore be regarded as being general for wheat.

The differences in final organ dimensions between the spring and winter wheat cultivars used in this study reflect the differences between spring and winter wheat in general. Since winter wheat main stems produce more phytomers than spring wheat, various parameters and functions are inevitably different. Good examples of this are the difference in sheath length for the first four to five phytomers, and the value of the parameter that determines the RPN of the first elongated internode. The relative ease with which the original winter wheat model could be adapted and parameterised for spring wheat implies that the approach provides a template for 3D modelling of Gramineae in general. The approach can be extended to account for effects of environmental factors such as water and nutrients and interplant competition. Such extension needs to be based on incorporating sink - source relations in the model. Steps in that direction are taken by Allen *et al.* (2004) and such efforts are on our research agenda.

Fig. 11. An example of a small simulated wheat plot.

Chapter 3

An architectural approach for modelling tillering in wheat: effects of plant density and shade, model evaluation and sensitivity analysis

Jochem Evers

Jan Vos

Christian Fournier

Bruno Andrieu

Michaël Chelle

Paul Struik

Abstract

ADELwheat is an architectural model that describes development of wheat in 3D. This chapter analyses the robustness of the parameterisation of ADELwheat for spring wheat cultivars in relation to population density and shading. The model was evaluated using data from two spring wheat experiments with three population densities and two light regimes. Simulation validation was done by comparing ground cover and leaf are index of simulated virtual wheat plots with actual data. A sensitivity analysis was performed by modulating variables defining leaf blade dimensions and leaf or tiller appearance rate, and its results are related to biological variability.

Parameterisation functions in the model that had been established previously applied to independent data for different conditions. GC and LAI were simulated adequately at three population densities. Sensitivity analysis revealed that calibration of phyllochron and blade area needs to be accurate to prevent disproportional deviations in output. In conclusion, the model adequately simulated spring wheat for various conditions. It is a complete architectural model for spring wheat, which can be used in several applications, e.g. plant-insect interaction, remote sensing, and light interception studies.

Keywords: functional-structural model, wheat, leaf shape, tillering, ground cover, L-system

Introduction

Architectural plant models provide the possibility to explicitly simulate plant and canopy structure, i.e. the three-dimensional geometry of leaves and other organs. For the Gramineae family, architectural models have been described for maize (Fournier and Andrieu, 1998; 1999), sorghum (Kaitaniemi *et al.*, 1999), barley (Buck-Sorlin, 2002) and rice (Watanabe *et al.*, 2005).

For wheat (*Triticum aestivum* L.) ADELwheat has been developed; ADELwheat is based on the L-system formalism (Lindenmayer, 1968; Prusinkiewicz, 1999) using the CPFG simulation program (Prusinkiewicz *et al.*, 2000; Měch, 2004). L-systems provide a modular approach to modelling, in which a basic unit is reproduced over time to simulate plant development. In ADELwheat, the basic unit is the wheat phytomer, which consists of an internode with a tiller bud at the bottom, and a node, a leaf sheath and blade at the top. These components are called modules. Each module is provided with its own set of variables and parameters, which define for example the module's current length or age, or geometrical properties like inclination. From a given initial spatial arrangement of plants, the model calculates growth and development, size, shape and orientation in space of each organ in relation to temperature. Simulation of tillers is comparable to main shoot simulation, taking into account a certain delay in tiller appearance relative to the development of the main stem. The concept of relative phytomer number, RPN (Fournier *et al.*, 2003), enables the derivation of properties of individual tiller phytomers from those of the main stem; to this end a 'phytomer shift' is added to the actual rank number of the phytomer, yielding the RPN, i.e. the main stem phytomer number from which properties are inherited. The model has two stochastic elements: curvature of the leaf blades, and tiller configuration (number in time and space) through thermal time. Other key variables in the model are phyllochron and leaf blade length and width. Previous work presented this model in detail, its concepts based on winter wheat (Fournier *et al.*, 2003) and the parameterisation for spring wheat (chapter 2).

In chapter 2, we determined model parameters of ADELwheat for spring wheat and discussed differences with the initial parameterisation for winter wheat (Fournier *et al.*, 2003). The objectives of the current chapter are (a) to measure the effect of population density and shade on model parameters under conditions ensuring ample supply of water and nutrients and absence of pests, diseases and weeds, (b) to evaluate model performance, and (c) to carry out sensitivity analysis of model parameters. Model evaluation was achieved by (I) comparing

the values of key model parameters, measured in an independent experiment, with the values obtained in the previous parameterisation experiment and the actual parameterisation as implemented in the model, and (II) comparing measured temporal changes of ground cover, GC, and leaf area index, LAI, with simulated ones. Time courses of GC and LAI are both model outputs incorporating effects of all parameters defining dynamics of development processes and dimensions of organs. Sensitivity analysis was performed by changing model parameters in a systematic way and analysing the effects on the temporal patterns of GC.

Model parameterisation is a laborious job. The current evaluation and sensitivity analysis yield insight in the options to use the model with standard parameter values for different applications, e.g. in remote sensing studies, interspecific and intraspecific competition studies and analysis of spatial aspects of relationships between pests or diseases and plants. Model evaluation as presented in the current chapter provides a necessary step towards a generic architectural model of tillering in Gramineae.

Materials and methods

Experimental setup
To validate the model parameterisation and the robustness of simulation of ground cover and leaf area index, two separate experiments were performed in Wageningen, the Netherlands (51º58′ N) in 2004.

An outdoor experiment was conducted from April to June 2004 (referred to in figures as '2004', to distinguish from the experiment '2003' which was used for model parameterisation for spring wheat, see chapter 2). Spring wheat plants (*Triticum aestivum* L., cv. Minaret) were grown in 70×90 cm containers. These contained a soil layer of approximately 35 cm and a 3 cm layer of coarse gravel on the bottom for drainage. The soil was enriched with fertilizer resulting in a soil nitrogen content of 15 g m^{-2}. The seeds were sown at a depth of approximately 5 cm below soil surface. Diseases, pests and weeds were controlled by using appropriate biocides. The containers were arranged closely together to ensure canopy homogeneity, and eight guard containers were placed around the test container to avoid border effects on the plants that were to be measured. Seeds were sown at three densities (100, 262 and 508 m^{-2}, one plot per density) in a regular square grid, i.e. no row structure. Distances between the plants were 10.0, 6.2 and 4.4 cm respectively. The containers were exposed to full light

(control). A similar plot (shade treatment) was placed in a tent constructed of shade material (XLF 17F, US Global Resources, Seattle, USA) that absorbed 75% of the incoming light. The tent was open to the sides at the bottom, at a height of approximately 80 cm. The six different treatment combinations are coded as D1c, D2c, D3c, D1s, D2s and D3s with the number indicating the population density (1 = low, 2 = middle, 3 = high) and the letters 'c' or 's' indicating control or shade treatment respectively. Treatment D1c is comparable to the experimental conditions in the parameterisation experiment of 2003 (reported in chapter 2), and data from D1c is therefore used as independent data to validate the model parameterisation. Due to the open mesh structure of the shade material, the tent had a negligible effect on temperature. Effects on humidity were not measured but can be expected to be virtually absent for the same reason. Light reflected from the inside of the tent had a negligible effect on the red/far-red ratio. An additional plot, exposed to full light, contained plants at the same three population densities for destructive measurements (harvests).

To collect additional data, spring wheat plants (cv. Minaret) were grown in eight similar containers at 100 plants m^{-2}, in a growth chamber (referred to in figures as '2004b'). Light period was set at 15 hours (6:00 until 21:00), with light intensity at ca 425 µmol m^{-2} s^{-1} PAR at the level of the top of the canopy. The light was emitted by 400 Watt SON-T Agro Philips lamps and 400 Watt HPI-T Plus Philips lamps (3.5 lamps m^{-2}). Temperature was 17 ºC from 9:00 until 21:00, and 11 ºC from 21:00 until 9:00; relative humidity was kept at 75%.

Experimental data collection and analysis
In the outdoor experiment, temperature was recorded (Datataker DT600, Datataker Data Loggers, Cambridgeshire, UK) with shielded thermocouples (type T, TempControl Industrial Electronic Products, Voorburg, NL) every hour. The thermocouples were placed 6 cm deep in the soil, and within the canopy at 20 cm above the soil surface; air temperature was measured at 1.5 m above soil surface. Thermal time was calculated from temperature data using a resolution of one hour. For the first two weeks soil temperature was used, since the apex was below soil surface; canopy temperature was used thereafter. The start of thermal time accumulation was set at appearance of the first leaf; the base temperature was set at 0 ºC.

In the outdoor experiment, the dimensions of all full-grown organs (blades, sheaths and internodes) of the main stem were measured by destructive sampling at two dates. The first sampling was at ligule appearance (i.e. leaf maturity) of the fifth main stem leaf (n = 10); the second sampling was at ligule

appearance of the ninth (flag) leaf (n = 10). In the growth chamber experiment, the dimensions of all fully grown organs were measured for main stem and tillers (the latter only in the growth chamber experiment) from destructive sampling at three dates (n = 6 per sampling). The first harvest was conducted at maturity of the fourth main stem leaf, the second harvest at maturity of the seventh main stem leaf, and the third at flowering. Final blade length distribution along a shoot was fitted to the Lorentz Peak Distribution function (Buck-Sorlin, 2002) (Eq. 1); y is blade length (cm), y_m is maximum blade length (cm), x is phytomer number, x_m is the number of the phytomer that contains longest blade, and k is the slope coefficient.

$$y = \frac{y_m}{\left(1 + \dfrac{x - x_m}{k}\right)^2}$$

(eq. 1)

For fitting final blade width distribution along the main stem the logistic equation was used (Eq. 2); y is blade width (cm), y_m is maximum blade width (cm), k is the slope coefficient, x is phytomer number, and x_m is phytomer number at the inflection point.

$$y = \frac{y_m}{1 + e^{-k(x - x_m)}}$$

(eq. 2)

Additionally, measurements of the distance of the blade margin to the midrib were done on eight randomly chosen fully grown leaves of plants from the growth chamber experiment (flag leaves were excluded because their shape diverges slightly from that of the other leaves). These measurements were used to fit a
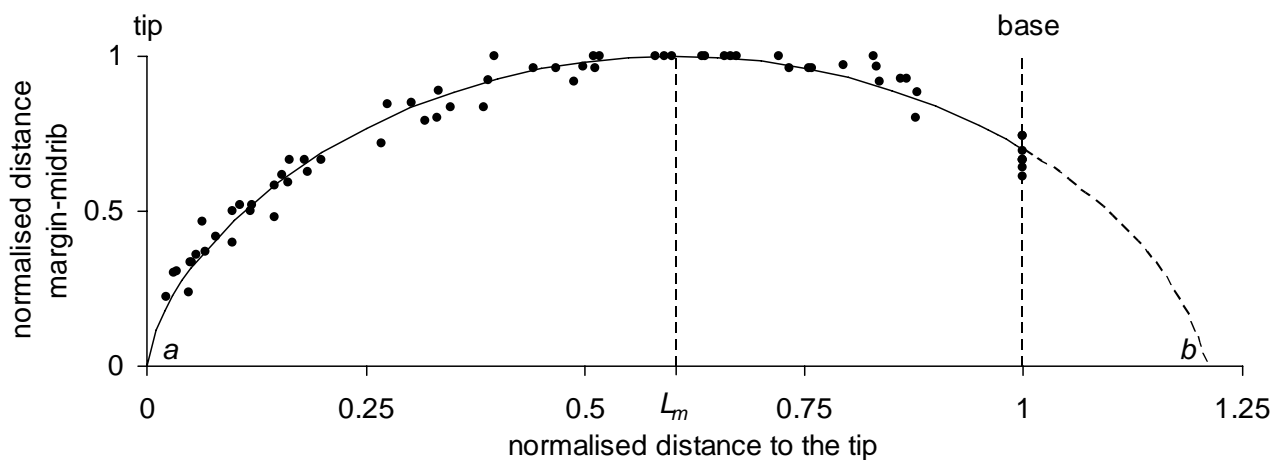

Fig. 1: Function describing the shape of a spring wheat leaf blade, i.e. the normalized distance from the leaf margin to the midrib as a function of the normalized distance to the blade tip. a and b indicate the x-intercepts (see appendix A), L_m indicates the location of the top.

function with two coefficients that describes the shape of the full-grown wheat blade by calculating distance of blade margin to midrib as a function of distance to the blade tip, see Eq. 3. W_{norm} is the normalised distance between margin and midrib (actual divided by final maximum margin-midrib distance), L_{norm} is the normalised distance of the base to the leaf tip (distance to leaf tip divided by final maximum blade length), L_m is the distance of the point of maximum margin-midrib distance to the blade tip as a fraction of the final length ($0.5 < L_m < 1$), and C is a curvature coefficient ($0 < C < 1$). For our spring wheat cultivar, coefficient values were $L_m = 0.603$ (SE = 0.0047) and $C = 0.63$ (SE = 0.015) ($R^2 = 0.97$, n = 68; see Fig. 1). For derivation of this new function, see appendix A.

$$W_{norm} = \left(\frac{-L_{norm}(L_{norm} - 2 \cdot L_m)}{L_m^2} \right)^C \qquad \text{(eq. 3)}$$

Eq. 3 is an alternative to the ones used for maize leaves in Sanderson *et al.* (1981), Prévot *et al.* (1991) and Bos *et al.* (2000), and for rice leaves in Elings *et al.* (1999), and provides an accurate description of blade shape of our wheat cultivar; Eq. 3 is used both in calculation of LAI (see below) and in the architectural model itself.

Leaf and tiller appearance, length of the appeared part of each leaf of ten plants per treatment (n = 60), and tiller senescence were monitored every 3 or 4 days. In the outdoor experiment (2004) this was done for main stem and all primary tillers, in the growth chamber experiment (2004b) (n = 24) for shoots of all orders. A leaf was considered to have appeared halfway between the last moment it was absent and the first it was recorded as being present. A tiller was considered to be senescing, when the youngest leaf had not gained length since the last measurement (Kirby and Riggs, 1978), and the starting date of senescence was chosen at halfway between the last moment it was not senescing and the first it was. A leaf was considered to be dead when at least half of the leaf area had turned yellow (measured in the growth chamber experiment only). Phyllochron values were calculated by linear regression of thermal time at leaf appearance vs. leaf number; the slope of the regression line is the phyllochron (ºCd per leaf). Tiller appearance delay (TAD, expressed in phyllochrons) was calculated by converting thermal time at tiller appearance into phyllochrons, using treatment specific leaf appearance data. Gross leaf area index (gLAI, expressed in m^2 leaf per m^2 soil) was calculated from these non-destructive measurements, by cumulating individual leaf areas (obtained from integration of Eq. 3) from the measured blade lengths. gLAI represents the total area of leaves that were

produced from appearance to the time of observation, disregarding senescence. gLAI was used in model validation instead of LAI, since measured data on leaf and tiller senescence was not sufficient to calculate net LAI, and data on secondary tillers was not present. gLAI data was fitted to thermal time using the classical logistic equation (Eq. 2). Here, *y* is gLAI, y_m is the maximum gLAI, *k* is the slope coefficient, *x* is thermal time since appearance of the first leaf, and x_m is the amount of elapsed thermal time at the inflection point, at which the rate of gLAI increase is highest.

To obtain ground cover (GC) data per plot four images of non-shaded plots were taken on seven occasions during canopy development, using a digital camera (from 40 to 70 cm above the top of the canopy), each covering an area of ca. 60x45 cm; field of view of the camera lens was 42º horizontally and 32º vertically (when held horizontally). GC percentages were calculated from the digital images, using Optimas v6.5 image analysis software (Media Cybernetics, Inc., Silver Spring, USA) and a ground cover analysis script capable of separating green vegetation and brown soil colours (see Andrieu, 1982; Andrieu *et al.*, 1997). GC data was fitted to thermal time using Eq. 2, with *y* being GC, and y_m maximum GC (restricted to ≤100% in the fitting process). The relation between GC and LAI is given by Eq. 4 (Lambert-Beer's law), which is used to calculate the extinction coefficient *K*.

$$GC = 1 - e^{-K \cdot LAI}$$

(Eq. 4)

Simulation output and its analysis

Initially, simulations were done based on the original spring wheat parameterisation (chapter 2). Individual simulation runs consisted of a plot of 36 (six by six) virtual wheat plants; time step was one day. Simulations were done at 100, 262 and 508 plants m^{-2} corresponding to the population densities used in the current experiments. As yet, ADELwheat lacks provisions to simulate the degree of tillering and senescence of leaves and tillers based on local processes. Therefore, to enforce simulation of tiller senescence, the distributions of tiller numbers, appearance and senescence were used in the model, as obtained from the 2004 outdoor experiment. Leaf senescence was introduced based on senescence data from the growth chamber experiment. Change of GC over time is an output of the model which embodies the cumulative effects of various variables such as tiller appearance, leaf area development and leaf angle, Therefore, GC is a good measure of overall simulation performance. GC percentages were calculated from top-down perpendicular views of the virtual

plots, using the 'histogram' function of the GNU Image Manipulation Program (the GIMP) v2.0.5. GC simulations were done at thermal time intervals corresponding to those of the actual measurements. Each data point of simulated GC represents the mean result of three separate simulation runs. These runs differed in the seed of the random number generator and in the height above the virtual canopy. The first affects the stochastic components of the model (leaf curvature and tiller configuration through thermal time); the latter mimics the variation in the camera height in reality. gLAI simulations of virtual plants were done by adding the individual surfaces of all leaf blade polygons present at a certain time step. Simulated GC and gLAI were fitted to thermal time using Eq. 2. Note that GC and gLAI time courses were not derived from the same simulations: for GC, leaf and tiller senescence were enforced to correspond to measurements; for gLAI, leaf and tiller senescence were disabled, as was secondary tillering, to make simulation output correspond to gLAI calculated from measurements (estimates of contribution of secondary tillers to maximum gLAI are ca. 20% at D1 and 5% at D2; at D3, no secondary tillering occurred).

Subsequently, simulations of the time courses of GC and LAI at 262 plants m^{-2} were done using a version of the model, with parameter values based on data from the D2c plot: refitting was done for final leaf blade length and width, final sheath length, phyllochron, and tiller appearance delay. Note that only the values of the coefficients that define the various functions were refitted; the functions themselves were similar to the ones in the original spring wheat model (with the inclusion of the improvements as described in Appendix B).

Sensitivity analysis

To test whether the output of the model is sensitive to modulation of a variable, a sensitivity analysis was performed using temporal dynamics of GC as the test output variable. Input parameters examined included width and length of the leaf blade, phyllochron, and tiller appearance delay, i.e. all variables determining the dimensions of organs and the dynamics of leaf production. The degree of sensitivity to input modulation was expressed in two ways: (a) linear regression (if applicable) of the relative change in output on the relative change in input; this serves to check for systematics in the effect of variable modulation. The slope of the regression line is the elasticity, i.e. the relative change in model output per amount of change in the value of the input parameter. If the relative effect is larger than the relative change (i.e. if elasticity is high), a small change in the input variable has a disproportional effect which means that the calibration of the variable in question has to be very accurate; and (b) the range of non-significant

effect, i.e. the range of decrease/increase in a variable that does not have a significant effect on the output parameters; obviously, this range only applies in case of a clear relation between relative change and effect.

The sensitivity analysis was done using three simulation runs of 6 × 6 plants at 100 m^{-2} per variable modulation, differing in random seed and in image height (see above). Random seed values were never reused, i.e. all simulations were done using a different random seed resulting in differences in leaf geometry and in tiller configuration in the canopy. This was preferred over fixed random seeds (in which case run 1 would always have seed x, and run 2 always seed y, etc.), because in this way, observed effects could be attributed to the variable modulation even though there was a difference in random variation. Both approaches were tested, and it appeared that both resulted in the same conclusions on effects of variable modulation; therefore, only the first approach is used here. To analyse the effects of variable modulation, GC was fitted to thermal time using Eq. 2, where $y_{(m)}$ is (maximum) GC, k is the slope coefficient, and $x_{(m)}$ thermal time (at the inflection point) (ºCd).

Statistics

Goodness-of-fit of the parameterisation and discrepancies between measured data and model output were expressed in their respective root mean squared errors (RMSE), see Eq. 5; i = sample number, n = total number of measurements, $X_{sim,i}$ = simulated value, and $X_{obs,i}$ = observed value. Note that an RMSE value has the same unit as the values of data it pertains to.

$$RMSE = \sqrt{\frac{1}{n}\sum_{i=1}^{n}\left(X_{sim,i} - X_{obs,i}\right)^2}$$
(Eq. 5)

Effects of treatment on phyllochron, tiller appearance delay, and final leaf number were compared using an analysis of variance and LSD post-hoc test. Tests on equality of coefficient values between observed and simulated data were performed using a t-test, based on the fitted values, their standard errors and the degrees of freedom (Motulsky and Christopoulos, 2003). Nonlinear fits were done using the NLIN procedure of the SAS System v8.02 (SAS Institute Inc., 2001); pseudo-R^2 values (referred to as R^2) were obtained by calculating 1–(SS$_{residual}$/SS$_{corrected\_total}$). In the sensitivity analysis, the range of change of significant effect was determined using an analysis of variance, including a test for normality and for equality of variance, and Dunnett's posthoc test for significant differences between modulated output and the 'control' (no

modulation) output. Further data analysis was done using R v1.8.1, SPSS v11.0.1, and Microsoft Excel 2003.

Results

Effects of plant population density and shade treatment on plant attributes

Phyllochron values of main stem leaves are separated into two groups (see model improvements section, appendix B): leaves 1 to 4, and leaves 5 and higher (Fig. 2). Main stem leaves 1 to 4 have a relatively low phyllochron compared to the leaves with higher phytomer number. For all categories of shoots phyllochron of the 2004 D1c plants was lower than observed in 2003 D1c (but not significantly so) except for main stem leaves 1 to 4 (at $P < 0.05$). Within the control group (full natural light), phyllochron of main stem leaves did not significantly differ between population densities. Shade generally reduced the rate of leaf appearance,

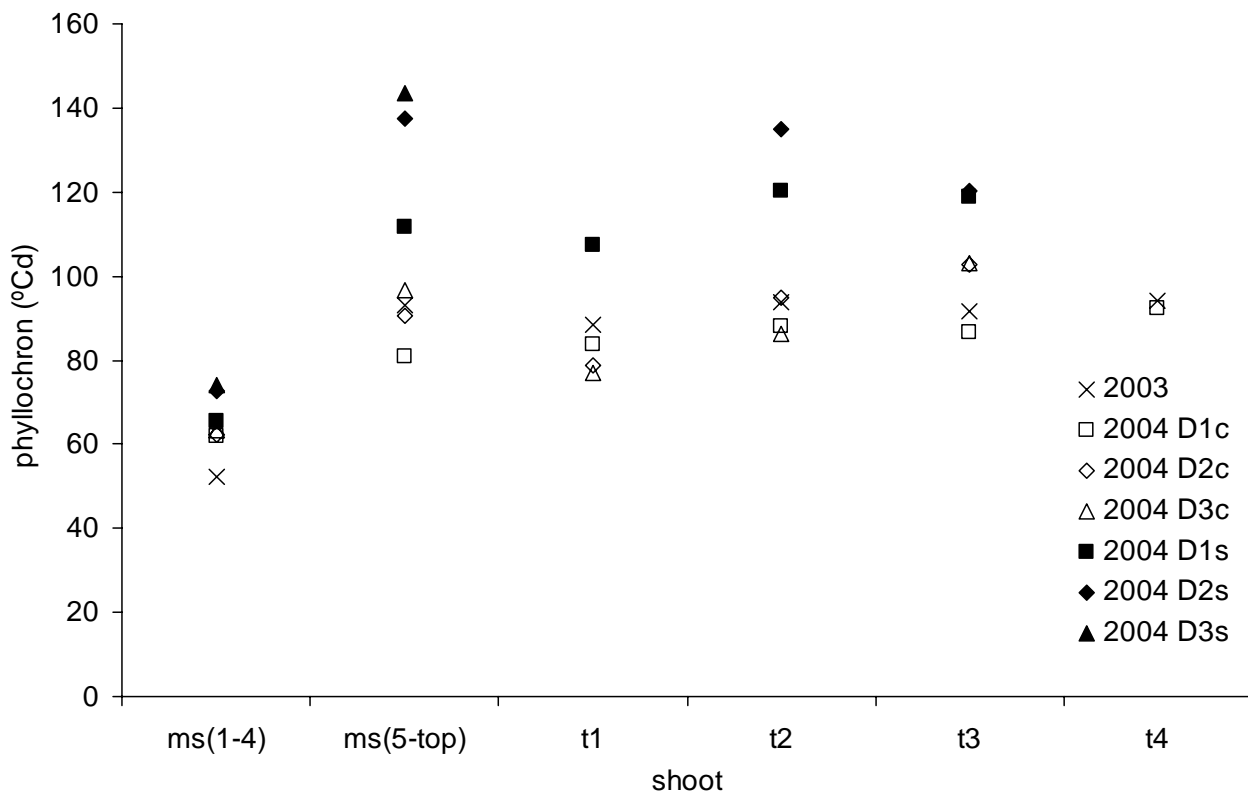Fig. 2: Phyllochron of main stem leaves 1 to 4, ms(1-4), main stem leaves 5 and higher, ms(5-top), and tiller leaves, t1 to t4, based on data from the parameterisation experiment (2003, cross) and validation experiment (2004, closed symbols indicate shade treatment, open symbols indicate control, for 100 (squares), 262 (diamonds) and 508 (triangles) plants m^{-2}). For clarity, SE values are not shown.
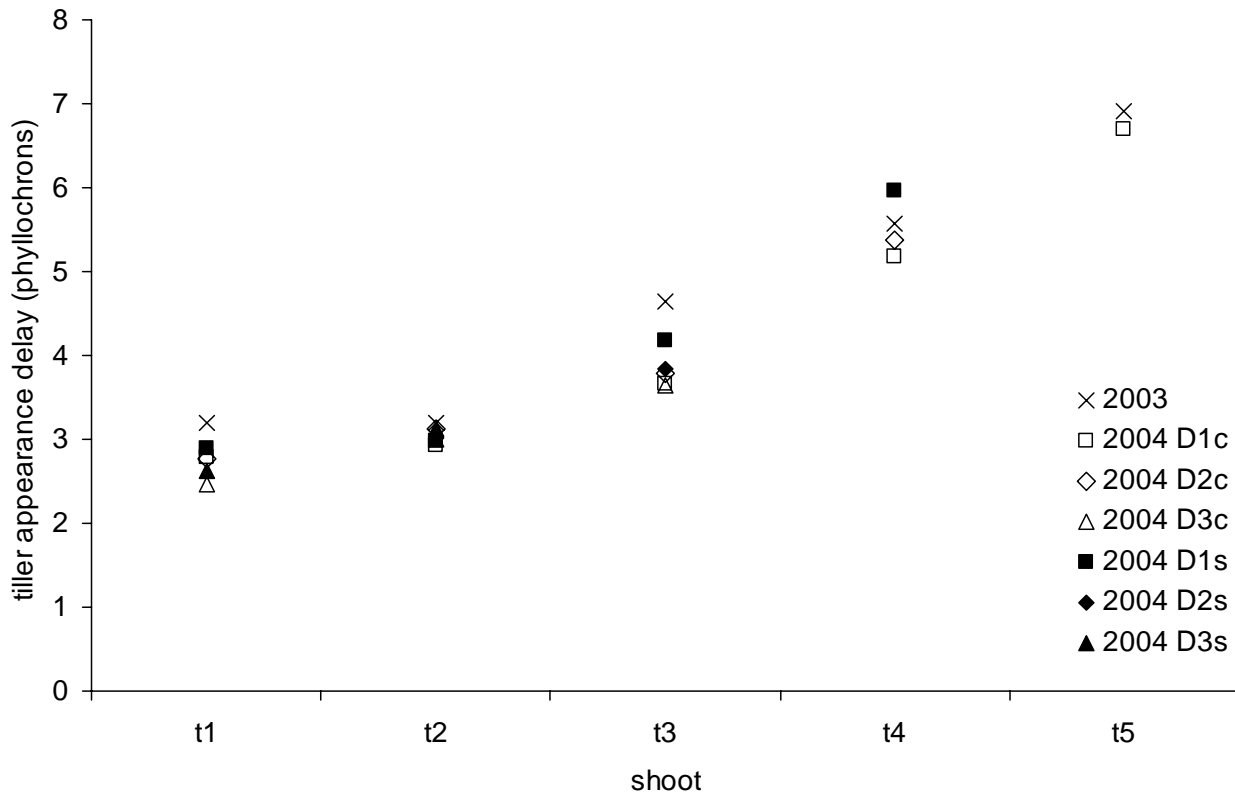
Fig. 3: Tiller appearance delay of tillers t1 to t5, based on data from the parameterisation experiment (2003, cross) and validation experiment (2004, closed symbols indicate shade treatment, open symbols indicate control, for 100 (squares), 262 (diamonds) and 508 (triangles) plants m^{-2}). For clarity, SE values are not shown.

resulting in a significantly higher phyllochron (P<0.001) in all shoot categories except for t1 (P = 0.07) (Fig. 2).

Tiller appearance delay (TAD) is defined as the difference between the appearance of the first leaf of a tiller and the appearance of the first leaf of its parent shoot, expressed in phyllochrons. TAD of the 2004 D1c plants showed the same relation to phytomer number as in 2003 (Fig. 3). Tillers t1 and t2 always had nearly identical TAD values (ca. 3 phyllochrons). Subsequent tillers had a TAD of approximately 1.25 phyllochron larger than the previous tiller. However, TAD of tillers in the 2004 D1c experiment was slightly lower than in 2003 for all tillers. Comparing the data with the parameterisation shows an RMSE of 0.81 and 0.31 phyllochrons for 2004 and 2003, respectively. Although the number of tillers that appeared differed greatly among treatments, TAD of those tillers that did appear, was not statistically different between population density treatments within tiller categories, except TAD for t3 and t4 in D1s (P<0.005).

Final leaf number on main stem and tillers were the same in 2004 D1c and 2003 (Fig. 4), as was its RMSE: 0.15 and 0.17 for 2004 D1c and 2003 D1c,
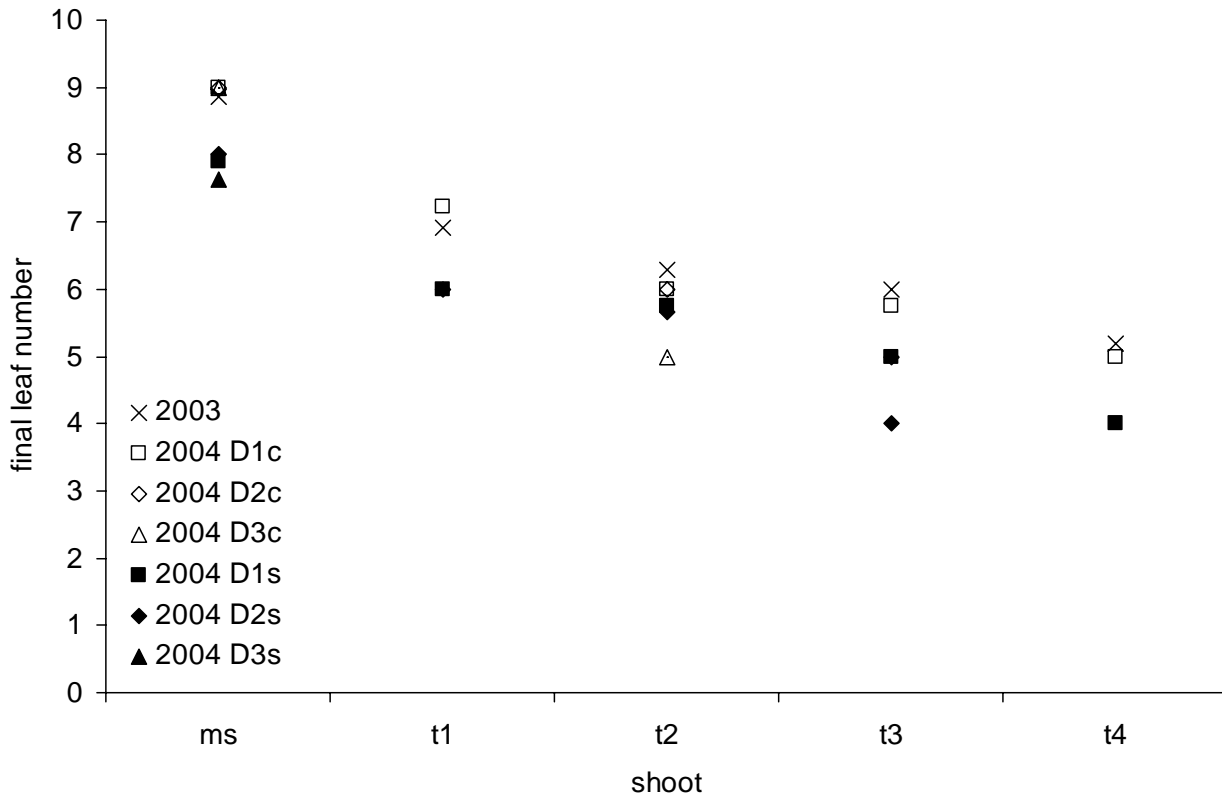
Fig. 4: Final leaf number of main stem and tillers t1 to t4, based on data from the parameterisation experiment (2003, cross) and validation experiment (2004, closed symbols indicate shade treatment, open symbols indicate control, for 100 (squares), 262 (diamonds) and 508 (triangles) plants m^{-2}). For clarity, SE values are not shown.

respectively. Final leaf number of main stem leaves was significantly (P<0.001) reduced by the shade treatment (Fig. 4) to 8 (full light 9) or 7 in 38% of the D3 plants; shade also significantly reduced final leaf number of tillers t1, t3 and t4 (P<0.001). Population density did not significantly alter final leaf number of the main stem. On tillers, increasing density significantly decreased final leaf number (P<0.05).

Final organ dimensions of plants from the 2004 D1c treatment and of the 2003 experiment were very similar. Final blade length showed a bell-shaped length distribution along the main stem, and final blade width showed a comparable sigmoidal shape (Fig. 5). These results confirm the parameterisation of the final dimensions for main stem organs as derived from the 2003 experiment. Also in all three population densities, final blade length data exhibited a similar bell-shaped distribution along the main stem, although the location of the peak appeared to be at lower phytomer ranks when population density increased (fractional rank number 7.2, 6.7 and 6.4 for D1c, D2c and D3c, respectively) (Fig. 5 and Table 1).

Table 1: Fitted coefficient values (±SE) of final blade length and width, using the Lorentz Peak Distribution (Eq. 1) and the logistic equation (Eq. 2) respectively, and their R^2 and RMSE values.

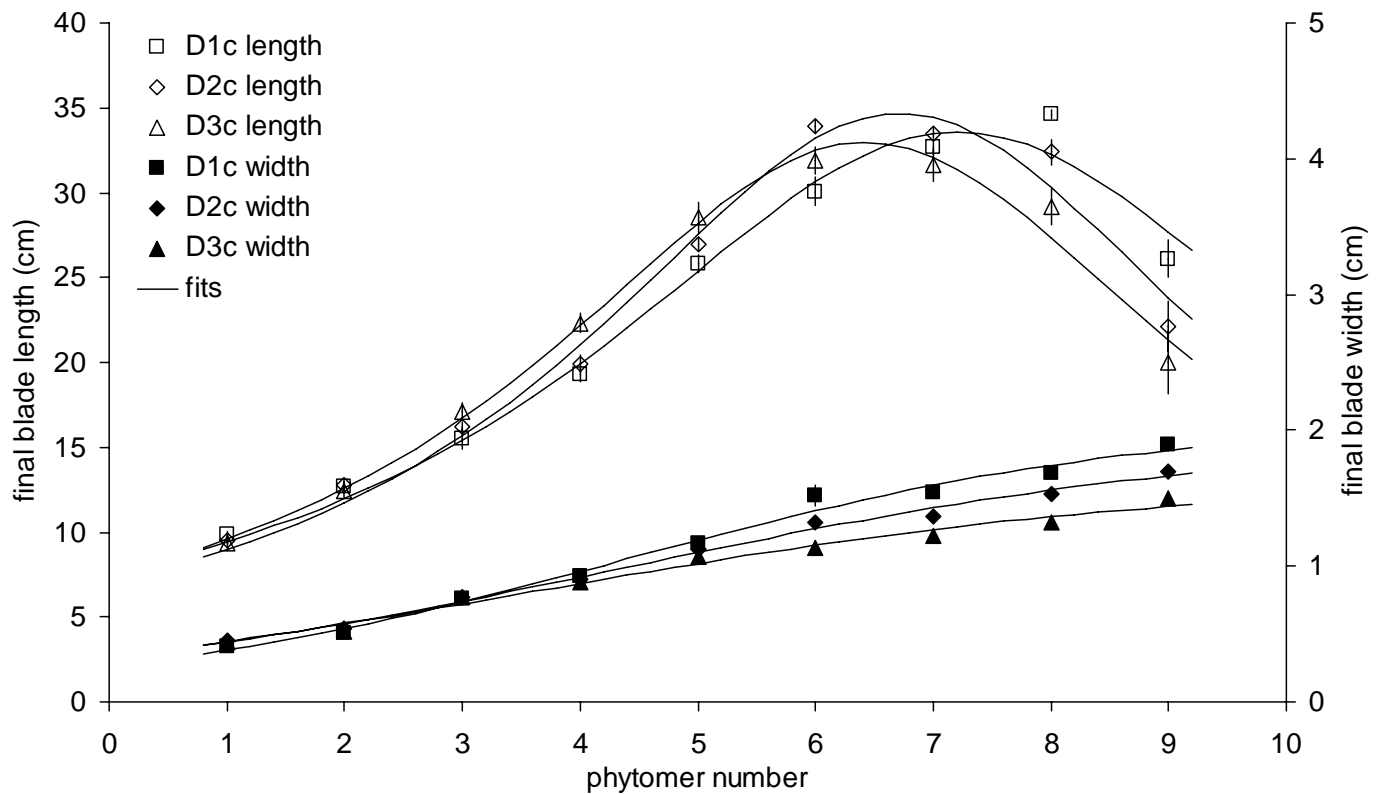| Leaf property	Population density	Coefficient fits			R^2	RMSE (cm)
		y_m (cm)	x_m	k		
final length	D1	33.6±0.82	7.2±0.13	3.8±0.23	0.983	1.07
	D2	34.7±0.93	6.7±0.10	3.4±0.19	0.982	1.15
	D3	33.0±0.64	6.4±0.07	3.5±0.14	0.990	0.80
final width	D1	2.1±0.14	4.4±0.40	0.44±0.05	0.990	0.052
	D2	1.9±0.13	4.3±0.44	0.37±0.04	0.993	0.035
	D3	1.6±0.14	3.6±0.55	0.37±0.06	0.983	0.044

Fig. 5: Final blade length (open symbols) and maximum width (closed symbols) for main stem leaves; lines show parameter fits of the Lorentz Peak Distribution function (lengths) and the classical logistic function (widths). Symbols indicate population density: 100 (squares), 262 (diamonds) and 508 (triangles) plants m^{-2}. Vertical lines show 2 × SE.
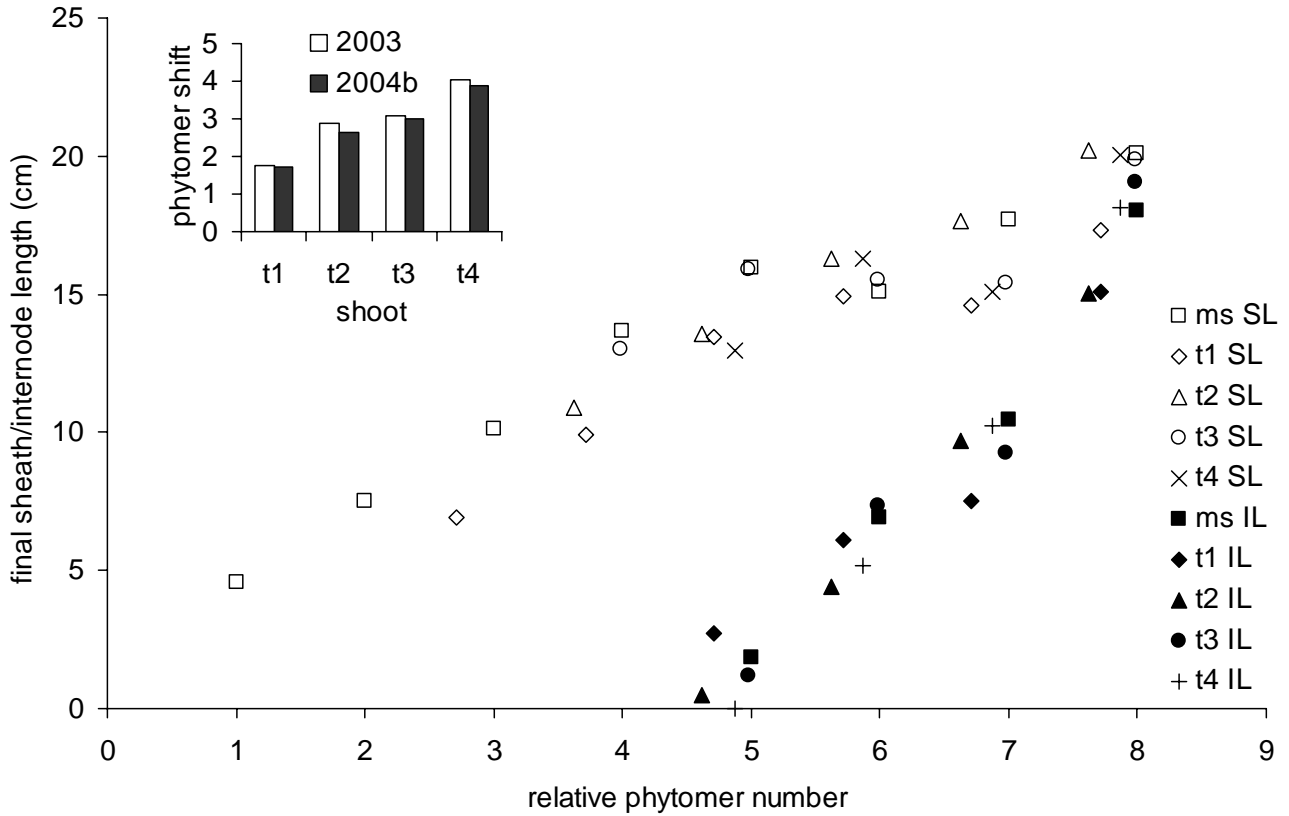
Fig. 6: Final sheath and internode length (SL and IL respectively) for main stem and tillers of plants grown in the growth chamber experiment vs. relative phytomer number (RPN). The inset shows phytomer shift values (dimensionless) for primary tillers 1 to 4, based on data from the parameterization experiment (2003) and the growth chamber experiment (2004b). Phytomer shift values provide the number of fractional phytomers that has to be added to the phytomer number on that tiller to obtain the relative phytomer number (Fournier et al., 2003).

Final maximum blade width for the top four leaves of the main stem decreased linearly with increase in population density (R^2 = 0.96) (Fig. 5 and Table 1). The increase in final blade width with phytomer number appeared to diverge between population densities at the transition of leaf 5 to leaf 6, creating the leaf width differences between population densities that can be observed for all later leaves.

The calculated phytomer shift values from the parameterisation (2003) and growth chamber (2004b) experiments were nearly identical (inset in Fig. 6). That these shift values were adequate is illustrated in Fig. 6 for sheath and internode length: when the rank number of a particular tiller phytomer was increased with the shift values (to yield RPN), data points from all shoot types formed one single relation with RPN.
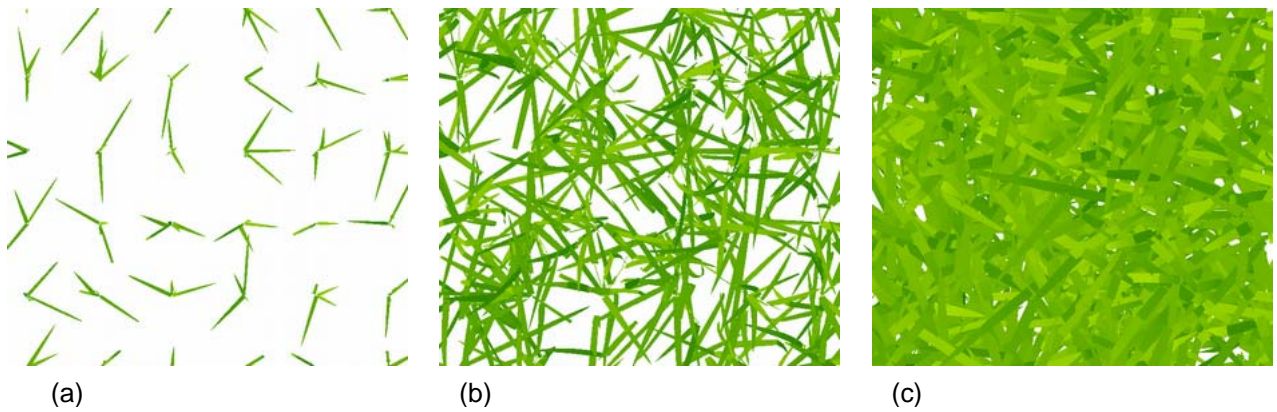
Fig. 7 a, b and c: Top-down view on simulated wheat plots at a population density of 100 plants m^{-2}, at (a) 183 ºCd, (b) 365 ºCd, (c) 620 ºCd.

Fig. 8: Temporal patterns of change in ground cover percentages in simulated (open symbols) and observed (closed symbols) plots, for 100 (squares), 262 (diamonds) and 508 (triangles) plants m^{-2}. The lines are fitted logistic curves (Eq. 2), see text and Table 1 for numerical values. Vertical lines show 2 $\times$ SE.

Model validation

Examples of pictorial top-down views on virtual wheat canopies are represented in Fig. 7. Fitted lines (Eq. 2) on temporal changes in observed and simulated GC percentages (Fig. 8) indicate that a higher population density resulted in full GC at lower thermal time. Though there were significant differences between simulation and observation in the coefficients k and x_m that describe the change in GC with thermal time, the general conclusion is that satisfactory agreement was achieved between simulated and observed GC for all population densities (Fig. 8, and Table 2: RMSE values < 4%).

Coefficients of Eq. 2, describing observed and simulated thermal time courses of gLAI, (Fig. 9) differed significantly between population density treatments (Table 2) within the simulation and the observation group (i.e. the inflection point coefficient x_m and maximum gLAI coefficient y_m; P<0.001 in all cases). Time courses of gLAI did not differ between simulations and observations during the early stages of development (D1 and D2: until ca. 350 °Cd, D3: 450 °Cd). At more advanced stages of canopy closure, gLAI was underestimated by
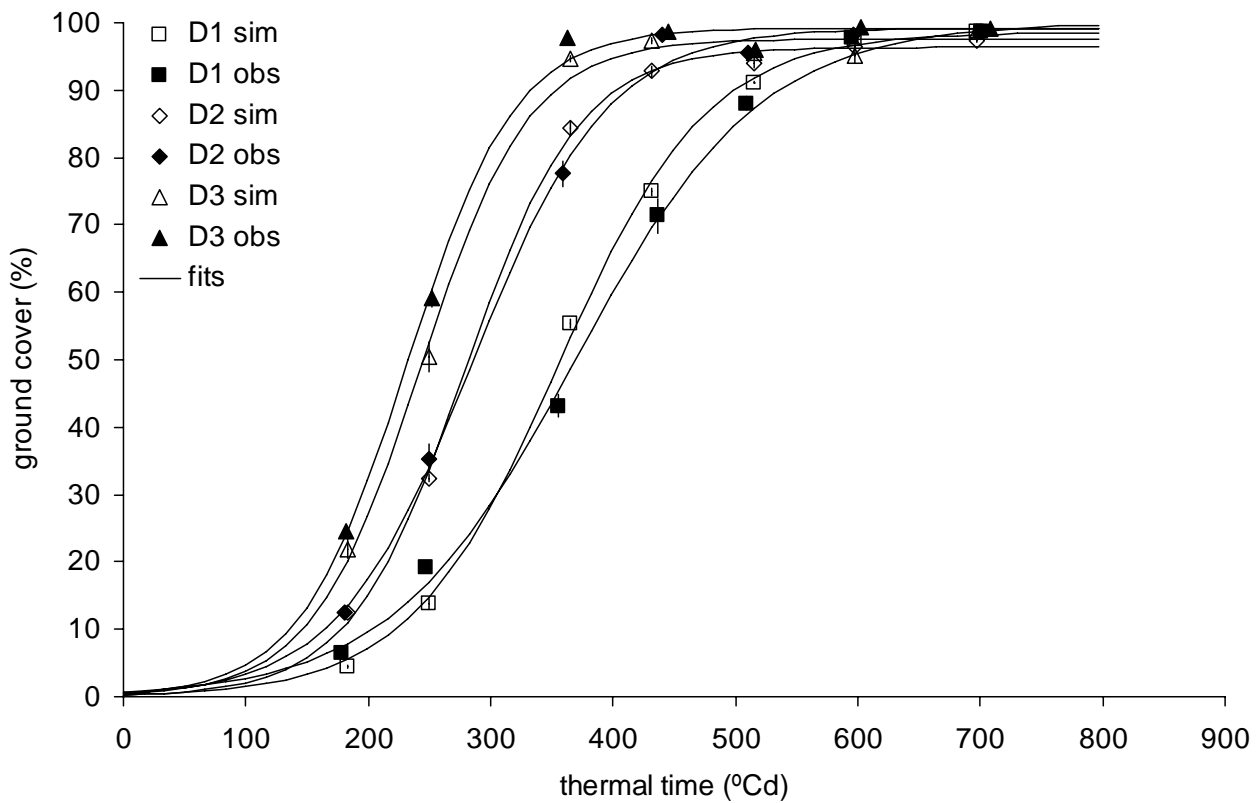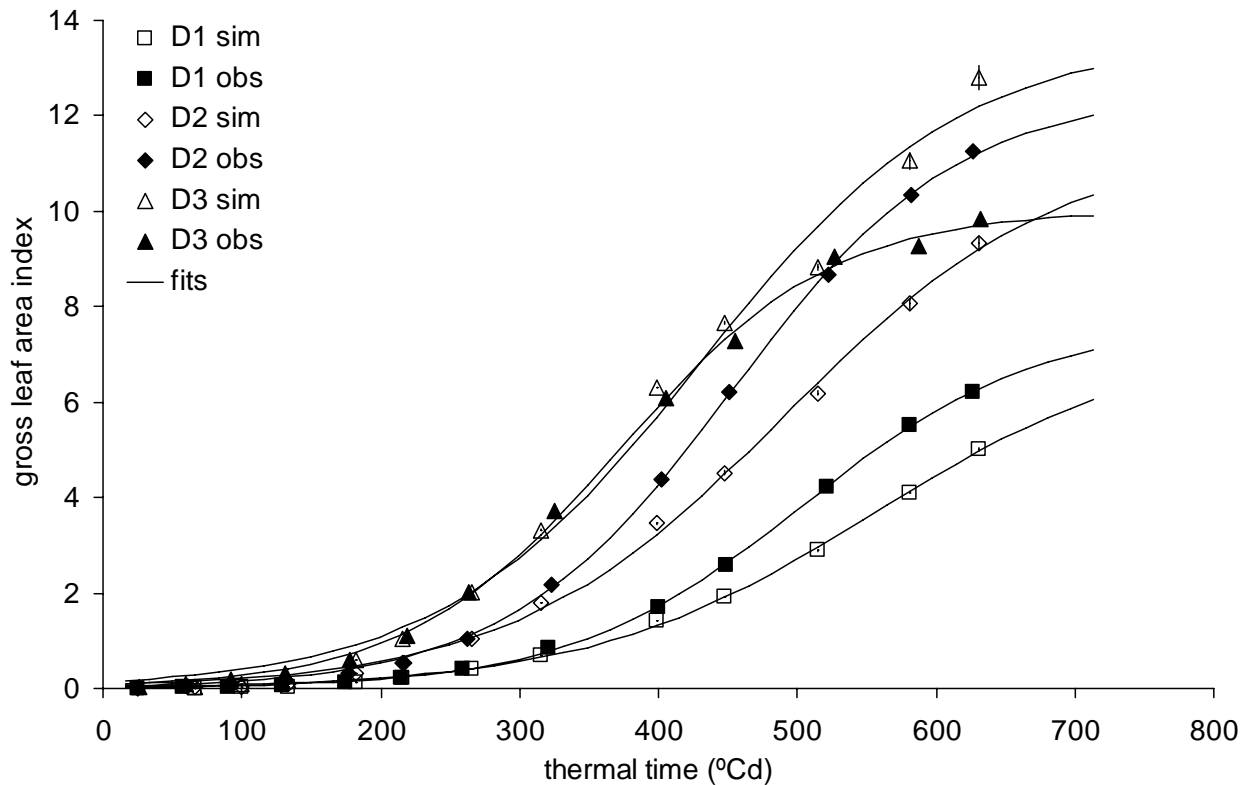

Fig. 9: Temporal patterns of change in gross leaf area index (gLAI) in simulated (open symbols) and observed (closed symbols) plots, for 100 (squares), 262 (diamonds) and 508 (triangles) plants m⁻². The lines are fitted logistic curves, see text and Table 1 for values. Vertical lines show 2 × SE.

*Table 2: Fitted coefficient values (±SE) of simulated (sim) and observed (obs) ground cover (GC) and gross leaf area index (gLAI) values, and their SE values, R^2 of the fits, and RMSE between observed and simulated values within density treatments. Indicators of significant differences between simulated and observed values of k and t_m within densities are * (P<0.01) and ** (P<0.001), denoted at the simulated value within a density. Note that due to the lack of replicates, these statistics were not computed for gLAI. Below 'reparameterisation' the coefficient fits are shown after reparameterisation of the model using experimental data from 2004 D2c on blade dimensions and leaf/tiller appearance.*

Test output variable	Density	Source	Coefficient fits			R^2	RMSE
			y_m	x_m (°Cd)	k		
GC	D1	sim	97.87±0.45	352.8±1.4	0.0171±0.0003	0.999	3.58
		obs	100±0[1]	369.0±2.8 }**	0.0132±0.0004 }**	0.997	
	D2	sim	97.46±0.42	279.8±1.5	0.0212±0.0005	0.999	1.80
		obs	99.22±0.86	284.9±3.1	0.0181±0.0008 }*	0.993	
	D3	sim	99.09±0.53	244.4±2.1 }**	0.0218±0.0011	0.995	2.73
		obs	99.18±0.53	231.8±1.7 }**	0.0227±0.0010	0.994	
gLAI	D1	sim	7.36±0.27	555.3±8.3	0.0097±0.0002	0.997	0.74
		obs	7.69±0.11	504.4±3.2	0.0119±0.0002	0.999	
	D2	sim	11.44±0.34	491.3±7.5	0.0101±0.0003	0.997	1.30
		obs	12.49±0.11	453.1±2.6	0.0123±0.0002	0.999	
	D3	sim	13.64±0.50	430.0±10.0	0.0119±0.0002	0.990	1.28
		obs	10.02±0.15	372.2±4.3	0.0131±0.0005	0.999	
Reparameterisation							
GC	D2	sim	98.62±0.47	261.2±1.6	0.0240±0.0009	0.998	2.20
gLAI	D2	sim	12.95±0.25	432.1±4.9	0.0118±0.0004	0.997	0.64

[1] *An SE of 0 is a result of the fact that the coefficient was constrained in the fitting process, as it was exceeding the imposed restriction (y_m < 100).*
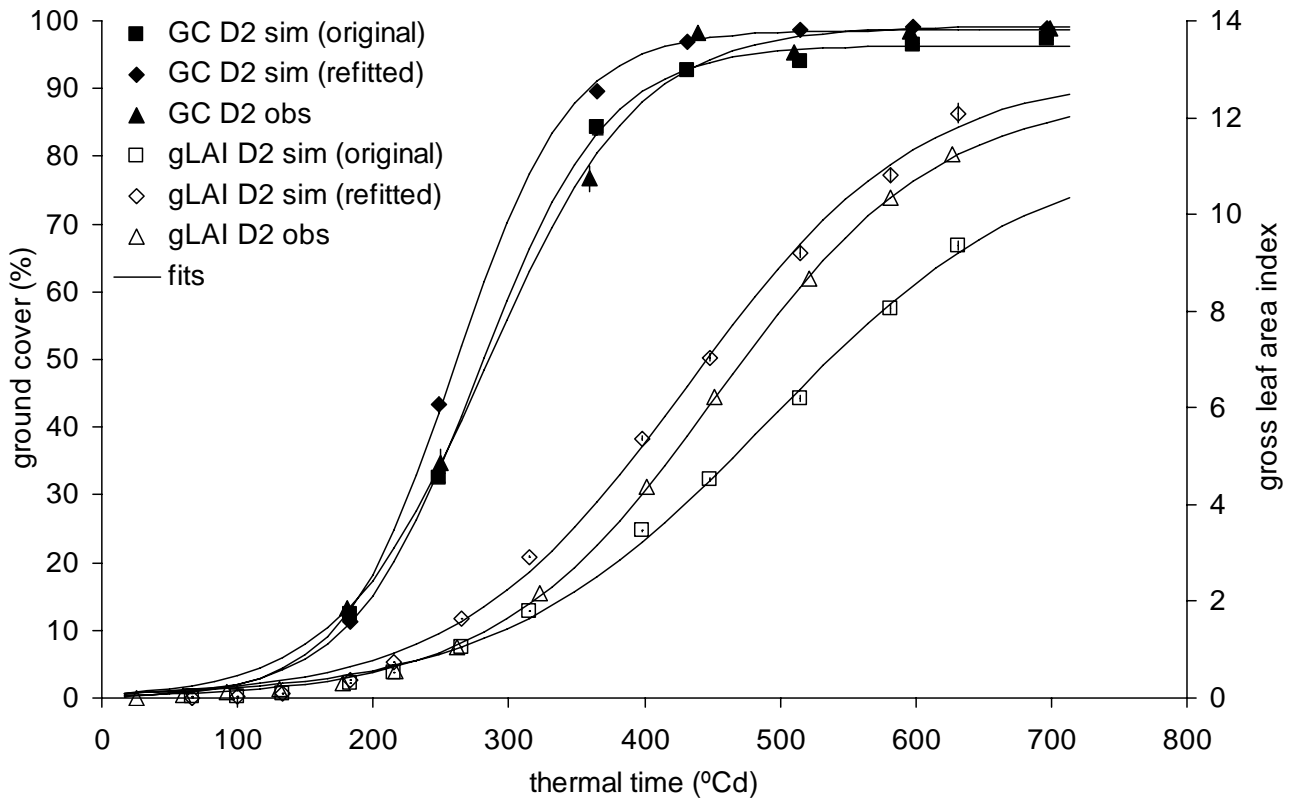
Fig. 10: Temporal patterns of change in ground cover percentages (closed symbols) and gross leaf area index (gLAI, open symbols) at 262 plants m^{-2}, for simulated plots based on the original parameterisation (squares, 'original'), based on D2c-specific parameterisation (diamonds, 'refitted') and for the observed plots (triangles). The lines are fitted logistic curves (Eq. 2), see text and Table 2 for numerical values. Vertical lines show $2 \times SE$.

the model in both D1 and D2, but overestimated in D3. The smallest RMSE value (0.74) was obtained at the lowest population density. Refitting the model parameters based on D2c data from the current experiment (i.e. accounting empirically for plant density effects on model parameters) improved the simulation of gLAI (Fig. 10 and Table 2). RMSE was reduced from 1.30 to 0.64, resulting in a simulated time course that overestimated the observed gLAI slightly, instead of underestimating it considerably. Simulation of GC was not improved when model parameters were adapted to accommodate measured population density effects; RMSE increased from 1.8% to 2.2%.

As an additional check on model performance the extinction coefficient *K* (Goudriaan, 1988) was calculated by fitting GC to gLAI using Eq. 4. For D2, *K* was 0.47 for the measured data, and 0.53 for the simulated data based on the original parameterisation. Reparameterisation of the model based on D2c data reduced *K* to 0.45. When GC is plotted on a logarithmic scale against gLAI (Fig. 11) the
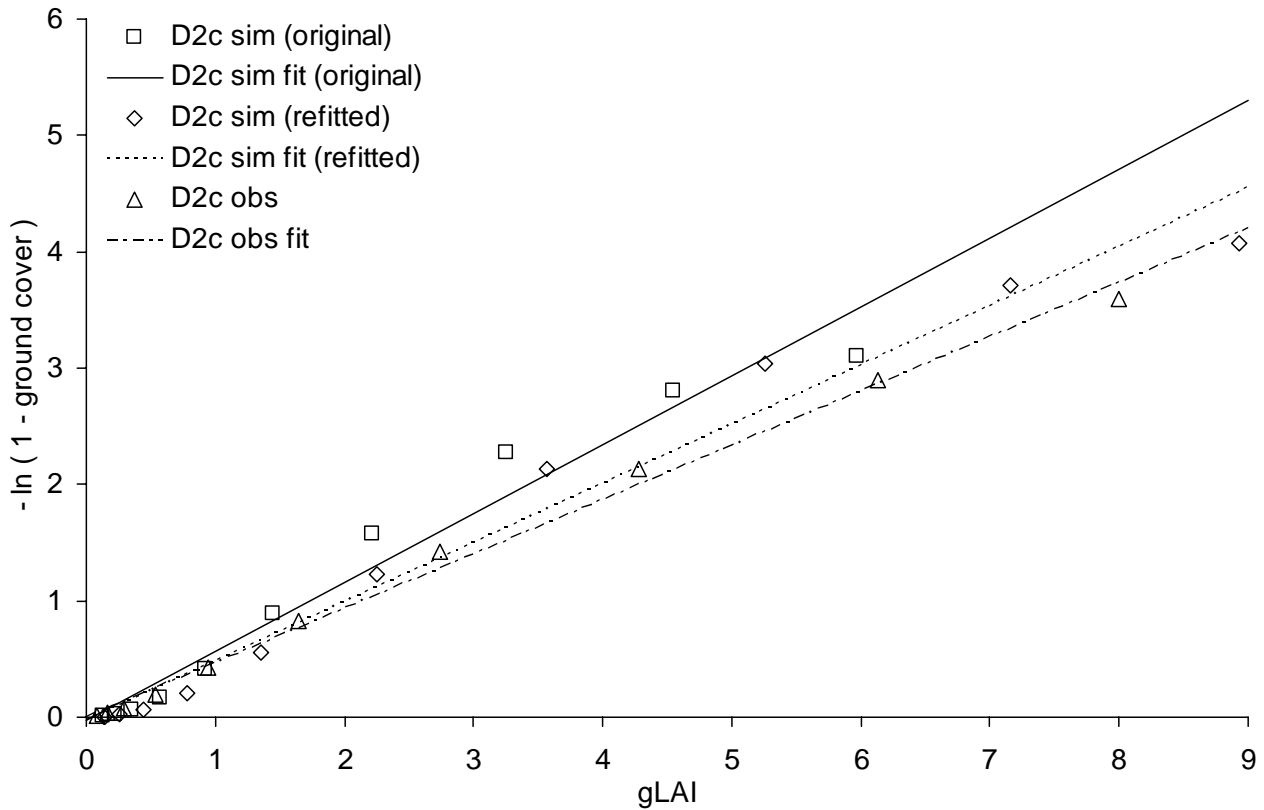
Fig. 11: (1 - Ground cover fraction) logarithmically plotted against gLAI for simulated plots based on the original parameterization (squares, 'original'), based on D2c-specific parameterization (diamonds, 'refitted') and for the observed plots (triangles); the slope of the regression lines represent extinction coefficient K.

slope of the regression line represents K. The simulated values based on the original parameterisation showed a slightly larger K until a gLAI of approximately 2.2, and a slightly lower K from 4.7 onwards, when compared to the regression line ($R^2 = 0.965$); this discrepancy was reduced by reparameterisation accounting for the population density effects ($R^2 = 0.976$). For observed data, data points did not show systematic change in deviation from linearity ($R^2 = 0.995$) (Fig. 11). For D3, K values were 0.41 for the simulation and 0.50 for the observations.

Sensitivity analysis

The standard parameterisation of leaf blade width calculation in the model was changed from -40 to +40 %. A decrease of at least 15% or an increase of at least 25% in blade width was needed to obtain a significant (P<0.05) effect on slope coefficient k of the GC thermal time course (Table 3). Over the whole range of changes in blade width, the effect (in %) of the change in blade width (in %) on k was linear (i.e. an increase in blade width results in a steeper GC thermal time

Table 3: Results sensitivity analysis. Description of the columns: 'Modulated input variable' shows which variable was changed; 'Affected parameter' shows the affected output coefficient (Eq. 2); 'Range of change for significant effect' shows the range of variable change within which the effect on the output coefficient is not significant (P<0.05), the values are exactly halfway between the last non-significant and the first significant percentage; elasticity' shows the value (±SE) of the elasticity in case of a significant linear relation (P<0.001 in all cases), i.e. the amount of effect (in %) when the variable is changed by 1 percent; when the absolute elasticity is larger than 1, the coefficient can be regarded as sensitive to the change (indicated in bold).

Modulated input variable	Affected parameter	Range of change for significant effect (%)		Elasticity
		lower limit	upper limit	
blade width	k	-15	+25	+0.27±0.017
	x_m	-2.5	+17.5	-0.22±0.015
blade width & length	k	-15	+15	+0.49±0.035
	x_m	-2.5	+7.5	-0.387±0.020
phyllochron	k	-7.5	+3.75	**-1.15**±0.193
	x_m	-1.25	+1.25	+0.84±0.037
tiller appearance delay	k	-7.5	+7.5	-0.89±0.075
	x_m	-2.5	+2.5	+0.59±0.013

course and v.v.), at a slope (elasticity) of 0.267% per %. In other words, for every percent of change in blade width, k changes 0.267%. The range of significance for t_m was -2.5 to 17.5%, indicating that a small decrease in blade width exerts a significant effect on t_m. The relation between change and effect was linear as well; the slope being -0.215, i.e. for broader leaves the inflection point of GC versus thermal time (as in Fig. 8) is shifted to the left and for narrower leaves to the right. Similar effects on the GC coefficients were found, when proportional changes in both blade width and length were enforced. However, the range within which the effect was not significant was smaller (-15 to 15% for k and -2.5 to 7.5% for t_m respectively) and the slope of the linear relation between change and effect was steeper for both coefficients.

Relative change in phyllochron was linearly related to its effect on both GC coefficients (Table 3). The effect of change in phyllochron was larger than the effects of blade width, indicated by rather high elasticity values (-1.15 and 0.841 for k and t_m respectively) and narrow significance ranges. Especially t_m was affected significantly at low percentages of change (less than -1.25% or more than 1.25%). k appeared sensitive to changes in phyllochron (elasticity larger than 1). Changes in tiller appearance delay and effect on GC were linearly related

for both coefficients, i.e. an increase in the delay of tiller appearance resulted in a decrease in canopy closure rate.

Discussion

Effects of population density and shade treatment on plant attributes

The observation that population density does not significantly affect phyllochron agrees with findings by Bos (1999) for the same spring wheat cultivar, and by Casal *et al.* (1990) for *Lolium multiflorum*, corroborating the view that main stem phyllochron responds conservatively to a variety of environmental factors (Hay, 1999) other than temperature (Jamieson *et al.*, 1995). Crop emergence is an event at which population density effects can be regarded negligible since no competition for light or nutrients is taking place yet at that point. The only environmental variable which is affected by population density at this early stage in development is the ratio between red and far red light, which has been shown to act as an 'early warning signal' for future competition (Ballaré *et al.*, 1987). Changes in red/far-red ratio have been shown to influence many aspects of crop development such as shoot length, tiller number and leaf angle (Casal *et al.*, 1985; Kasperbauer and Karlen, 1986; Smith and Whitelam, 1997). However, wheat phyllochron remains unaffected by artificially altered red/far-red ratios (Casal, 1988), at least for main stem leaves, which is in accordance with the current data. From Fig. 2, it appears that phyllochron was increased when light intensity was low, which has been found earlier for this spring wheat cultivar (Bos and Neuteboom, 1998a), for maize (Birch *et al.*, 1998; Bos *et al.*, 2000), but also for a dicotyledon like pigweed (Rajcan *et al.*, 2002). The current observations suggest that a more general modelling of leaf appearance can be obtained by incorporating a function that calculates phyllochron based on temperature and daily intercepted PAR (Volk and Bugbee, 1991).

Tiller appearance delay was conservative across population densities. However, replacing the current parameterisation of TAD with a more general one, in which t1 (the coleoptile tiller) and t2 have a TAD value of 3 phyllochrons, and every subsequent tiller 1 phyllochron extra (i.e. a 'tillochron' of 1) (see Hay and Kirby, 1991; Hay, 1999, and references therein), results in RMSE values of TAD of 0.37 and 0.57 phyllochrons when comparing to data from 2004 and 2003, respectively. This suggests a more general parameterisation of TAD is appropriate in a generic architectural model of wheat. Variation in TAD between population densities was small (Fig. 3); considering the small differences in phyllochron (Fig.

2), this is not surprising since TAD is expressed in phyllochrons, and leaf and tiller appearance are strongly coordinated (Kirby *et al.*, 1985). However, compared to full light, in D1s the shade treatment had a significant reducing effect on TAD for tillers 3 and 4, suggesting that coordination of leaf and tiller appearance is not intimate and can be changed under the influence of light.

Final leaf number on a shoot is affected by photoperiod and temperature in spring wheat (Rawson and Zajac, 1993; Brooking *et al.*, 1995), both of which did not differ between treatments. Nevertheless, a significant effect of shading on final leaf number was observed (Fig. 4). A possible explanation is a direct effect on the fate of 'labile' primordia that are initiated as vegetative primordia, but become committed to differentiate into a spikelet (Brooking and Jamieson, 2002) under low light.

Current findings (Fig. 5 and Table 1) confirm the conclusion in chapter 2, that blade length distribution along a shoot of a Gramineae species can be parameterised using the Lorentz Peak Distribution function (Buck-Sorlin, 2002). This proposition was based on data from literature on several species of Gramineae (Fournier and Andrieu, 1998; Kaitaniemi *et al.*, 1999; Tivet *et al.*, 2001; Buck-Sorlin, 2002; Cattani *et al.*, 2002; Lafarge *et al.*, 2002). Recently published data on rice (Jaffuel and Dauzat, 2005; Watanabe *et al.*, 2005) support this view. The exact shape of the 'bell' in terms of location of the peak, its amplitude and its width, depends on environmental conditions, in our case population density, and on plant species. For our spring wheat cultivar, it is justified to conclude that main stem and tiller blade length can be modelled using the Lorentz Peak Distribution function as well, the latter using a certain phytomer shift value. From Fig. 6, it can be concluded that these phytomer shift values for tillers are robust and independent of the growing conditions (outdoors or indoors).

The observation that the top four leaves of a shoot show a decrease in blade width with increasing population density corroborates findings by Bos (1999). Interestingly, top four phytomers are also the ones having an elongated internode; from this, one could speculate that internode elongation and leaf growth compete for limiting resources, resulting in reduced dimensions. Alternatively, processes related to floral transition might be the cause of the simultaneous internode extension and changes in blade width responses to the environment.

Model validation and sensitivity

The current study showed that key parameters of the model showed conservative values in the different experiments. Hence, there was good agreement between model simulation and data obtained from an independent experiment, considering individual parameters and cumulative effects as manifest in GC and LAI. Both simulated and observed temporal patterns of increase in GC differed between population density treatments (Fig. 8). The number of tillers per plant was up to 12 tillers in D1 compared to 8 in D2 and 7 in D3. Apparently more tillers per individual wheat plant at the lowest density did not compensate for the lower plant number as regards GC. gLAI simulation was improved when the model parameters had been refitted using data from the D2c plots (Fig. 10), resulting in a slight overestimation in both cases. A probable cause is deviation from reality in the degree of tillering that is enforced in the model. Improvement can be expected here when tillering kinetics of the canopy is the result of intercepted radiation, which will be the focus of subsequent study.

Correct simulation of leaf and tiller numbers does not necessarily mean perfect simulation of the orientation of the leaves in the canopy space. Plants are inclined to fill open spaces with leaves (Maddonni *et al.*, 2002; Andrieu *et al.*, 2004) or tillers (Matthew *et al.*, 1998). However, at present the model does not provide means for the virtual plant to react to its immediate environment in terms of leaf reorientation or tillering. This leads to the observation that gaps in the young canopy, emerging from the random variation in tiller configuration, are not preferred over more crowded parts of the canopy by the developing plants. Future implementation of photomorphogenetic responses and photosynthesis at the leaf level will provide an improvement in the simulation of the spatial aspects of ground cover.

In spite of the abovementioned limitations of the model, it can be concluded that the architectural model simulates canopy closure and leaf area development of spring wheat well; a view which is confirmed by the equivalent values for calculated and simulated light extinction coefficients K (Fig. 11).

The sensitivity analysis has shown that: (a) Phyllochron appears to be very influential on the time course of GC. This is not surprising because phyllochron, being a prime determinant of developmental rate, is included in many sections of the model code. Therefore, phyllochron is a variable that requires accurate calibration, even more so when taking into account the observed differences in phyllochron between population density and light treatments. (b) The ranges out of which variable modulation has a significant effect are generally quite narrow (a larger number of simulations is likely to decrease the width of the significance

ranges even further), indicating that although the effect of a modulation might not yield a sensitive response, a small change can result in a significant effect.

Conclusions

The ADELwheat model for spring wheat cultivars adequately simulated the architecture of a spring wheat canopy. The previously established parameterisation (chapter 2) of various parts of the model proved adequate for the simulation of canopy development for different population densities and light conditions; though still better simulation of gLAI was obtained when key parameters of the model were empirically refitted, based on data from the corresponding treatment. The current model is suited for use in applications, requiring a 3D representation of a wheat canopy, e.g. studies on herbivore-plant interactions (Skirvin, 2004) and remote sensing studies (Lewis *et al.*, 2004). Future introduction of mechanisms to simulate the effect of environment on the architecture of the crop is expected to eliminate the need for refitting coefficient values. To this end, the model will be extended with the calculation of intercepted PAR (photosynthetically active radiation), assimilate production and distribution based on source-sink principles (see e.g. Fournier and Andrieu, 1998; de Visser *et al.*, 2004; Allen *et al.*, 2005) and photomorphogenetic responses to spectral distribution of the light in the canopy (e.g. Gautier *et al.*, 2000). These mechanisms drive organ growth and development, and thereby determine canopy architecture. A first step in this direction will be the implementation of tillering responses to the local light environment. Tillering has a crucial effect on blade area development in wheat (Bos, 1999) and is therefore an important factor in the array of plastic responses of wheat to its environment.

Appendix A: derivation of blade shape function

Eq. 3 describes the normalised margin-midrib distance of a wheat leaf blade as a function of the normalised length (distance to the tip) (Fig. 1). Two coefficients are used: L_m and C, which indicate the location of the top of the curve and the curvature coefficient, respectively. Derivation of the function starts with the polynomial part, i.e. without coefficient C. In general, a parabola $f(x)$ which is zero in points a and b has the following form (coefficient p will be derived later):

$$f(x) = p(x-a)(x-b)$$

A leaf blade has a width of zero at the tip (for $x = 0$), therefore either a or b is zero, forcing the function to go through (0,0). The location of the top of the parabola (here L_m), is located halfway between a and b, a relation which can be used to express b:

$$L_m = \tfrac{1}{2}(a+b) \qquad a=0 \rightarrow \qquad b=2L_m$$

Therefore:

$$f(x) = px(x-2L_m)$$

At L_m, the normalised distance of the blade margin to the midrib is 1. This relation can be used to express p:

$$f(L_m) = 1 \qquad \rightarrow \qquad p \cdot L_m(L_m - 2L_m) = 1 \qquad \rightarrow \qquad p = \frac{-1}{L_m{}^2}$$

This results in:

$$f(x) = \frac{-x(x-2L_m)}{L_m{}^2}$$

Adding coefficient C, which improves flexibility in curvature, and substituting $f(x)$ and x by their respective variables, leads to Eq. 3.

Appendix B: model improvements

Since the model parameterisation (chapter 2) was published two changes have been made after re-analysis of the same dataset. As correct simulation of leaf blade length is needed for the intended model application we propose a slightly modified parameterisation here (Fig. 12): for main stem phytomers 1 to 5, a linear model is used to model final blade length (coefficients: slope a = 4.19 cm phytomer^{-1} (SE = 0.11), y-intercept b = 4.41 cm (SE = 0.35); R^2 > 0.99), for all other leaves the original nonlinear parameterisation function (Eq. 1) is maintained, refitted for the dataset without data for main stem leaves 1 to 5 (y_m = 31.97 cm (SE = 0.62), k = 3.32 (SE = 0.19) and x_m = 7.49 (SE = 0.09); R^2 = 0.92). This resulted in a reduction in RMSE from 2.30 cm to 1.69 cm.

A second improvement in the parameterisation which primarily affects early main stem leaves is the value of the phyllochron. In chapter 2, two distinct phyllochron values were used: one for main stem, and one for tillers (Kirby *et al.*, 1985; Bos and Neuteboom, 1998a). However, it appeared that the difference in phyllochron of the main stem compared to the tillers was primarily caused by the
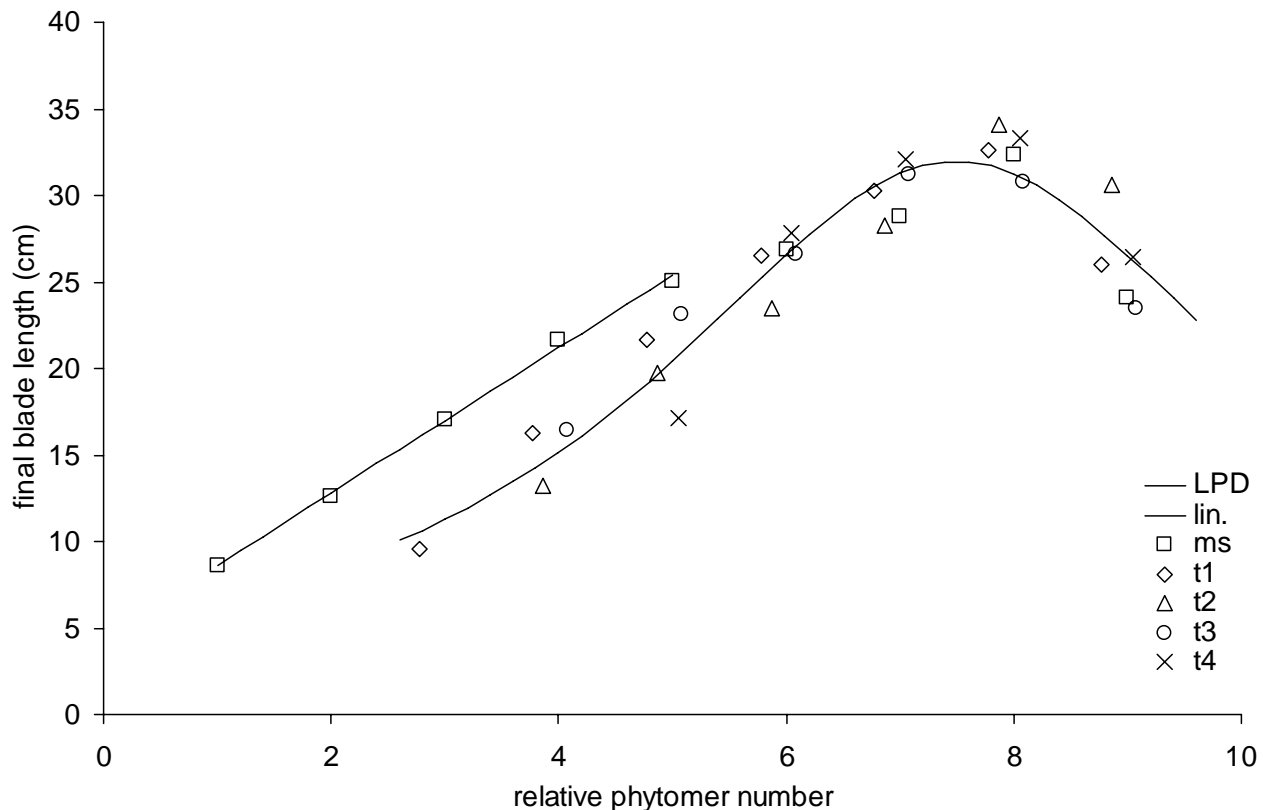
Fig. 12. Final blade length versus relative phytomer number of the main stem (ms) and primary tillers t1 to t4. The line indicates linear fit (lin.), the curve indicates Lorentz Peak Distribution function fit (LPD).

high rate of appearance of the early main stem leaves. When disregarding the first four leaves of the main stem, phyllochron of higher phytomers compared well to that of the tiller; a similar distinction between early and late leaves was made by Jamieson *et al.* (1995) for wheat and by Abeledo *et al.* (2004) for barley. Therefore, phyllochron parameterisation was adapted to 52.172 ºCd (SE = 1.24, n = 56) for main stem leaves 1 to 4, and to 91.98 ºCd (SE = 2.42, n = 546) for all other main stem and tiller leaves. Apart from a better simulation of early main stem leaf appearance, we believe that this is an improvement for main stem leaf appearance in general as the simulation of the appearance of the later appearing leaves is also more accurate.

Chapter 4

Cessation of tillering in spring wheat in relation to light interception and red/far-red ratio

Jochem Evers

Jan Vos

Bruno Andrieu

Paul Struik

Abstract

The production of axillary shoots (tillering) in spring wheat (*Triticum aestivum*) depends on intraspecific competition. The mechanisms that underlie this competition are complex, but light within the wheat canopy plays a key role. The main objectives of this chapter are to analyse the effects of plant population density and shade on tillering dynamics of spring wheat, to assess the canopy conditions quantitatively at the time of tillering cessation, and to analyse the relationship between the tiller bud and the leaf on the same phytomer.

Spring wheat plants were grown at three plant population densities and under two light regimes (25% and 100% light). Tiller appearance, fraction of the light intercepted, and red/far-red ratio at soil level were recorded. On six sampling dates the growth status of axillary buds was analysed.

Tillering ceased earlier at high population densities and ceased earlier in the shade than in full sunlight. At cessation of tillering, both the fraction of light intercepted and the red/far-red ratio at soil level were similar in all treatments. Leaves on the same phytomer of buds that grew out showed more leaf mass per unit area, than those on the same phytomer of buds that remained dormant.

Tillering ceases at specific light conditions within the wheat canopy, independent of population density, and to a lesser extent independent of light intensity. It is suggested that cessation of tillering is induced when the fraction of PAR intercepted by the canopy exceeds a specific threshold (0.40 - 0.45) and red/far-red ratio drops below 0.35 - 0.40.

Keywords: *Triticum aestivum*, wheat, tiller, bud, plant density, shade, PAR, red/far-red ratio, functional-structural model

Introduction

Like most gramineous species, wheat (*Triticum aestivum*) produces tillers, which develop from axillary buds on the parent shoot, located at the bottom of the internode of the parent phytomer, just above the node and the sheath insertion point of the preceding phytomer. Theoretically, the parent shoot can be any existing shoot on the plant. Tillers that grow from the main stem are called primary tillers and those from primary tillers are secondary tillers, etc. (see Kirby and Appleyard, 1981). In practice, however, only a few tiller buds grow into a tiller, and only a proportion of these tillers survive to become ear-bearing shoots. The ultimate number of tillers is therefore a result of tiller appearance and tiller survival. The main factors that affect the appearance and survival of tillers in Gramineae are nitrogen (N) availability (see for example Davies, 1971) and plant population density (Darwinkel, 1978). Population density affects tillering cessation primarily via two mechanisms. By the first, tillering appears to cease earlier in the development of the plant the higher the population density, due to the severely reduced PAR (Photosynthetically Active Radiation) intensity at the lower levels inside the canopy, especially near complete canopy closure (Simon and Lemaire, 1987). In this context, a relationship has been assumed between outgrowth of tiller buds, PAR intensity, and LMA (leaf mass per unit leaf area) of the associated 'parent' leaves (i.e. the leaf on the same phytomer as the bud) (Bos, 1999). By the second mechanism, increase in population density is associated with a lower red/far-red ratio (R:FR) at the base of the individual plants because there is more surrounding vegetation that can scatter red and far-red light differentially (Holmes and Smith, 1977). A low R:FR ratio reduces the phytochrome photoequilibrium (Pr:Pfr) (Smith, 2000), and has been related to reduced tillering (Casal *et al.*, 1986; Barnes and Bugbee, 1991). Decline in R:FR has been shown to herald mutual shading, acting as an early warning signal for future competition (Ballaré *et al.*, 1987; Franklin and Whitelam, 2005).

Wheat plants, as for gramineous species in general, do show variable degrees of tillering. There are two patterns of cessation of tillering. In the first, all tiller outgrowth is arrested, usually at the time of formation of the terminal spikelet on the parent shoot apex (Baker and Gallagher, 1983; Gomez-Macpherson *et al.*, 1998), which coincides with stem elongation (Hay, 1999). The plants switch to the reproductive phase and axillary buds differentiate into floral structures. In the second pattern, only vegetative tiller buds are initiated, the plant has not become reproductive, but buds stop producing tillers. The current

study deals with this second type of cessation of tillering during the vegetative phase.

The objectives of the current work are (a) to study the kinetics of tiller appearance and the probability of tiller occurrence in spring wheat at three population densities and two light intensities; (b) to analyse cessation of tiller appearance in relation to the light conditions inside the canopy (in terms of PAR intercepted and R:FR when tillering ceases); and (c) to establish a possible link between the time of cessation of tillering and the LMA of the parent leaves.

Materials and methods

Experimental setup
Data used in this chapter is taken from the same experiment as was used for chapter 3; therefore, the experimental setup is not repeated here.

Data collection and analysis
Temperature was recorded every hour with shielded TempControl thermocouples (type T, TempControl Industrial Electronic Products, Voorburg, NL) and a Datataker DT600 datalogger (Datataker Data Loggers, Cambridgeshire, UK). Thermocouples were placed in the soil (6 cm deep; 'soil temperature') and in the canopy (20 cm above soil level; 'canopy temperature'). Thermal time was calculated from temperature data using a resolution of one hour. For the first two weeks, soil temperature was used, since the apex was still below soil surface; canopy temperature was used thereafter. The start of thermal time accumulation was set at the appearance of the first leaf and the base temperature used was 0 ºC.

Tiller appearance from the surrounding sheath tissues, leaf appearance, and length of the appeared part of each leaf of ten plants per treatment (n = 60) were monitored every three or four days; this was done for main stem and all primary tillers (denoted according to the main stem phytomer number from which the tiller originated: t1 (the coleoptile tiller), t2, t3, etc.). A leaf was considered to have appeared halfway between the last observation when it was absent and the first observation when the tip was visible. A tiller was considered to be senescing, when the youngest leaf stopped extending (Kirby and Riggs, 1978); this could be clearly discerned in the current experiment. The starting date of senescence was defined as halfway between the last observation when a tiller was not observed to be senescing and the first observation when it was judged to

be senescing. To determine additional information on tillering kinetics, tiller appearance and senescence were recorded on tillers of all orders for ten extra plants per treatment, bringing the total number of plants for which records were taken to 120.

To express the mean developmental stage of the plants in a specific treatment, thermal time was converted into elapsed phyllochrons by fitting a second order polynomial to the relationship between number of appeared leaves and thermal time. This was done to obtain an index of developmental stage (physiological age) that was not biased by the effect of treatment on phyllochron. Phyllochron is the most important determinant of rate of tillering due to the co-ordination of leaf and tiller appearance (Kirby *et al.*, 1985), and physiological age, expressed in phyllochrons, is a measure of plant development, comparable to Haun stage (Haun, 1973). However, Haun stage increases by one unit at leaf ligule appearance, whereas physiological age increases by one unit at appearance of the tip of a new leaf. Physiological age at maximum tiller number was studied in more detail by calculating it for individual plants for which exact leaf appearance kinetics were known (n = 60), and calculating means for each treatment. Similarly, tiller appearance was expressed using individual plant-based physiological age.

Bud growth of plants grown in natural light was assessed by harvesting three plants per population density on six sampling dates (at ligule appearance of leaves three to eight on the main stem respectively; n = 54). For each individual plant, the status of each main stem tiller bud that had not yet appeared was classed as either dormant or growing. A bud was considered to be dormant when the length of the prophyll was less than 7 mm. This threshold value was derived from the data in this investigation, as larger prophylls were nearly all longer than 1 cm. This threshold value did not differentiate between dormant buds and growing buds that were still less than 7 mm in length of the prophyll, but the probability that the latter is the case is very small since buds grew rapidly after escaping from their cavity in the internode (Williams and Langer, 1975). Dimensions and dry weights of leaves on the parent phytomers of the examined buds were determined. Leaf mass per unit leaf area (LMA, in mg cm^{-2}) was calculated by dividing blade dry weight by blade area; the latter was obtained by calculating length × width × *S*. The value of the shape coefficient *S* was 0.81, obtained by integration of the blade shape function as presented in chapter 3, appendix A.

To examine the possible relationship between LMA of the leaf, and the bud on the same phytomer as the leaf, the bud development dataset was split into

two groups, one group containing data from phytomers with buds that grew out ('outgrowth' group) and one group with buds that were dormant ('dormant' group).

Light penetration at ca. 2 cm above soil level was measured once every week around noon, at six randomly chosen locations in the microcanopy of each of the population density × light intensity combinations, using the SunScan Canopy Analysis System (Delta T Devices, Cambridge, UK). This device measures PAR along a light sensitive bar. A separate reference sensor, which measured PAR input, was placed just above the canopy. The fraction of incoming PAR intercepted by the canopy, P_{int}, was fitted to thermal time using the beta growth function (Yin *et al.*, 2003), which allows for asymmetry in the curve around the inflection point and does not have the x-axis for asymptote but originates from (0,0) (Eq. 1):

$$P_{int} = P_{int,m} \left(1 + \frac{t_e - t}{t_e - t_m} \right) \left(\frac{t}{t_e} \right)^{\frac{t_e}{t_e - t_m}}$$
(Eq. 1)

where P_{int} is the fraction of PAR intercepted, $P_{int,m}$ is the maximum fraction of PAR intercepted (which was restricted to ≤1 in the fitting process), t_e is the amount of elapsed thermal time at $P_{int,m}$, t_m is the amount of thermal time (ºCd) at the inflection point where the slope has its maximum value, and t is thermal time (ºCd) since the appearance of the first leaf.

Weekly measurements of red/far-red ratio (R:FR) at ca. 2 cm above soil level were made using the Skye SKR100/116 Fibre Optic Probe Measuring System (Skye Instruments Ltd., Powys, UK). Measurements were made parallel to the soil surface, with the sensor facing north. The device was equipped with a glass fibre probe that measured R:FR at its tip, with an angle of view of 40º relative to the soil surface. In each microcanopy, six measurements were made at random locations. R:FR was fitted to thermal time using a two-parameter exponential decline function, see Eq. 2:

$$R = a \cdot exp(-b \cdot t)$$
(Eq. 2)

where R is red/far-red ratio, a and b are coefficients, and t is thermal time (ºCd). Equations 1 and 2 were used to convert thermal time to the fraction of PAR intercepted and R:FR respectively, in order to express canopy development and
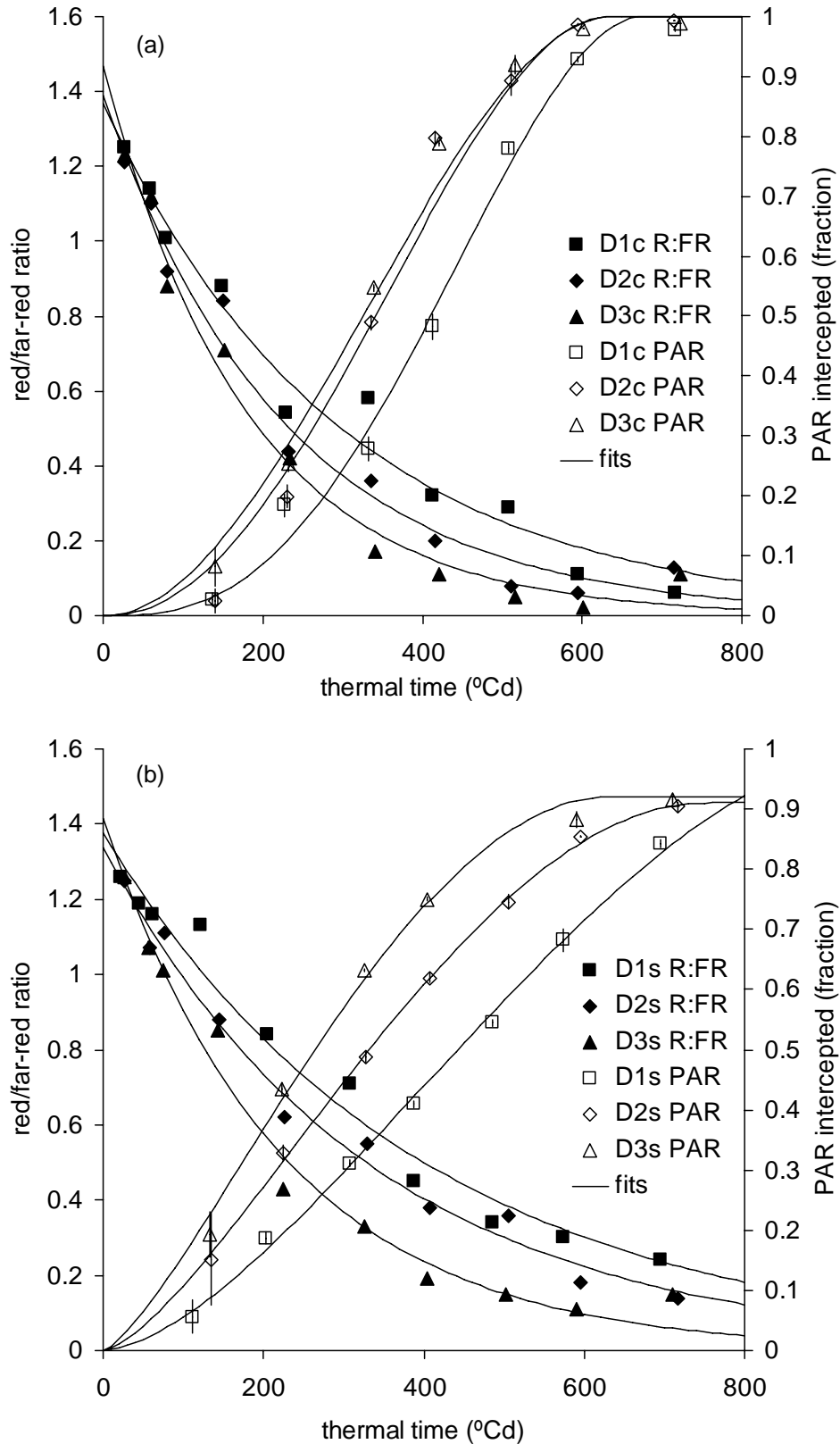
Fig. 1a, b: Time courses of the fraction of PAR intercepted (open symbols) and red/far-red ratio (closed symbols) in full light (a) and shade (b), at 100 (squares), 262 (diamonds) and 508 (triangles) plants m^{-2}. Bars indicate 2 × SE.
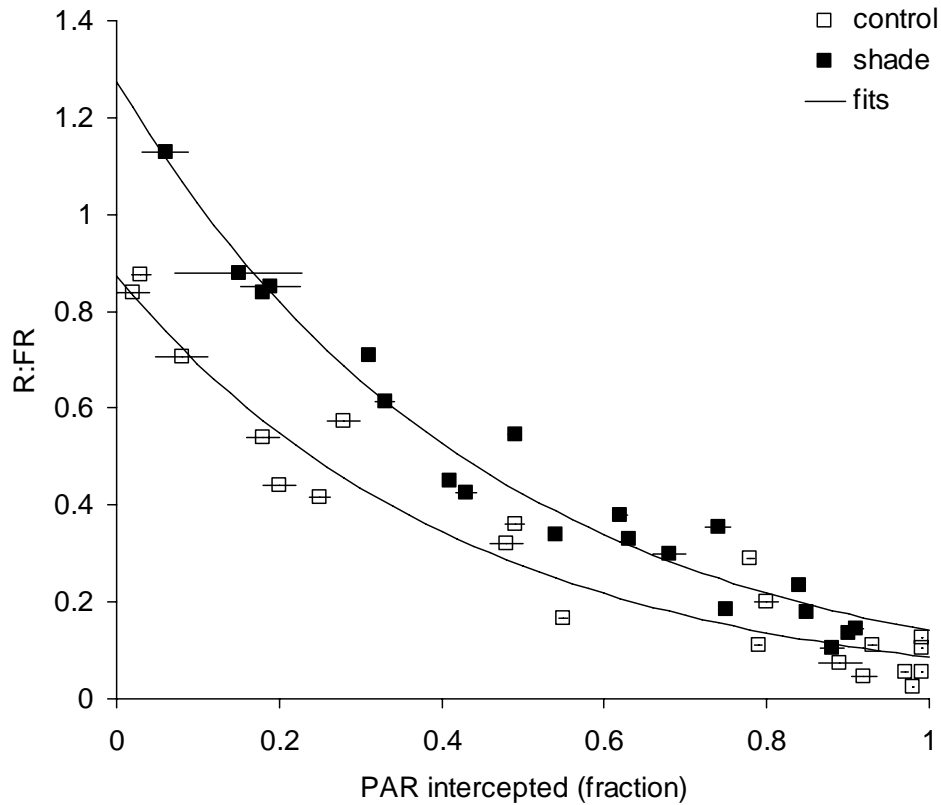
Fig. 1c: Time course of R:FR vs. PAR intercepted (c) for the full light (open symbols) and shade (closed symbols) treatments. Bars indicate 2 × SE.

tillering kinetics as functions of these two measures of plant development. To fit the R:FR data to fraction PAR intercepted, a similar two-parameter exponential decline function was used, see Eq. 3:

$$R = c \cdot exp(-d \cdot P_{int}) \hspace{4cm} \text{(Eq. 3)}$$

where *R* is red/far-red ratio, *c* and *d* are coefficients, and P_{int} is the fraction of PAR intercepted.

Statistics

The difference between population densities on PAR intercepted and R:FR was tested using a t-test on the fitted coefficients. Statistical analyses of physiological age, PAR and R:FR at the time of maximum tiller number included analysis of variance and LSD post-hoc tests. Nonlinear fits were done using the NLIN procedure of The SAS System v8.02; further data analysis was done using SPSS v11.0.1 and Microsoft Excel 2003.

Table 1. The values of the fitted coefficients of Eqs. 1, 2 and 3. The coefficients of Eq. 1 were fitted to data on the fraction of PAR intercepted (P_{int}) versus thermal time. The coefficients of Eq. 2 were fitted to R:FR (R) data versus thermal time. The coefficients of Eq. 3 were fitted to R:FR (R) data versus fraction PAR intercepted. Eq. 1 and Eq. 2 were fitted for plots at three population densities (D1, D2 and D3, i.e. 100, 262 and 508 plants m^{-2}) and two light regimes (c = control, s = shade). Eq. 3 was fitted for the two light regimes only (population densities combined). In parentheses: SE.

		D1c	D2c	D3c
P_{int} vs t	$P_{int,m}$	1 (0[1])	1 (0[1])	1 (0[1])
(Eq. 1)	t_m	445 (5.9)	355 (10.2)	328 (9.9)
	t_e	676 (11.8)	633 (12.0)	639 (11.4)
R vs t	a	1.37 (0.06)	1.39 (0.06)	1.47 (0.06)
(Eq. 2)	$b \cdot 10^{-4}$	33.8 (2.9)	43.8 (3.8)	55.4 (4.4)
		control		
R vs P_{int}	c	0.87 (0.04)		
(Eq. 3)	d	2.32 (0.19)		

		D1s	D2s	D3s
P_{int} vs t	$P_{int,m}$	1 (0[1])	0.91 (0.04)	0.92 (0.02)
(Eq. 1)	t_m	394 (13.8)	238 (36.1)	171 (24.4)
	t_e	997 (25.3)	752 (83.0)	634 (24.7)
R vs t	a	1.38 (0.04)	1.34 (0.04)	1.42 (0.06)
(Eq. 2)	$b \cdot 10^{-4}$	25.3 (1.8)	29.9 (1.7)	44.8 (3.4)
		shade		
R vs P_{int}	c	1.27 (0.05)		
(Eq. 3)	d	2.20 (0.12)		

[1] An SE of 0 is a result of the fact that the coefficient was constrained in the fitting process, as it was exceeding the imposed restriction ($P_{int,m} \leq 1$).

Results

Fraction of PAR intercepted and red/far-red ratio

The increase in P_{int} with thermal time was very similar in D2c and D3c, because unconstrained coefficients t_m and $t_{e,}$ describing the temporal change, did not differ significantly (Table 1, Fig. 1a, b). This means that the thermal time of steepest increase and maximum PAR intercepted were reached simultaneously. The course of PAR intercepted by D1c over thermal time was shifted to the right compared with those of D2c and D3c, as values of both coefficients for D1c were significantly higher (P<0.001 for t_m and P<0.05 for t_e) than those for D2c and D3c. For the shaded plants, the two coefficients describing the course of P_{int} over thermal time did not differ significantly between the treatments D2s and D3s, but

Fig. 2: Relationships between mean number of (non-senescing) tillers and physiological age of the main stem, calculated using leaf appearance data for each population density × light intensity combination, in full light (open symbols) and shade (closed symbols), at 100 (squares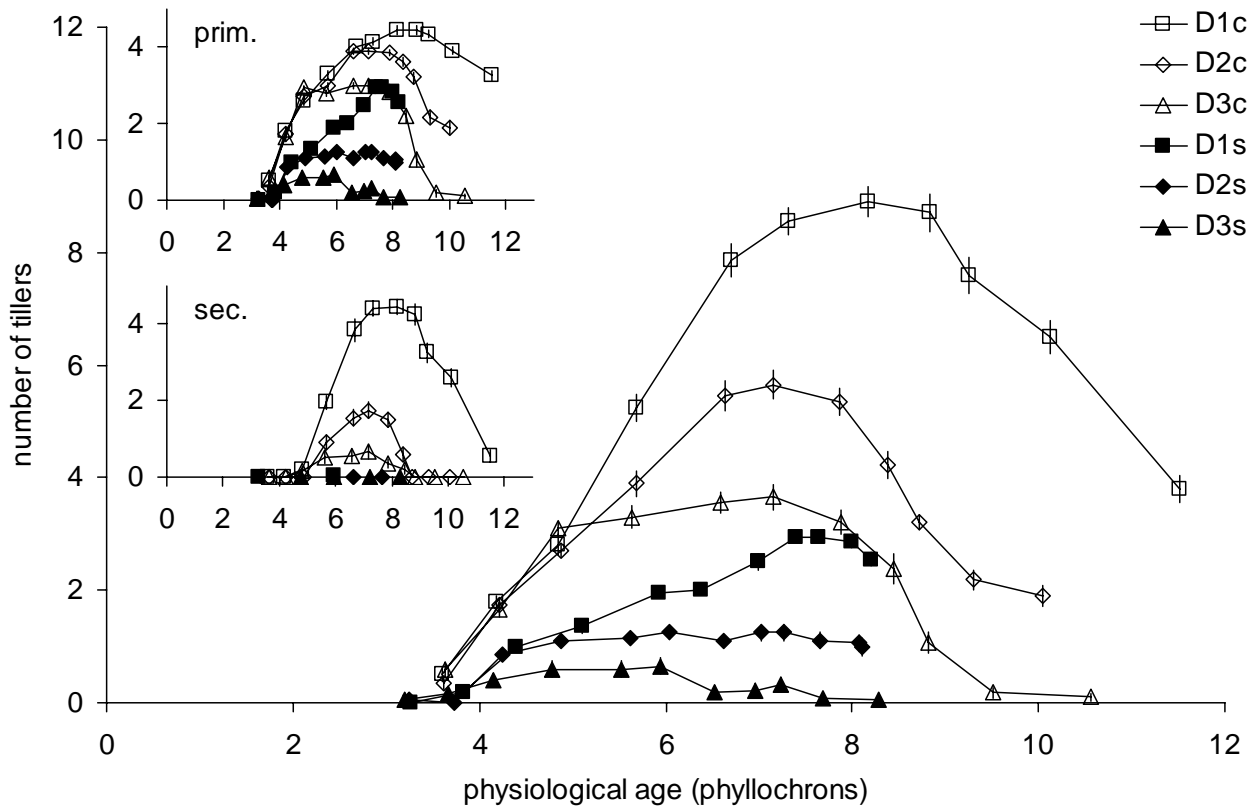), 262 (diamonds) and 508 (triangles) plants m⁻². The insets show the same data split into two groups containing primary (above) and secondary (below) tiller data. Vertical bars indicate 2 × SE, n = 120.

coefficients of D1s differed from those of D2s and D3s (P<0.05) (Table 1, Fig. 1b). The red/far-red ratio (R:FR) at the soil surface declined as the canopy expanded (Table 1, Fig. 1a, b). Both in control and shaded canopies, R:FR declined faster with thermal time when the population density was higher. However, significantly smaller values for *b* (Eq. 2) were found only for D1c compared with D3c, and for both D1s and D2s compared with D3s (Table 1). For the relationship between R:FR and P_{int} (Fig. 1c, Table 1), population densities were combined since the separate fits were not significantly different. The difference between fitted lines for the shade and non-shaded treatment was significant for coefficient *c* (P<0.001).

Dynamics of tiller numbers

Tillering started at a physiological age of ca. three phyllochrons (Fig. 2), i.e. around appearance of the third leaf of the main stem. The shaded plants did not
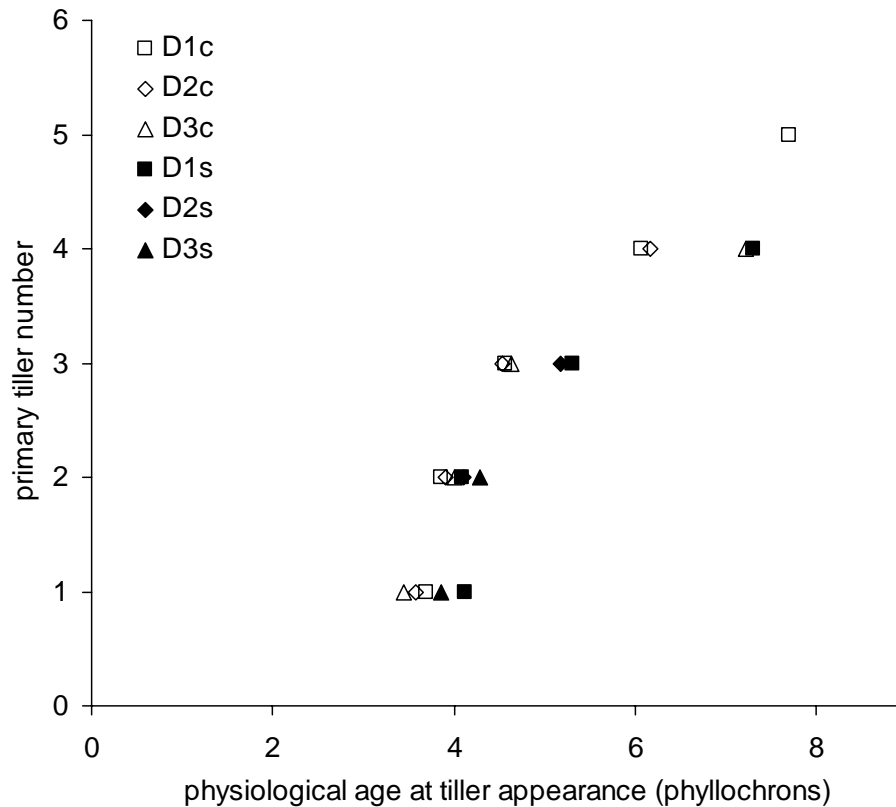
Fig. 3: Relationships between the appearance of primary tillers and the physiological age of the main stem, in full light (open symbols) and shade (closed symbols), at 100 (squares), 262 (diamonds) and 508 (triangles) plants m^{-2}, n = 60.

produce any secondary tillers (inset in Fig. 2). In the control plants, grown in full sunlight, progress in tillering was similar for all population densities up to a physiological age of approximately 4.8 phyllochrons, at which time the plants had approximately three appeared tillers. After this point tiller production diverged, as fewer additional tillers appeared at higher population densities.. The maximum number of appeared tillers was lower at higher population densities, with more tillers being produced by plants in full light than by shaded plants (8.9, 5.7 and 3.7 tillers for D1c, D2c and D3c, and 3.0, 1.3 and 0.7 tillers for D1s, D2s and D3s, respectively). After reaching a peak, tiller number declined by senescence to 3.8, 1.9 and 0.1 tillers per plant for D1c, D2c and D3c, and to 2.6, 1.0 and 0.1 tillers for D1s, D2s and D3s, respectively. The final number of tillers did not decrease any further beyond the data points shown in Fig. 2. In none of the treatments did tiller senescence occur before the last tiller appeared (data not shown), i.e. there was no overlap between tiller appearance and senescence.

Within the non-shaded and within the shaded plants, population density did not affect the physiological age at which primary tillers appeared (Fig. 3); in D3c, appearance of t4 occurred in only one out of ten plants, and therefore the
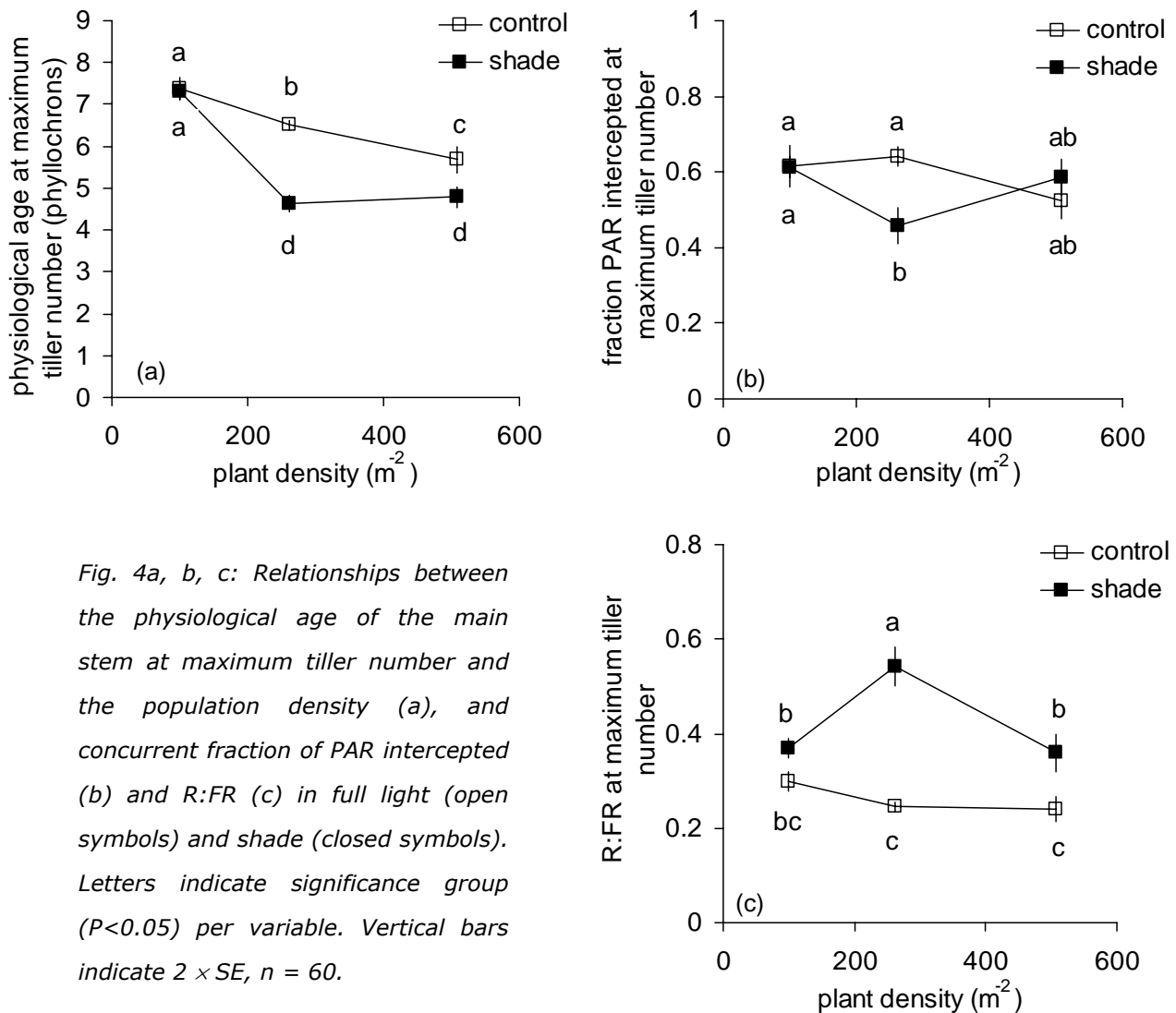
Fig. 4a, b, c: Relationships between the physiological age of the main stem at maximum tiller number and the population density (a), and concurrent fraction of PAR intercepted (b) and R:FR (c) in full light (open symbols) and shade (closed symbols). Letters indicate significance group (P<0.05) per variable. Vertical bars indicate 2 × SE, n = 60.

data point for this tiller does not count as evidence. In the shaded plants, appearance of a tiller type occurred consistently at a slightly higher physiological age than in control plants under full sunlight. The maximum delay in tiller appearance caused by shade was approximately 1 phyllochron for any population density, as observed for t3 in the D1s treatment.

Cessation of visible tiller appearance

For D1, control and shaded plants reached maximum tiller number at the same physiological age (ca. 7.4 phyllochrons, when calculated on an individual plant basis; Fig. 4a). For D2 and D3, physiological age at maximum tiller number was significantly lower for the shaded plants (P<0.05) than for the plants in full light, whose physiological age at maximum tiller number was significantly lower (P<0.05) at higher population densities. In the shaded plants, D2 and D3 had a significantly lower physiological age at maximum tiller number than D1 (P<0.05), but the values for D2s and D3s did not significantly differ from each other.

Table 2: Probability of occurrence of primary tillers t1 to t5 for plants at three population densities (D1, D2 and D3, i.e. 100, 262 and 508 plants m^{-2}) and two light regimes (c = control, s = shade).

tiller	D1c	D2c	D3c	D1s	D2s	D3s
t1	1.0	1.0	1.0	0.2	0	0.3
t2	1.0	1.0	1.0	1.0	1.0	0.5
t3	1.0	1.0	1.0	1.0	0.2	0
t4	1.0	0.9	0.1	0.9	0	0
t5	0.3	0	0	0	0	0

P_{int} and R:FR (both calculated from the fitted functions, Table 1, Fig. 1) at maximum tiller number were stable across population densities within the control and shaded treatments (Fig. 4b, c), with the control treatments intercepting 0.53 to 0.62 PAR and having R:FR ratios of 0.24 to 0.30 at maximum tiller number. In the shaded plants, treatments D1s and D3s had similar values for P_{int} (0.61 and 0.59, respectively) and for R:FR (0.37 and 0.36 in D1s and D3s, respectively), values that were similar to those of all control plants. However, the D2s treatment intercepted less PAR and had a higher R:FR ratio (P<0.05) at maximum tiller number than the D1s and D3s treatments.

Occurrence of different tiller types and arrest of outgrowth of tiller buds

In full sunlight, the probability of occurrence of tillers t1, t2 and t3 was not affected by population density (Table 2), with a probability of 1 in all cases. The probability of occurrence of t4 was 0.8 in D2c and 0.1 in D3c. Tiller t5 appeared only at the lowest population density (probability 0.1). In the shaded plants, increasing population density reduced the probability of occurrence of most tillers, the extent of which depended on tiller position. For D1s only t2 and t3 were present on all plants and, in D2s, t2 was the only tiller type with a probability of 1.0. The probability of occurrence of t1 under shade was conspicuously low and erratic (0.2, 0 and 0.3 in D1s, D2s and D3s, respectively). Plotting these probabilities against mean P_{int} by the canopy during a window of opportunity for bud outgrowth (starting at ligule appearance of the bud's parent leaf, and ending at ligule appearance of the next leaf), and excluding the t1 probabilities under shade, a clear relation was found (Fig. 5a). Independent of population density and with little effect of shade, the probability of any primary tiller to occur was 1 until P_{int} reached approximately 0.4. After this point, the probability dropped until it reached 0 at values of P_{int} of ca. 0.55, and remained 0 beyond that value of P_{int}. The only exception was t1 in the shaded plants, for which there was no relationship between P_{int} and probability of occurrence: t1 showed low probability of occurrence when the P_{int} was still considerably lower than 0.4 (Fig. 5a). A
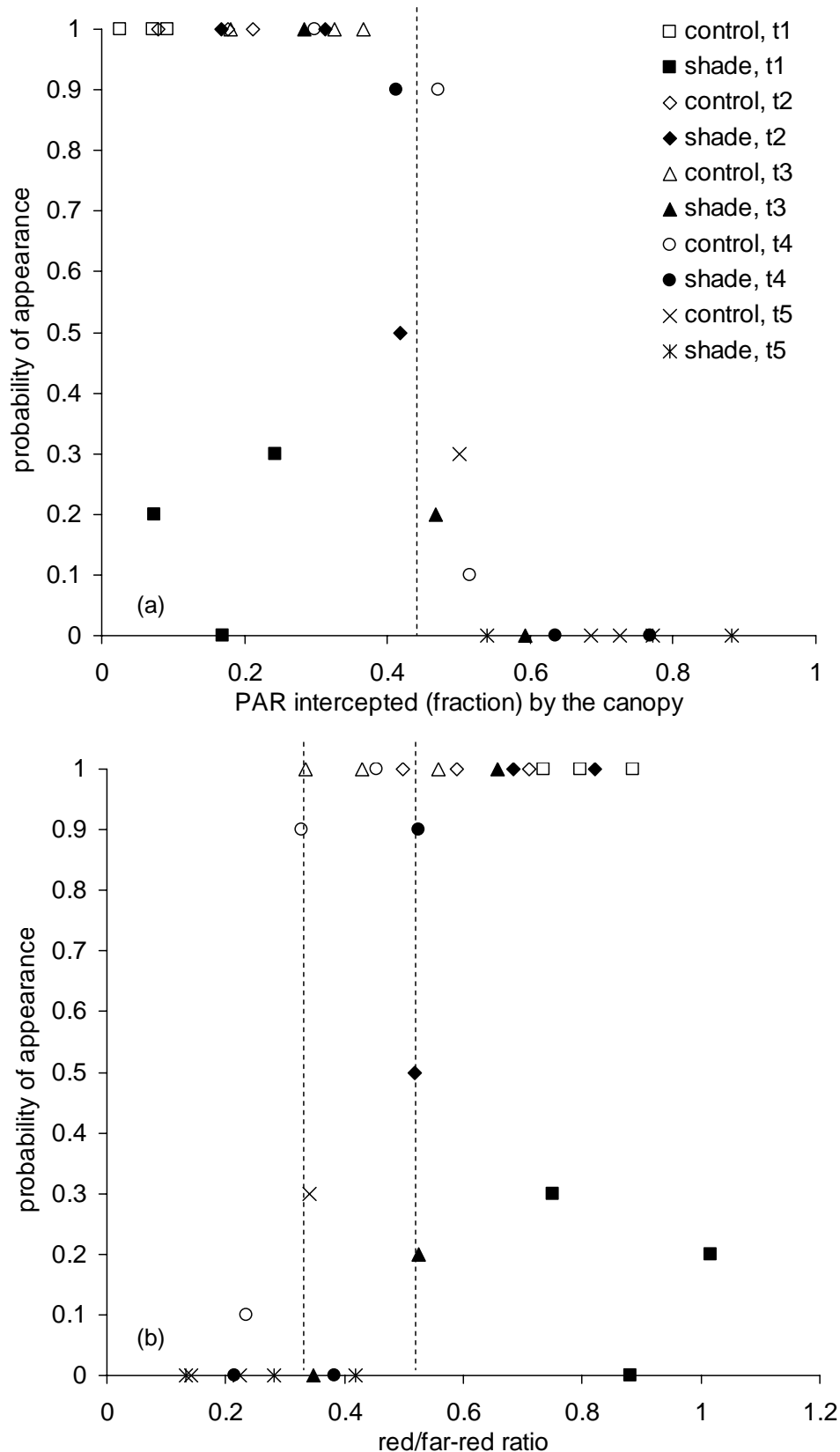
Fig. 5a, b: Relationships between probability of occurrence of tillers t1 to t5 and the fraction PAR intercepted (a) and R:FR (b) by the canopy, during a window of opportunity for bud outgrowth starting at ligule appearance of the parent leaf and ending at ligule appearance of the next leaf. The vertical dashed lines show the threshold levels at which probabilities of occurrence decrease. For clarity, population densities are not distinguished from one another; n = 60. Note that in (b) the course of R:FR over thermal time should be read from right to left.

Fig. 6: Probability distribution of leaf mass per unit leaf area (LMA) of parent leaves of buds t1 to t5 that either remained dormant ('dormant' group, open bars) or grew out ('outgrowth' group, closed bars), of bud 1 to 5 on the main stem, n = 82. The dashed line indicates the class limit below which the distribution for the dormant group has a higher probability, and above which the outgrowth group has a higher probability.

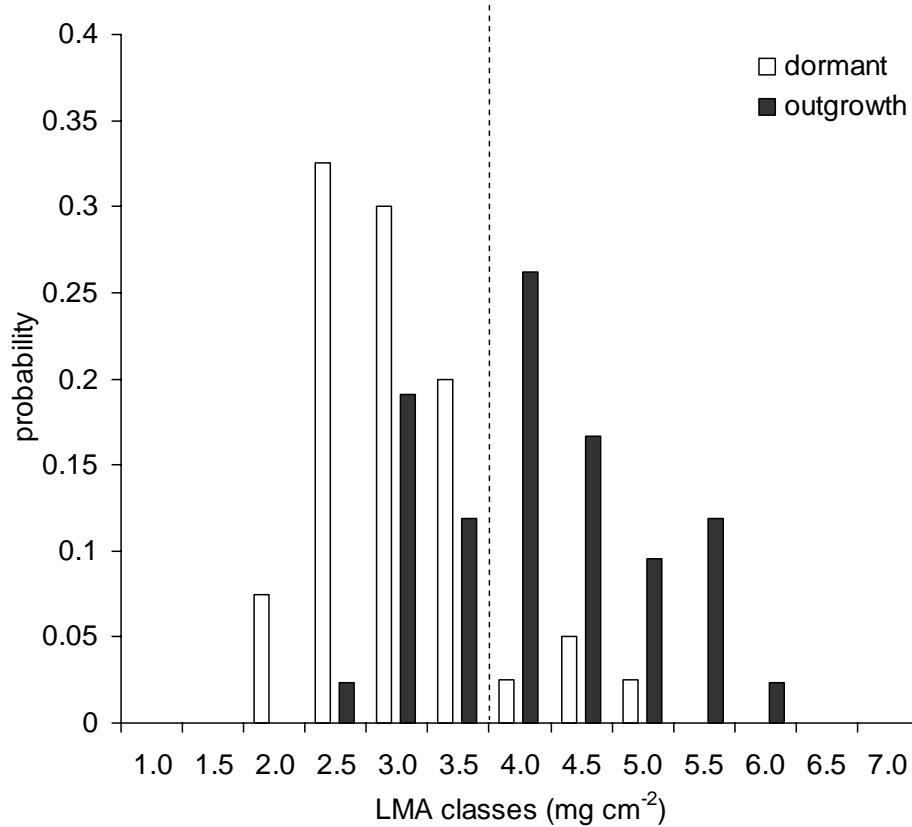similar plot for R:FR shows that a clear distinction was visible between non-shaded and shaded plants (Fig. 5b): the threshold R:FR values below which the probability of occurrence approached zero, were ca. 0.51 for plants grown in shade and 0.32 for control plants.

LMA of parent leaves and outgrowth of buds

Both within the group of buds that had grown out, and the group of buds that remained dormant, there was no significant difference between population densities in LMA of the parent leaf blades. LMA of the parent leaves of buds of t1 to t5 in the 'dormant group' (all population densities combined) was 2.78 mg cm^{-2} (SE = 0.09, n = 40), in the 'outgrowth group' LMA was 3.86 mg cm^{-2} (SE = 0.13, n = 42), a highly significant (P<0.001) difference. The probability distribution of LMA data for the 'dormant' and 'outgrowth' groups (Fig. 6) indicates that the class limit beyond which the tillers of the outgrowth group had a higher probability of

appearing than those of the dormant group (dashed line in Fig. 6) was 3.75 mg cm^{-2}. The probability of dormancy of buds for which the parent leaf's LMA was lower than 3.75 mg cm^{-2} was 0.63. For LMA > 3.75 mg cm^{-2}, the probability of outgrowth was 0.84. Separate analysis on data from phytomer number four showed highest variation among population densities in probability of occurrence of tiller appearance (Table 2), resulting in a balanced distribution between the 'outgrowth' and 'dormant' groups with n = 8 and n = 11, respectively. A significant difference (P<0.01) between the two groups was found, i.e. LMA was 3.99 (SE = 0.30) mg cm^{-2} for the 'outgrowth group' and 1.99 (SE = 0.16) mg cm^{-2} for the 'dormant' group. This difference was primarily caused by longer and heavier leaves in the 'outgrowth' group compared with the 'dormant' group. The frequency distribution indicated a threshold LMA value of 3.25 mg cm^{-2} (not shown), with an outgrowth probability of 0.83 when the LMA of the parent leaf was above the threshold, and a dormancy probability of 0.77 when it was below the threshold.

Discussion

Tiller numbers
In full light, population density had no effect on total number of tillers per plant until approximately 4.8 phyllochrons had been produced (Fig. 2) but, from that point on, tillering rates started to diverge between population densities. A similar divergence in tillering rate in relation to population density has been observed in pearl millet (van Oosterom *et al.*, 2001) and sorghum (Lafarge and Hammer, 2002). In the current study, this divergence can be attributed partly to the appearance of more secondary tillers (inset in Fig. 2) at lower population densities. Furthermore, at the divergence, primary tiller number (inset in Fig. 2) in D3c plants reached a plateau of ca. 3 tillers, a value which was maintained for three phyllochrons. This plateau was caused by constant tiller numbers, and not by compensation between appearance and senescence of tillers, as senescence occurred later; the first tillers started to senesce from a physiological age of 7.1 phyllochrons onwards, and the senescence of later tillers did not start till a physiological age of 8 (data not shown). In D1c and D2c, the plateau in tiller numbers was either not present or much less distinct than in D3c (inset in Fig. 2) due to the higher probability of occurrence (Table 2) of t4 and t5 at those population densities. Similar effects of population density on tiller appearance of t2 to t5 in spring wheat have been reported by Bos (1999) (note: t1 was absent

in his experiment), while Kirby and Faris (1972) showed that development of barley tiller buds up to t4 was not affected by population density, but that subsequent buds appeared later at higher population densities due to the delaying effect of population density on developmental rate of the plant.

Cessation of tillering in relation to fraction of PAR intercepted

The appearance of new tillers has been found to decrease strongly at a particular leaf area index (Simon and Lemaire, 1987; Lafarge and Hammer, 2002). The current analysis (Fig. 4b) indicates that, in full sunlight, tiller appearance stopped at a particular value of P_{int} (0.59 on average) rather than at a fixed physiological age. In shade treatments, the appearance of tillers in D1s and D3s ceased at approximately the same P_{int} as in full sunlight. However, in D2s, cessation of tillering occurred at lower P_{int} than in D1s and D3s (0.45, P<0.05). Omitting the results of D2s results in a mean P_{int} of 0.60 in the shaded plants, a value similar to that of the plants in full light (0.59). The data shown in Fig. 5 is independent of Fig. 4, which relates cessation of appearance of leaves to conditions in the canopy. However, the 'decision' of a tiller bud to remain dormant instead of growing out must have been taken approximately one phyllochron before the time of maximum tiller number, because the period of time during which the bud extends within the surrounding sheath has to be taken into account. The analysis of Fig. 5 pertains to that period. Therefore, these results reinforce the proposition that tiller appearance ceased at a similar P_{int} in full sunlight and in shaded plants. On the basis of the data in Fig. 5a, it may be surmised that the probability of a tiller to grow out starts to decrease when $P_{int} > 0.40$, and that it has fallen to zero by the time that P_{int} exceeds 0.55. This translates to a time window of around 0.75 phyllochrons for the fully lit plants, and 0.85 phyllochrons for the shaded plants. In other words, well within the time it took for two successive leaves to appear, complete tillering cessation had taken place.

LMA of parent leaves and tiller outgrowth

Bos (1999) hypothesised that low PAR intensity at the level of a bud's parent leaf, and therefore its low rate of assimilate supply, prevents the bud from developing into a tiller. Bos (1999) reported a relationship between the mean LMA of a particular leaf rank and the probability of occurrence of the tiller. He found a 'threshold' value for LMA of 2.9 to 3.1 mg cm^{-2} for t1 and 2.0 to 2.4 mg cm^{-2} for t3, below which buds did not grow out and above which they did. These results appear to be consistent with the present results, but there are some important differences. In the current study the parent leaf is regarded to be the leaf on the

same phytomer, being the leaf directly above the tiller bud (chapter 2) and not the leaf in the axil of which the bud resides as in Bos (1999). The current interpretation of the association between parent leaf and bud is preferred to that of Bos because it has been shown for barley that an initiated bud is nutritionally dependent on the leaf above the bud rather than the subtending leaf. This view is based on anatomical grounds and on the relationship between the photosynthetic activity of that leaf and bud growth (Fletcher and Dale, 1974). Analysis of the relationship between tiller appearance and LMA of the subtending leaf, as was done by Bos (1999), yielded largely the same segregation in LMA distributions for parent leaves of dormant buds than of buds that grew out, but less distinctively so that found for the parent leaves (as defined here). Yet, if bud growth is directly or indirectly associated with LMA of leaves, it is not only the LMA of the parent leaf, but it may also be LMA of the leaf on the preceding phytomer (the subtending leaf) that counts. The LMA threshold values for arrest of tiller growth in Bos (1999) were lower than that of the present study (3.75 mg cm^{-2}), a result which may be explained by the difference in growing conditions (growth chamber lamps *vs*. full sunlight). The current investigation advances understanding because the association between LMA and bud growth was evaluated on an individual plant basis, resulting in probabilities of bud outgrowth in relation to LMA values (Fig. 6) rather than population means reported by Bos (1999).

The red / far-red ratio and cessation of tillering
It has been argued that, in ryegrass (Simon and Lemaire, 1987) and sorghum (Lafarge and Hammer, 2002), cessation of tillering can be explained by photomorphogenetic effects particularly changes in R:FR (e.g. Casal *et al.*, 1990), rather than reduction in the rate of photosynthesis per (parent) leaf, since no association could be found between availability of assimilates in the tiller bases and cessation of tillering in the case of ryegrass (Davies and Thomas, 1983). Such photomorphogenetic effects on tillering are mediated mainly by R:FR of horizontally propagated light perceived by vertically orientated organs such as elongating leaves, sheaths of mature leaves, and internodes (Cordukes and Fisher, 1974; Morgan *et al.*, 1980; Skinner and Simmons, 1993). Next to the R:FR ratio, the supply of blue light has also been shown to play a role in modulation of tillering (Barnes and Bugbee, 1992). R:FR is closely related to P_{int} (Fig. 1c), because light 'emitted' (reflected and transmitted) by the surrounding vegetation is strongly depleted in the red region of the spectrum compared with the far-red region (Holmes and Smith, 1977), but this is not true for direct light. At the time of maximum number of tillers, horizontally measured R:FR at soil

level was 0.26 in the full light treatment, irrespective of population density (Fig. 4c), whereas physiological age varied significantly among population densities. In the shaded plants, D2s had a significantly higher R:FR value (0.54, P<0.001) at the time of cessation of tiller appearance than D1s and D3s which had an identical average R:FR of 0.36. Therefore, in full light conditions, an R:FR of ca. 0.25 to 0.3 represented a 'threshold' value above which (at least indirectly) tiller appearance ceased. In shaded conditions, the value may be higher, due to the difference in the relation between P_{int} and R:FR (Fig. 1c). When taking into account the time it takes for a tiller to appear from its surrounding sheath, the R:FR threshold value for cessation of outgrowth was 0.35 to 0.40 in full light, and 0.45 to 0.50 in shade (Fig. 5b). However, the former value is much more representative for agricultural systems than the latter, since 75% shading does not occur in the field.

Thresholds in P_{int}, R:FR and LMA of parent leaves: different sides of the same coin?

A low R:FR results in lower LMA values in chrysanthemum (Rajapakse and Kelly, 1992) and tall fescue (Wherley *et al.*, 2005). Wherley *et al.* (2005) hypothesised that the decrease in tillering in their low R:FR treatment was due to the decreased LMA and the associated decrease in photosynthetic capacity of the leaves. The existence of an association between LMA and photosynthetic capacity was argued by Oguchi *et al.* (2003), although in some cases no association has been found over a substantial range of LMA values (Vos and van der Putten, 1998). A general reduction in LMA with increase in population density was not found in the current study, but has been described for potato (Vos, 1995) and ryegrass (van Loo, 1993). Van Loo ascribed the effects of a high population density on LMA to reduced light intensity (Silsbury, 1971). However, critical evidence supporting that mechanism seems to be lacking; there is no data showing divergence in LMA of (full grown) leaves that initially showed the same LMA but diverged in LMA after being subjected to high and low light regimes, respectively. Most evidence suggests an environmental trigger (i.e. R:FR), which results in a morphogenetic change in LMA. If variation in LMA of leaves of a particular phytomer rank is brought about by a photomorphogenetic response, this variation in LMA reflects the range of light conditions experienced by these leaves and also underlines the local nature of the response: the light conditions (R:FR) of each parent leaf × bud combination are apparently decisive for the LMA of the parent leaves and outgrowth of the tiller bud.

Several authors have proposed a relationship between tiller outgrowth and substrate production per plant or per parent leaf (e.g. Bos and Neuteboom, 1998a; Gautier *et al.*, 1999). Obviously, bud growth requires substrates, but the question is whether or not substrate availability is the main determinant of the fate of a tiller bud. If it were, one would not expect a conservative value across population densities and shading for P_{int} that marks the cessation of tiller appearance. Therefore it is concluded, in this investigation, that light quality dominated over substrate availability as a determinant of the fate of tiller buds.

Nevertheless, the differences in probability of occurrence of t1 in the shaded plants between population densities (Table 2, Fig. 5), could be a direct result of the reduced amount of PAR on (parent) leaf 1, rather than being triggered by P_{int} or the value of R:FR (Fig. 5a, b). At the early stage of development of the canopy, at which the window of opportunity for t1 to grow out has opened, R:FR is still high but the absolute amount of incident PAR is low in the shaded plants. Under those conditions the small size of leaf 1 may limit the resources provided by this leaf for the t1 bud to grow out, resulting in much reduced occurrence of t1 in shade as compared with those in full sunlight.

In conclusion, the current results, along with evidence from the literature, support the theory that tillering ceases at a fixed R:FR and P_{int} inside the canopy. Particularly in the case of fully sunlit plants, the time of maximum tiller number occurred at a similar P_{int} and at similar red/far-red ratio, independent of population density, in spite of the fact that plant development, expressed in physiological age, was significantly different between population densities. This suggests that particular light conditions, related to canopy development stage, suppress bud outgrowth. During the window of opportunity for outgrowth of buds it appears that a value of 0.40 to 0.45 for P_{int}, marked the transition between bud growth ($P_{int} < 0.40$ to 0.45) and suppression of bud growth ($P_{int} > 0.40$ to 0.45). Furthermore, for plants grown in full light, bud outgrowth was suppressed when R:FR dropped below a threshold value (0.35 to 0.40). The population density used in the field usually does not exceed the range of population densities used in this trial, and the light intensity caused by the shade treatment is far below natural light intensity. Therefore, the main conclusions drawn from treatments exposed to full sunlight are probably valid for common agronomic conditions for wheat growth, provided that water and N are applied in non-limiting amounts.

Chapter 5

Tillering in spring wheat: a 3D modelling study on the effects of the local light environment

Jochem Evers

Jan Vos

Michaël Chelle

Bruno Andrieu

Christian Fournier

Paul Struik

Abstract

The outgrowth of tiller buds in Gramineae is influenced by the intensity of photosynthetically active radiation (PAR) and the ratio of the intensities of red and far-red light (R:FR). At each point in the plant canopy volume, both components are affected by surrounding plant tissues (shading and multiple scattering, respectively). Evidence exists that light properties operate on a local level (i.e. the 'parent' leaf blade of the tiller bud (this is the leaf blade of the same phytomer), and the tube of sheaths, respectively). This chapter presents a virtual plant modelling approach to simulate the local effects of light on tillering in spring wheat (*Triticum aestivum* L.), and explores the hypothesis that tillering can be explained by local effects of the fraction of PAR intercepted and R:FR.

A virtual plant model of spring wheat (ADELwheat) was interfaced with a light model (Nested Radiosity) capable of calculating the distribution of PAR and R:FR in the 3D architecture. The virtual plant model was modified to make tiller bud outgrowth dependent on (a) the fraction of PAR intercepted by the parent leaf blade of the bud, or (b) R:FR perceived by either the tube of sheaths (the pseudostem, which is known to act as an R:FR sensor), or by the bud's parent leaf blade. Simulations were done for three plant population densities. Bud outgrowth was expressed as a 'go / no go' process, depending on threshold values of fraction PAR intercepted by the parent leaf blade (P_{loc}), and on R:FR at the two sites of R:FR perception indicated above.

In accordance with reality, fewer tillers per plant were simulated for higher plant population density. However, bud outgrowth was not simulated equally adequate for each tiller position. P_{loc} was a good indicator for outgrowth of tillers of a low rank, but outgrowth of tillers of a high rank was overestimated. Assuming R:FR is perceived by the pseudostem resulted in overestimation of the number of tillers. Assuming that leaf blades act as R:FR sensors gave lower simulated maximum number of tillers, but still at least as many as experimentally observed. It is suggested that a combination of photomorphogenetic effects and the effects of shading on carbon assimilation may improve model performance.

The current study showed that the open L-system approach is a promising tool to analyse crop morphological and ecological research questions in which the determinants act on the level of the individual plant organ.

Keywords: plant architecture, virtual plant, functional-structural model, wheat, tillering, PAR, light interception, red/far-red ratio

Introduction

Tillering is an important property of the wheat plant. It enables the crop to cope with intraspecific competition by optimising the formation of grain-bearing ears in relation to the available resources (Darwinkel, 1978). Nitrogen availability affects tillering (Davies, 1971; Longnecker *et al.*, 1993). Light, however, plays a key role in the regulation of tiller appearance. Number of tillers per plant and rate of tiller appearance have been related to the intensity of photosynthetically active radiation (PAR), e.g. in wheat (Bos, 1999) and perennial ryegrass (Bahmani *et al.*, 2000), especially in nearly closed canopies (Simon and Lemaire, 1987). Also, a lower ratio between the intensity of red and far-red light (R:FR) has been related to reduced tillering rate in Gramineae, e.g. in Italian ryegrass (*Lolium multiflorum* Lam.) and dallisgrass (*Paspalum dilatatum* Poir.) (Casal *et al.*, 1986), barley (*Hordeum vulgare* L.) (Skinner and Simmons, 1993) and weeping lovegrass (*Eragrostis curvula* Schrad.) (Wan and Sosebee, 1998). R:FR is lowered by plant tissues through differential reflection and transmission of red and far-red light (Holmes and Smith, 1977). R:FR has been shown to be perceived by vertically orientated organs such as elongating leaves, sheaths of mature leaves, and internodes (the 'sites of perception') (Cordukes and Fisher, 1974; Morgan *et al.*, 1980; Skinner and Simmons, 1993). Changes in R:FR have been shown to precede mutual shading, consequently serving as an early signal that competition for light will likely occur in the near future (Ballaré *et al.*, 1987; Franklin and Whitelam, 2005).

An experimental study (chapter 4) on the light conditions inside the canopy of spring wheat (*Triticum aestivum* L.) plants showed that new tillers stop emerging when fraction PAR intercepted by the canopy exceeds 0.4. That threshold value was fairly stable over a wide range of intensities of incoming light and plant population densities. In the same study, observations were also done on R:FR values within the canopy at soil level at the time of cessation of tiller appearance. Again, it was observed that tillering ceased at specific values of R:FR, but these values appeared to be affected by light intensity (0.32 in full light and 0.51 in 75% shade). These findings on cessation of tillering at specific light conditions within the canopy confirmed suggestions by Simon and Lemaire (1987) for perennial ryegrass (*Lolium perenne* L.) and Italian ryegrass (*Lolium multiflorum* Lam.), and by Lafarge and Hammer (2002) for sorghum (*Sorghum bicolor* (L.) Moench).

The PAR intensity and R:FR inside the wheat canopy are largely determined by the architecture of the canopy itself, i.e. the distribution in the

canopy volume of tissue (selectively) reflecting, absorbing and transmitting light. Light properties influence the pattern of tillering, which in turn determines the architecture of the canopy. The current work attempts to analyse this feedback mechanism in tillering behaviour of spring wheat plants, using a modelling approach called virtual plant modelling (Room *et al.*, 1996), or functional-structural plant modelling (Sievänen *et al.*, 2000; Godin and Sinoquet, 2005). The virtue of virtual plant models is that each element in the 3D architecture of the canopy is explicitly described. This enables simulation of processes at the level of the organ instead of at the level of the whole plant or crop. The model used in this study is an architectural model called 'ADELwheat' (Fournier *et al.*, 2003), which has been calibrated and validated for spring wheat (chapters 2 and 3), in conjugation with a light interception model called 'nested radiosity' (Chelle and Andrieu, 1998; Chelle *et al.*, 1998).

The primary objective of the current work is to analyse whether a 3D virtual plant model of spring wheat is capable of simulating tillering appearance in accordance to experimental observations, merely based on the local (i.e. organ level) influence of light.

Materials and methods

Experiment
The experimental data used in this chapter are derived from the experiment described in chapter 3 and 4, and are therefore not repeated here.

ADELwheat
ADELwheat (Fournier *et al.*, 2003) is an architectural model of wheat, based on the open L-system principles and the CPFG language and simulation program (Lindenmayer, 1968; Prusinkiewicz, 1999; Prusinkiewicz *et al.*, 2000; Měch, 2004). In ADELwheat, the basic unit is the phytomer, which is repeated over time to simulate development of the wheat plant. From top to bottom, the wheat phytomer consists of the following plant organs: a leaf (composed of a blade and a sheath) inserted on a node, an internode, and a tiller bud. From a given initial planting pattern of seeds, the model calculates growth and development, size, shape and orientation in space of each organ in relation to thermal time. Leaf blade curvature and orientation in space are stochastic elements based on distributions derived from experiments.

In ADELwheat, tiller simulation is similar to simulation of the main shoot. The concept of relative phytomer number, RPN (Fournier *et al.*, 2003), enables the derivation of properties of individual tiller phytomers from those of the main stem. This is done by adding a specific 'phytomer shift' value to the actual rank number of the phytomer, yielding the RPN, i.e. the (fractional) main stem phytomer number from which properties are derived. Previous work presented the concepts of ADELwheat based on winter wheat (Fournier *et al.*, 2003), the parameterisation of the model for spring wheat (chapter 2), and the evaluation of model performance in varying conditions (chapter 3). Initially, the probability and timing of tiller appearance followed experimentally derived distributions. In the present work, probability and timing of tiller appearance is dependent on the fraction PAR intercepted and R:FR (see below).

Nested radiosity

To simulate the influence of the local light environment on tillering, light variables such as PAR intensity or R:FR have to be estimated for each individual leaf and internode. This requires calculation of direct (sun) light and diffuse (sky) light in the canopy, as well as calculation of multiple scattering (reflection and transmission) of light by plant organs. Direct light interception can be calculated using a projection technique (Chelle and Andrieu, 1999). The classical radiosity method (Goral *et al.*, 1984) is numerically limited to a restricted number of modules (plant organs), and requires a finite canopy description resulting in border effects. Therefore, the classical radiosity method is not suitable for a canopy composed of a number of virtual plants. However, the radiosity method was adapted for crop canopies (Chelle and Andrieu, 1998; Chelle *et al.*, 1998). This model, called nested radiosity (NR), calculates both the irradiance on and the energy absorbed by each virtual plant organ. To avoid border effects, NR infinitely repeats the simulated canopy. The link between NR and the L-system simulation program CPFG is an interface called CARIBU (Chelle *et al.*, 2004). This interface drives the different calls to NR in order to simulate the spectral bands requested by the L-system (PAR, red, far-red, etc.). In ADELwheat a leaf is defined by a set of polygons, the coordinates of which determine their positions in space. NR calculates absorption and irradiance at the level of individual polygons of which a virtual organ is composed, CARIBU converts the variables and parameters of the organs to and from those of the polygons used by NR. In other words, the light properties of a module are calculated by averaging the light properties of the polygons that comprise the module, e.g. a leaf blade.

In the NR model, the source of the incoming light is a virtual hemisphere. The description of this hemisphere contains both a direct component (sunlight) and a diffuse component (skylight). For the current work, the virtual hemisphere was parameterised for Wageningen conditions on 1 May. Since the time step of NR was set at one day, the definition of the direct light part of the virtual hemisphere contained an arc of light corresponding to the solar trajectory on one day, and the cumulative light intensity on one day. This trajectory was composed of 42 light sources (Fig. 1), each at a relative light intensity corresponding to the elevation of the source. The diffuse component of the virtual hemisphere was composed of 72 sources, arranged in 6 rings (Fig. 1), each emitting light with an intensity relative to its elevation. Similar to direct light, the light intensity values of the diffuse sources added up to the total daily amount of diffuse radiation. The R:FR of the light (both direct and diffuse) was set at 1.15 (Smith, 1982).

PAR interception and R:FR perception in ADELwheat

To introduce the capability of response to daily values of input of environmental variables, in this case solar radiation, ADELwheat was extended with the communication module ?E (Měch and Prusinkiewicz, 1996; Měch, 2004), which enables bidirectional communication between the L-system and the interface to NR (CARIBU). The communication modules were provided with variables for PAR, red and far-red light. Modules in ADELwheat representing foliar organs (blades, sheaths) were provided with reflection and transmission coefficients. To obtain reflection and transmission coefficients for PAR, seven randomly chosen leaves were measured at three sites on each blade (bottom, middle, top), using an Ocean Optics SD 2000 spectrometer with a HL-2000-FHSA Tungsten halogen lamp. Coefficient values were obtained by taking the average value for the wavelengths 400-700 nm. For red and far-red, values were taken from recent measurements on wheat by F. Baret (INRA-CSE Avignon, unpublished), which were acquired according to the methodology described by Jacquemond and Baret (1990). Reflection coefficients used in the model were 0.092, 0.048 and 0.377 for PAR, red and far-red, respectively; transmission coefficients were 0.013, 0.033 and 0.485, respectively.

For the simulation of PAR interception by the leaves, the ?E module was associated with the leaf modules. The perception of R:FR was not associated with a specific plant organ. Vertically oriented organs are the sites of perception for R:FR of horizontally propagating light (Cordukes and Fisher, 1974; Morgan *et al.*, 1980; Skinner and Simmons, 1993). In line with that, the vertically orientated base of the plant is lit by a red light source in experiments studying
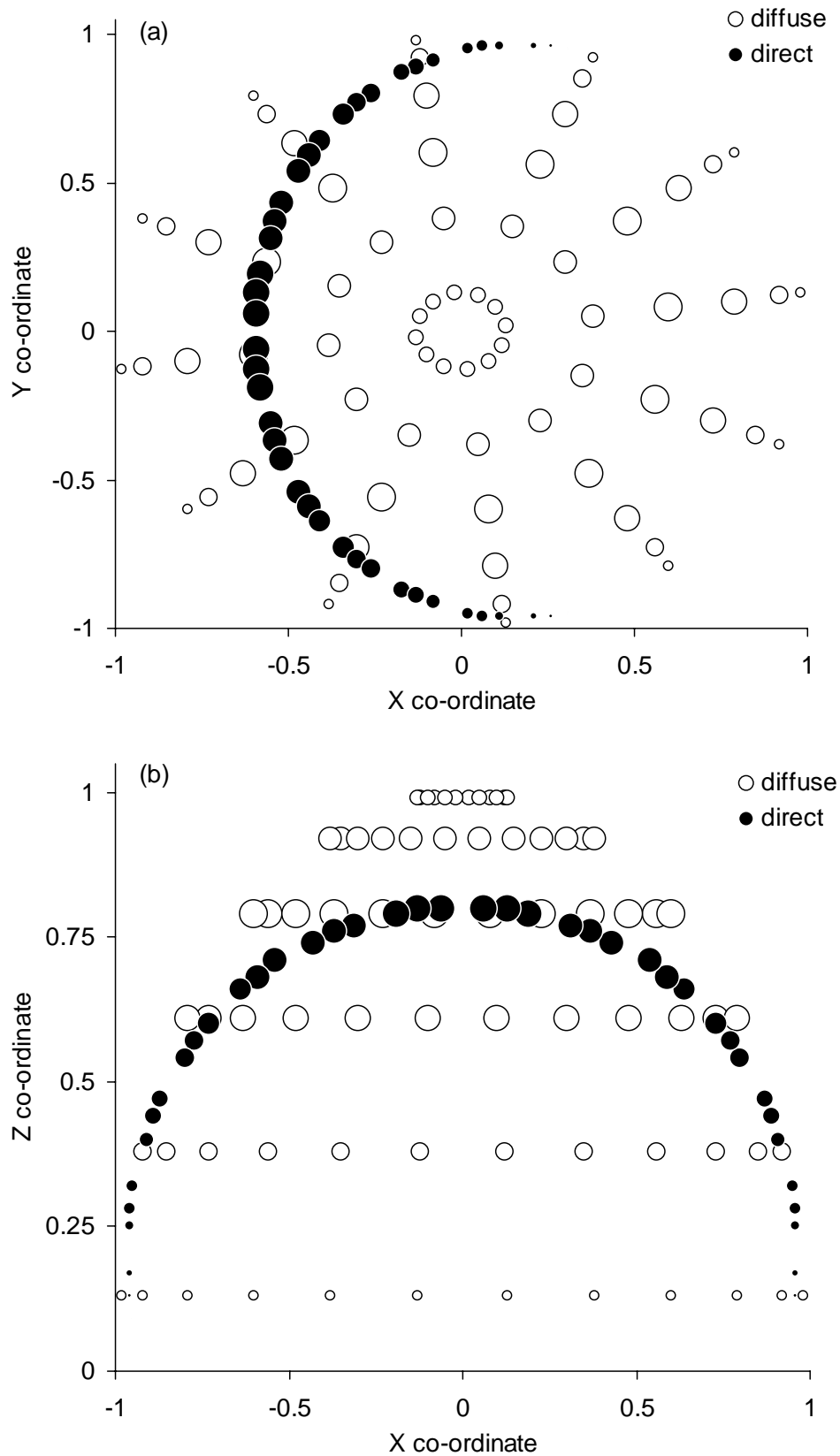
Fig. 1a, b: Configuration of the light sources in the virtual hemisphere, for both direct (solid circles) and diffuse (open circles) light; (a) shows a top-down view, (b) shows a side view. The axes represent the co-ordinates of the light sources; the diameter of the circles represents the relative intensity of the light source.

photomorphogenetic responses to R:FR (e.g. Casal *et al.*, 1986). In ADELwheat, this part of the plant is represented by a single module, representing sheaths and parts of elongating blades which form a tube from which leaf tips appear and within which the ear finally develops. This tube, or pseudostem, is located at soil level in the case of un-elongated stems (internodes), and was used to perceive R:FR of the incoming light ('R_t-tube' simulations). Additionally, simulations were run using the upper side of fully grown leaf blades as sites of perception ('R_t-blade' simulations). Note that perception by fully grown leaf blades does not occur in real plants (Skinner and Simmons, 1993). Fully grown leaf blades have a considerable horizontal component, in contrast to R:FR sensitive organs which are vertically oriented.

For each time step, the calculated fraction of PAR intercepted on each leaf (P_{loc}) was stored in a four-dimensional array, making the PAR values globally accessible through the four identifiers of a leaf module (plant, parent shoot, shoot, and phytomer numbers). In the case of the R_t-blade simulations the R:FR values were stored similarly. In the case of the R_t-tube simulations, the R:FR values were stored in a one-dimensional array (plant number being the only identifier). The stored values of P_{loc} and R:FR were used by the tiller bud modules in a rule that determines the moment of outgrowth.

Rules for bud outgrowth

A previous study (chapter 4) has shown that, although the probability of tiller appearance decreased earlier in canopy development at higher population densities, both the fraction of PAR intercepted at soil level (0.40) and R:FR were similar at that point (0.32), i.e. independent of population density. Additionally, it has been discussed that the PAR intercepted by the 'parent' leaf blade of a tiller bud (i.e. the leaf blade on the same phytomer) is particularly important for tiller bud outgrowth (Bos, 1999, and chapter 4). These triggers of cessation of tillering have been implemented in the model, using a conditional statement associated with the bud outgrowth rule: outgrowth was allowed as long as P_{loc} or perceived R:FR did not drop below a threshold value (P_t and R_t, respectively). The decision to grow out was irrevocable. Also, a bud was not allowed to grow out when the internode of the preceding phytomer had started to extend.

Simulations

Each simulation consisted of 12 virtual plants, divided into three runs of four (two by two) plants. Time step was one day. Simulation runs were done at population densities of 100, 262 and 508 m^{-2} corresponding to the population densities used

Fig. 2: Number of tillers per plant versus the physiological age of the plants for 100 (squares), 262 (diamonds), and 508 (triangles) plants m^{-2}, from simulations using a P$_t$ value of 0.6. Error bars show 2 × SE.
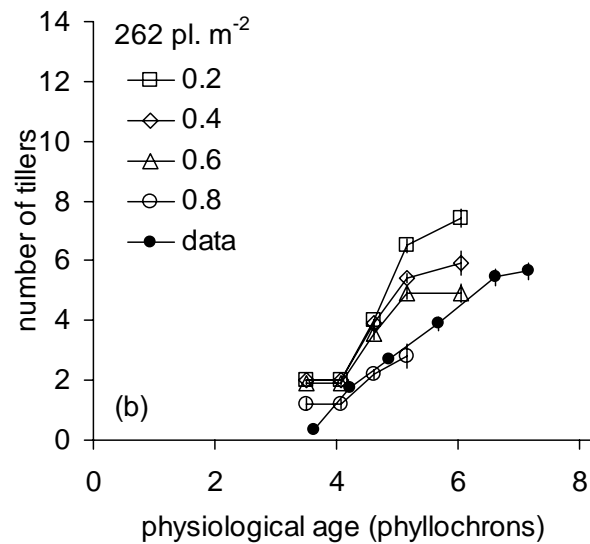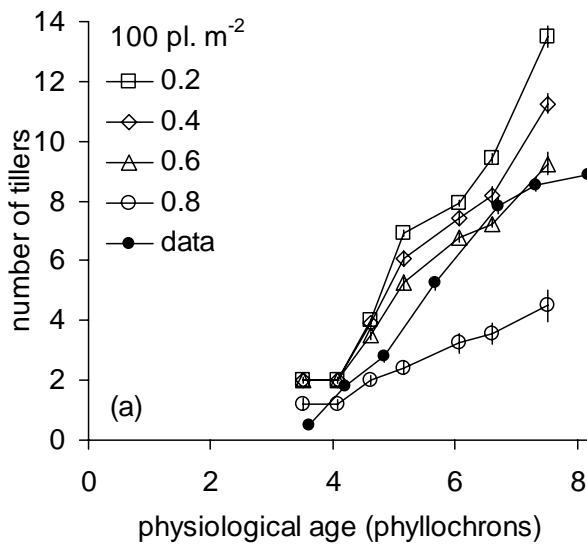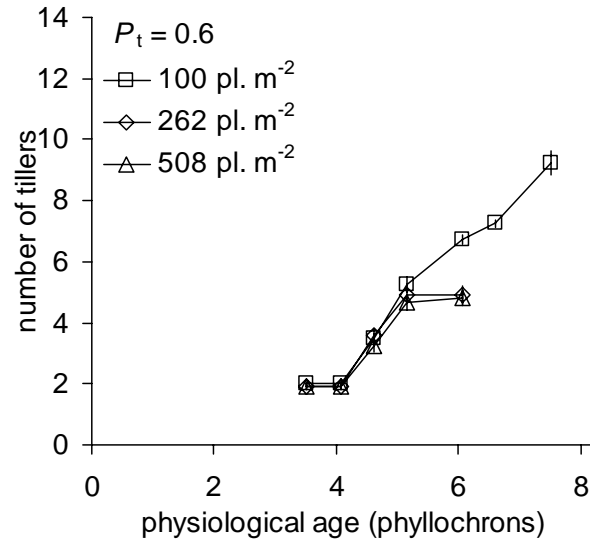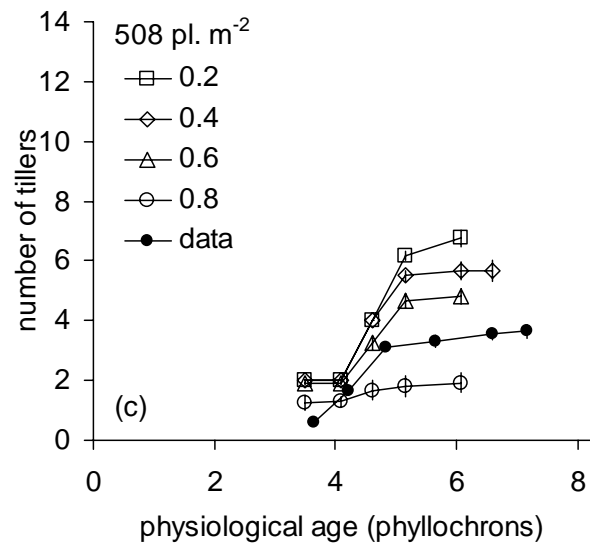

Fig. 3a, b, c: Number of tillers per plant (shown until maximum value) versus the physiological age of the plants for (a) 100, (b) 262, and (c) 508 plants m^{-2}, from simulations using P$_t$ values of 0.2 (squares), 0.4 (diamonds), 0.6 (triangles), 0.8 (circles), and from experimental data (dots). Error bars show 2 × SE.
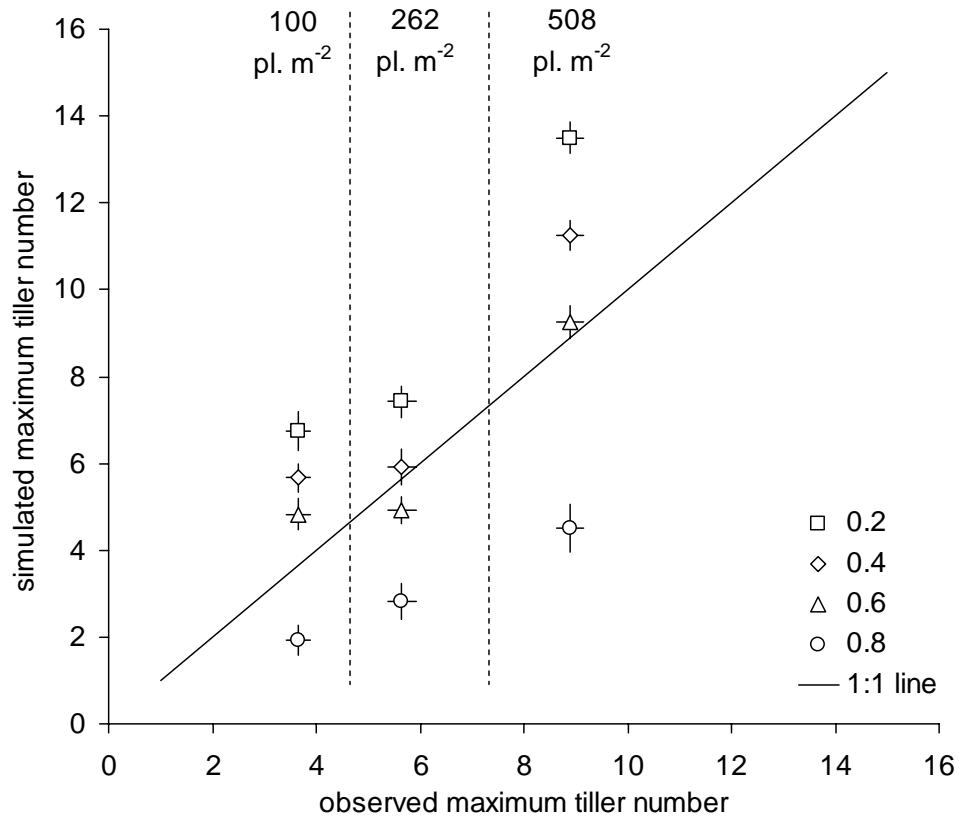
Fig. 4: Simulated vs. observed average maximum number of produced tillers per plant using P_t values of 0.2 (squares), 0.4 (diamonds), 0.6 (triangles), 0.8 (circles). Error bars show 2 × SE.

in the experiment. The runs differed in the starting value of the random number generator, which affects the stochastic components of the model (leaf curvature). In the P_t simulations, the P_t values for bud outgrowth were set at 0.2, 0.4, 0.6 and 0.8. Both in the R_t-tube and in the R_t-blade simulations, the value of R_t was set to 0.32 (value taken from chapter 4).

The simulation output consisted of (a) the time course of the number of tillers present per plant (a tiller was regarded to be present when its first leaf had appeared), (b) the maximum number of tillers produced per plant (c) the probability of individual tiller occurrence, and (d) the time course of leaf area index (LAI, in unit leaf area per unit soil area).

Results

Tillering constrained by P_{loc}

At any of the three P_{loc} threshold (P_t) values, the rate of increase of the number of tillers per plant was similar across population densities until a physiological age of

Fig. 5: Example of the visual output at four moments in thermal time, from simulations runs at (a) 100 and (b) 262 plants m⁻².

216 ºCd   531 ºCd   780 ºCd   1029 ºCd

(a)

(b)
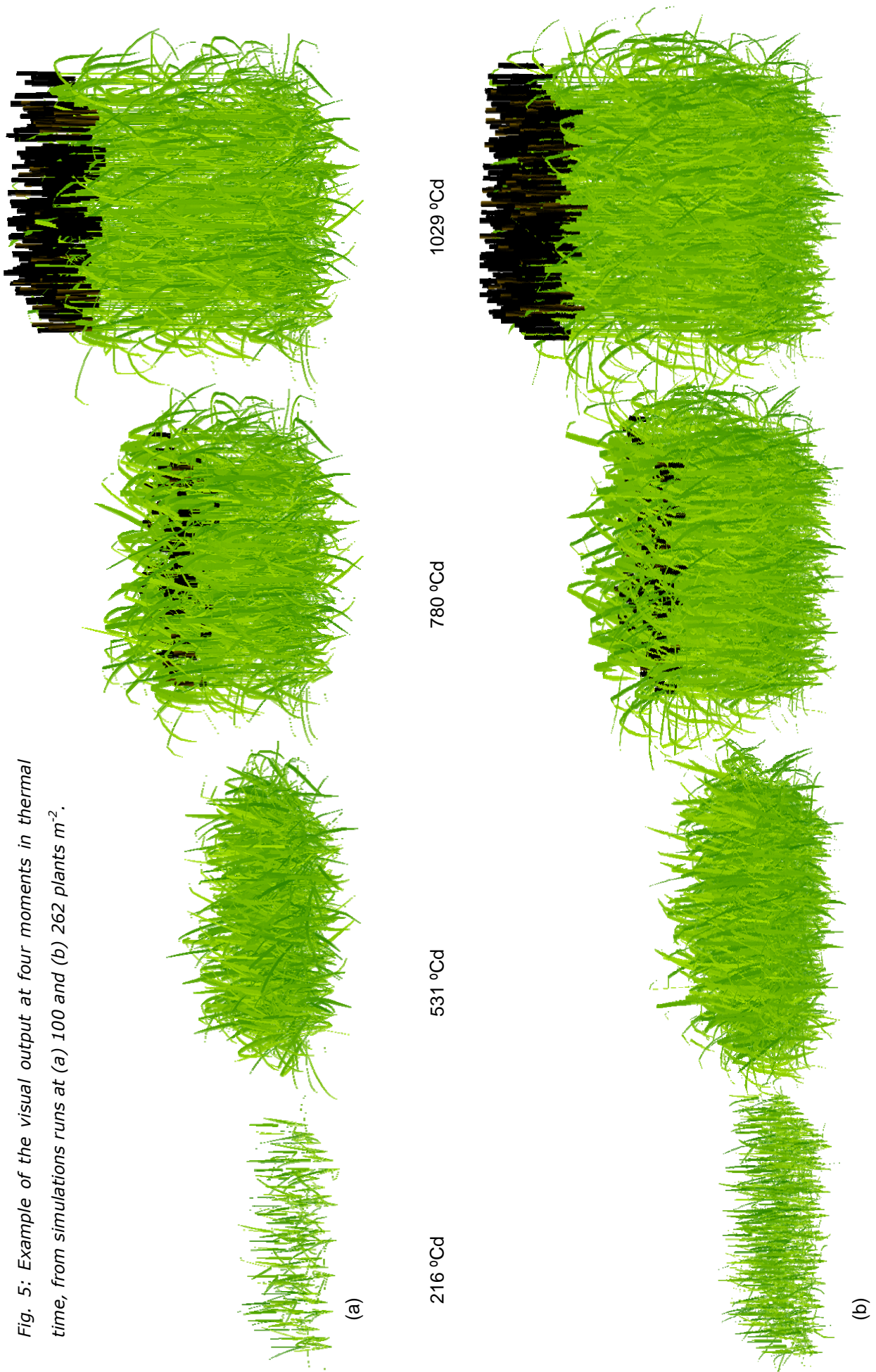
ca. 5 phyllochrons (Fig. 2, showing the case of P_t = 0.6). Beyond that physiological age, tiller numbers per plant of the lowest population density continued to increase, whereas increase nearly stalled at the two higher population densities. A higher P_t value generally resulted in reduction in the number of tillers per plant at any physiological age (Fig. 3). The experimentally observed number of tillers per plant was generally between the simulation lines of P_t = 0.6 and P_t = 0.8 (Fig. 3). Both a higher P_t and a higher population density decreased the simulated average maximum number of appeared tillers per plant (Fig. 4): in conditions most favouring tillering (population density = 100 plants m^{-2}, P_t = 0.2), 13.5 tillers appeared per plant on average, whereas in least favourable conditions (population density = 508 plants m^{-2}, P_t = 0.8) only 1.9 tillers appeared per plant. The maximum number of appeared tillers in the experiment was always within the range of numbers obtained in the P_t simulations (Fig. 4). Illustrations of the visual output of two simulations at 100 and 262 plants m^{-2} are given in Fig. 5.

Probability of occurrence of tillers generally decreased with increasing phytomer number of the parent shoot (exemplified for 262 plants m^{-2} in Fig. 6).
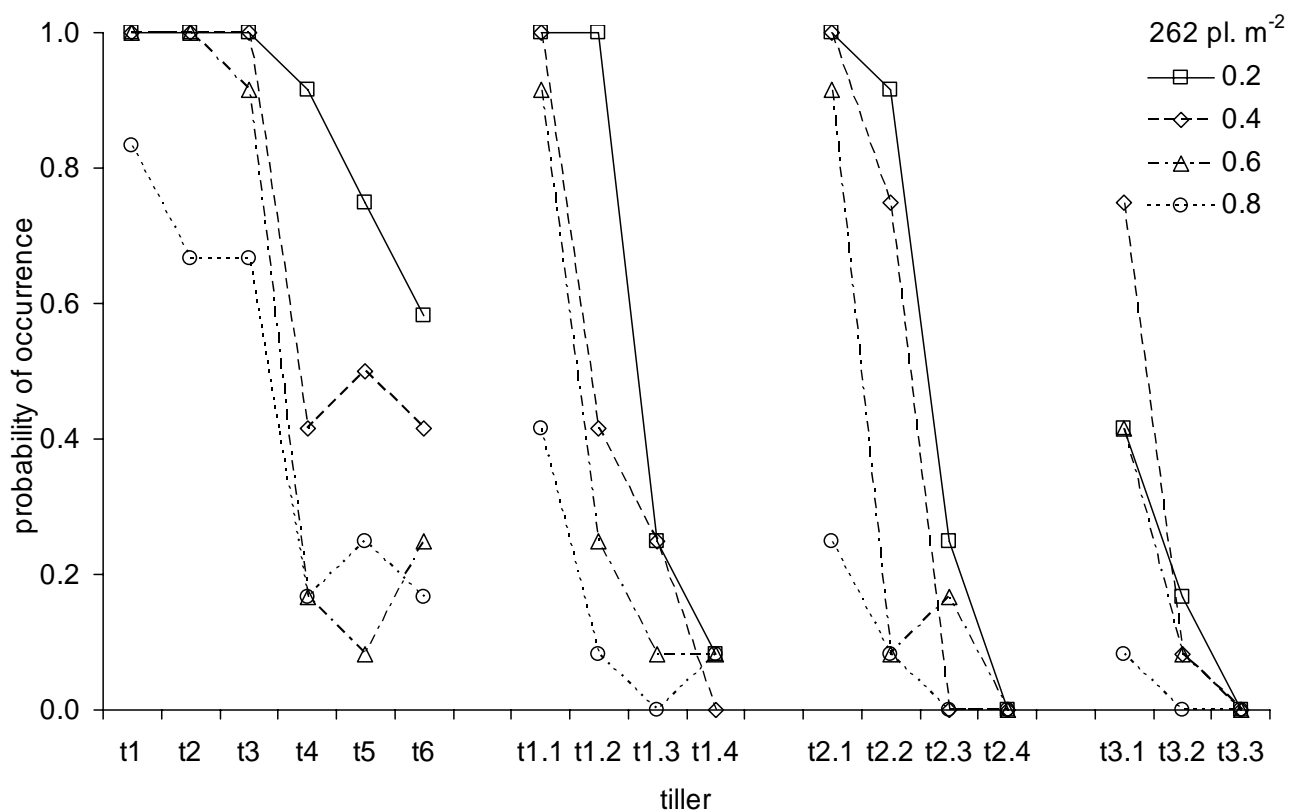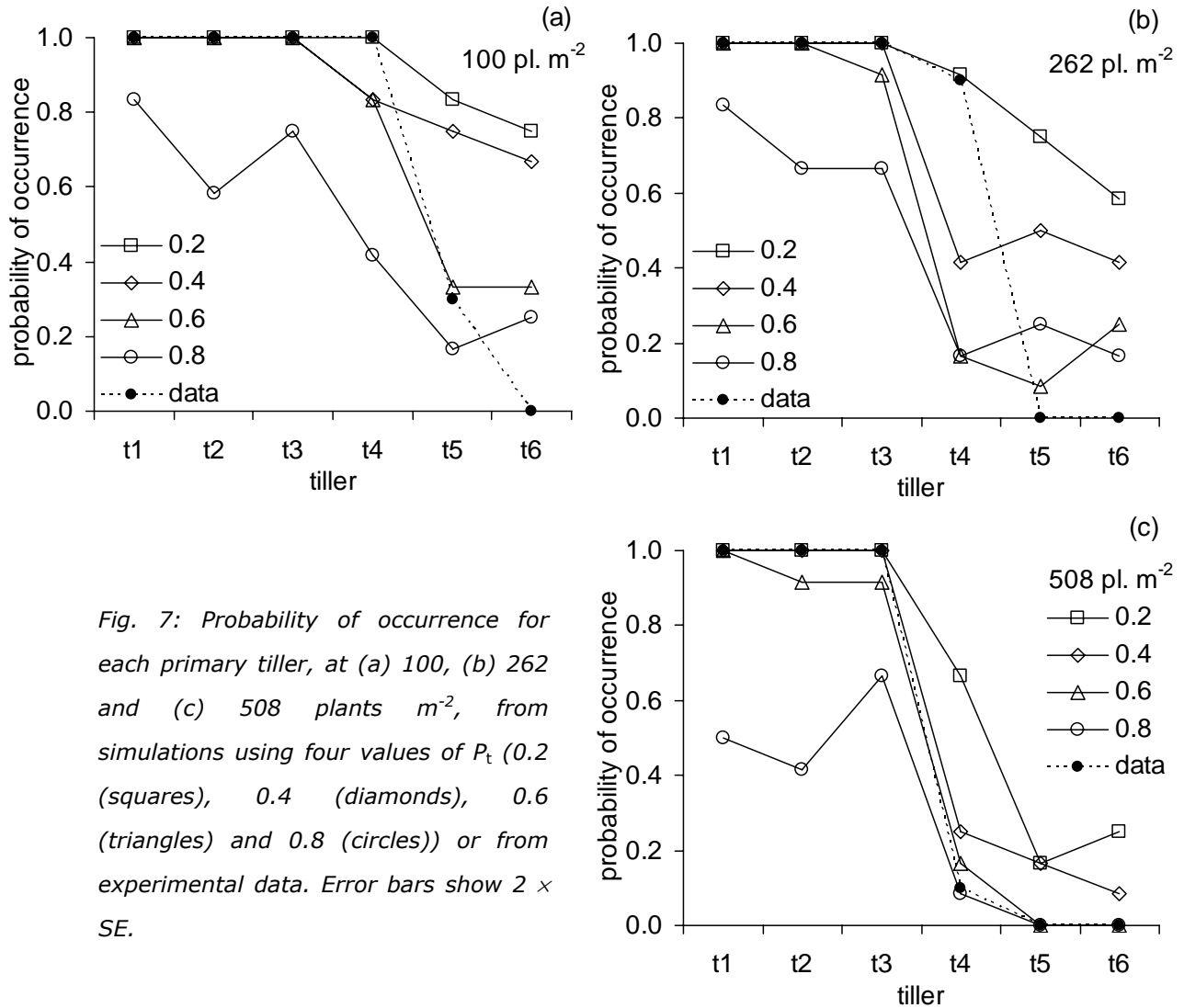

Fig. 6: Probability of occurrence for each tiller, from simulations at 262 plant m^{-2} using four values of P_t: 0.2 (squares), 0.4 (diamonds), 0.6 (triangles) and 0.8 (circles).

Fig. 7: Probability of occurrence for each primary tiller, at (a) 100, (b) 262 and (c) 508 plants m^{-2}, from simulations using four values of P_t (0.2 (squares), 0.4 (diamonds), 0.6 (triangles) and 0.8 (circles)) or from experimental data. Error bars show 2 × SE.

In some cases t5 or t6 had a higher probability of occurrence than the preceding tiller, which was never experimentally observed (Fig. 7). Similar simulation results were obtained for secondary tillers: also here in some cases the tillers of higher rank number occurred more frequently than the tillers of lower rank number. Secondary tillers t2.4 and t3.4 (and other secondary tillers of higher rank) never appeared, and the same was true for secondary tillers originating from the fourth (or higher) main stem phytomer (t4.1, t5.1 etc.) However, t4.2 was the exception as it appeared at the lowest population density and P_t values of 0.2 and 0.4. Probability of occurrence of primary tillers was either equal across population densities, or lower at higher population densities than at the lowest population density (Fig. 7). Primary tiller t1 (the coleoptile tiller) was fully present in most of the 12 population density × P_t combinations, except that tiller t1 occurrence was < 1.0 for P_t value of 0.8.

Maximum LAI values reached were 9.7, 9.2, 8.9 and 6.7 (100 plants m^{-2}), 8.9, 8.7, 8.2 and 7.7 (262 plant m^{-2}), and 11.0, 10.4, 12.7 and 10.7 (508 plants
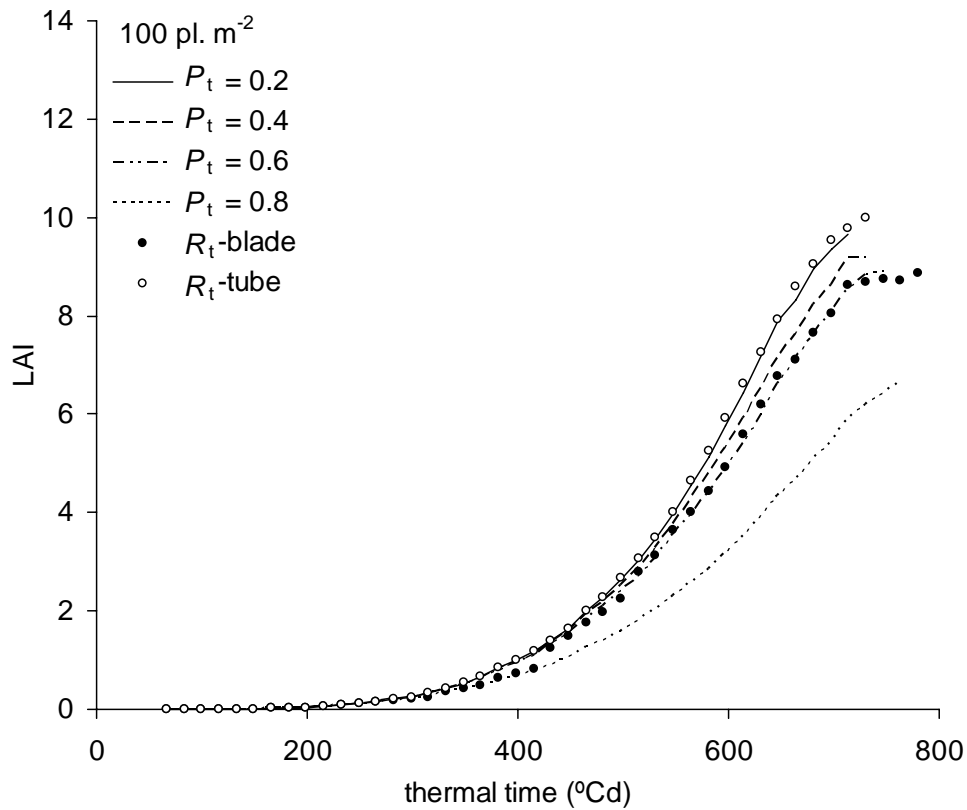
Fig. 8: LAI (in m^{-2} leaf area per m^{-2} soil area) versus thermal time for 100 plants m^{-2}, from simulations using P$_t$ values of 0.2, 0.4, 0.6, and 0.8, and from simulations using either the tube or the blades as sites of R:FR perception.

m^{-2}) for P_t values of 0.2, 0.4, 0.6 and 0.8, respectively. At the lowest population density, the difference in LAI during canopy development between P_t values 0.2, 0.4 and 0.6 was very small; a value of 0.8 resulted in a much slower LAI increase (Fig. 8). At 262 and 508 plants m^{-2} differences in LAI development between P_t values were relatively small, with higher values resulting in a lower rate of LAI increase (not shown).

Tillering constrained by R:FR

At either of the three population densities, the average number of tillers per plant was higher in the R_t-tube simulations than in the R_t-blade simulations (Fig. 9) at any physiological age. The R_t-tube simulations produced more tillers per plant than experimentally observed, in contrast to the R_t-blade simulations which produced fewer tillers per plant than experimentally observed. The lowest population density resulted in the highest simulated number of tillers per plant. In the R_t-tube simulations at 508 plants m^{-2} at maximum more tillers per plant were produced than at 262 plant m^{-2} (7.1 vs. 7.8). (Fig. 10). Generally, the model overestimated the maximum number of tillers produced per plant.
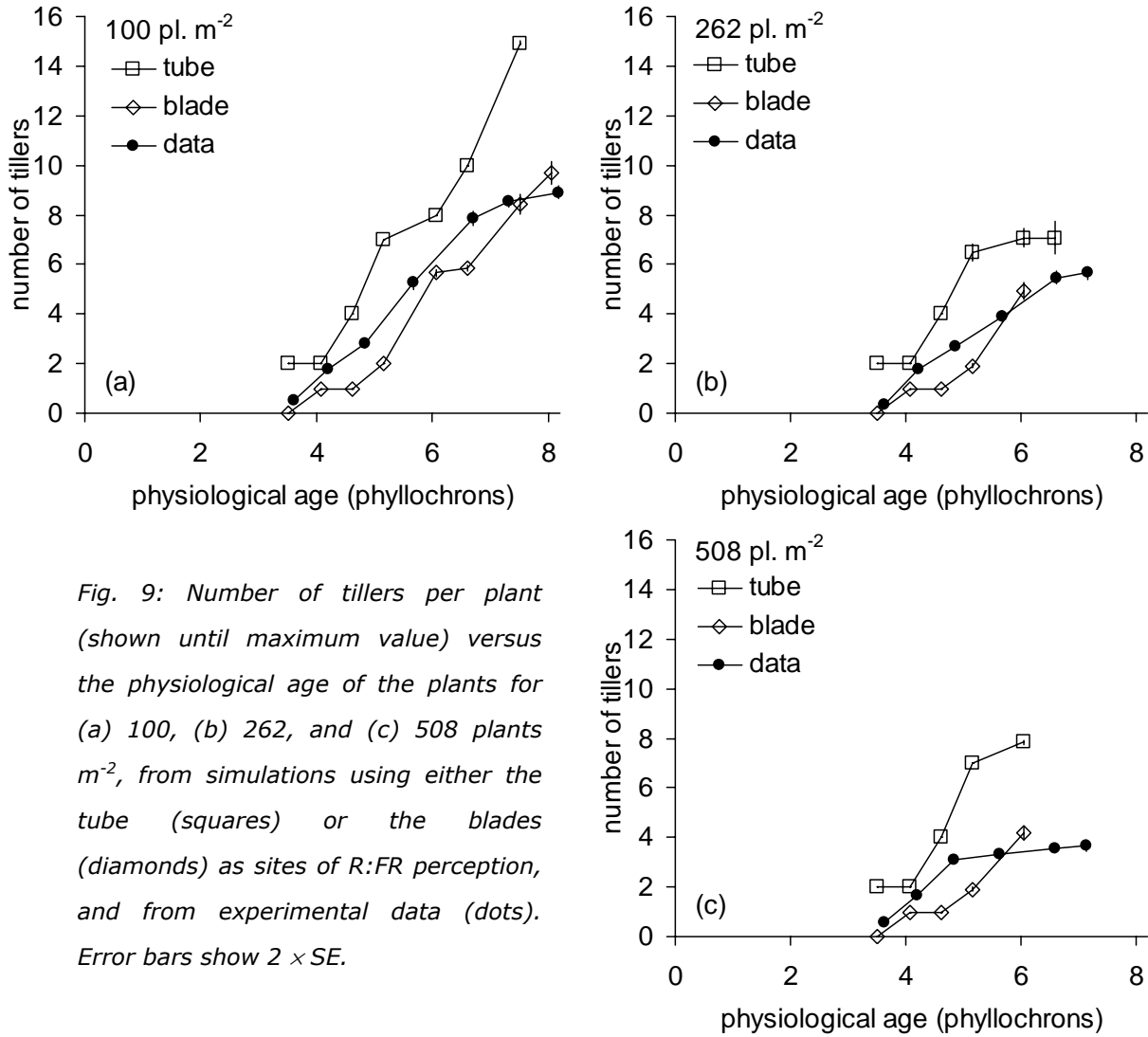
Fig. 9: Number of tillers per plant (shown until maximum value) versus the physiological age of the plants for (a) 100, (b) 262, and (c) 508 plants m^{-2}, from simulations using either the tube (squares) or the blades (diamonds) as sites of R:FR perception, and from experimental data (dots). Error bars show 2 × SE.

The probability of occurrence of individual tillers was either identical (both 1.0) or higher in the R_t-tube simulations than in the R_t-blade simulations (Fig. 11). Tillers t5 and t6 did not show this higher probability in comparison to their preceding tiller, in contrast to the P_t simulations (Fig. 11). Similar to the P_t simulations, the R_t-blade simulations showed a higher probability of occurrence for some highly ranked secondary tillers compared to the preceding tiller (t2.3 and t4.2 at 100 plants m^{-2}); this was not the case for the R_t-tube simulations. In the R_t-tube simulations at 100 plants m^{-2}, nearly all tillers had a probability of occurrence of 1.0, in contrast to the higher population densities. In both R_t-tube and R_t-blade simulations, probability of occurrence of primary tillers was higher than in the experimental data (Fig. 11) At population densities of 100 and 262 plants m^{-2}, the difference in LAI between the R_t-tube simulations and the R_t-blade simulations was small (Fig. 8 for 100 plants m^{-2}). Maximum LAI reached was
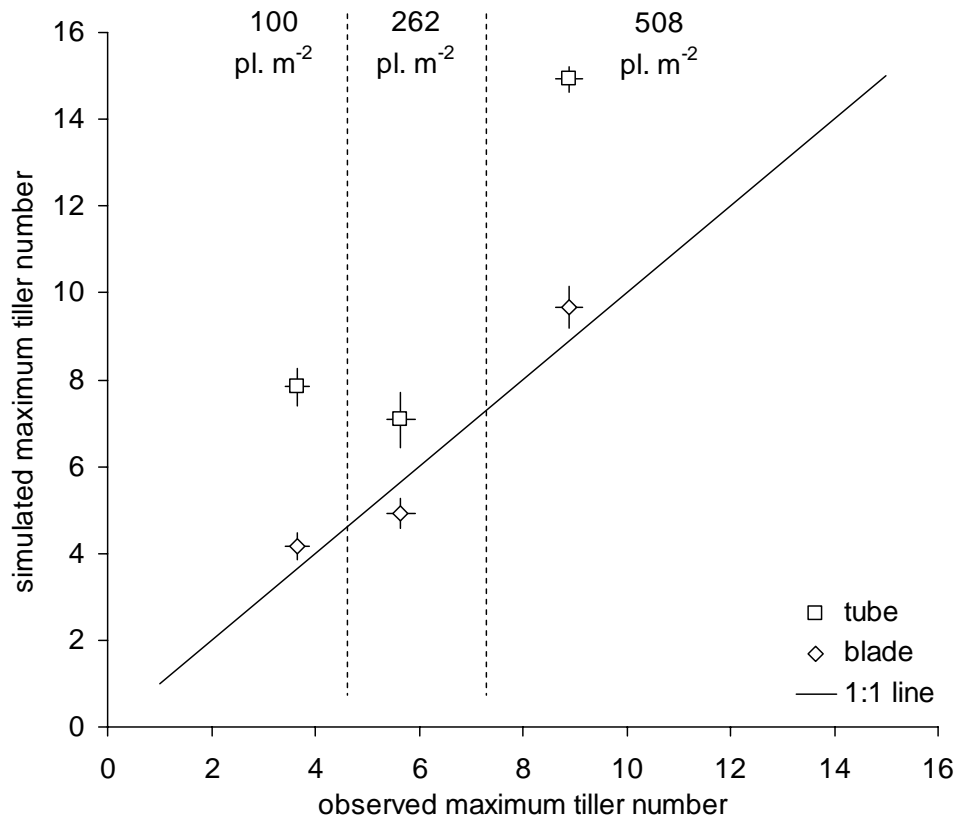
Fig. 10: Simulated vs. observed average maximum number of produced tillers per plant using either the tube (squares) or the blades (diamonds) as sites of R:FR perception. Error bars show 2 × SE.

10.0, 8.9 and 11.3 for the R_t-tube simulations and 8.9, 9.8 and 12.1 for the R_t-blade simulations at 100, 262 and 508 plants m^{-2}, respectively.

Discussion

Difference between tillers of low and high rank

In the P_t simulations and in the R_t-blade simulations the probability of occurrence for tillers t5 and t6 and for higher-ranked secondary tillers was in some cases higher than for tillers originating from lower phytomers. This was caused by their higher position in the canopy, and the consequent lower degree of shading the parent leaf blades of these tillers generally experienced compared to lower leaves. Consequently, P_{loc} and R:FR of these parent leaf blades decreased at a lower rate, which resulted in a higher probability for their tiller buds to grow out before the end of their window of opportunity. In the R_t-tube simulations this effect was never observed. This was caused by the fact that the tube was situated near soil level and not at increasing height in the canopy (like blades), and that
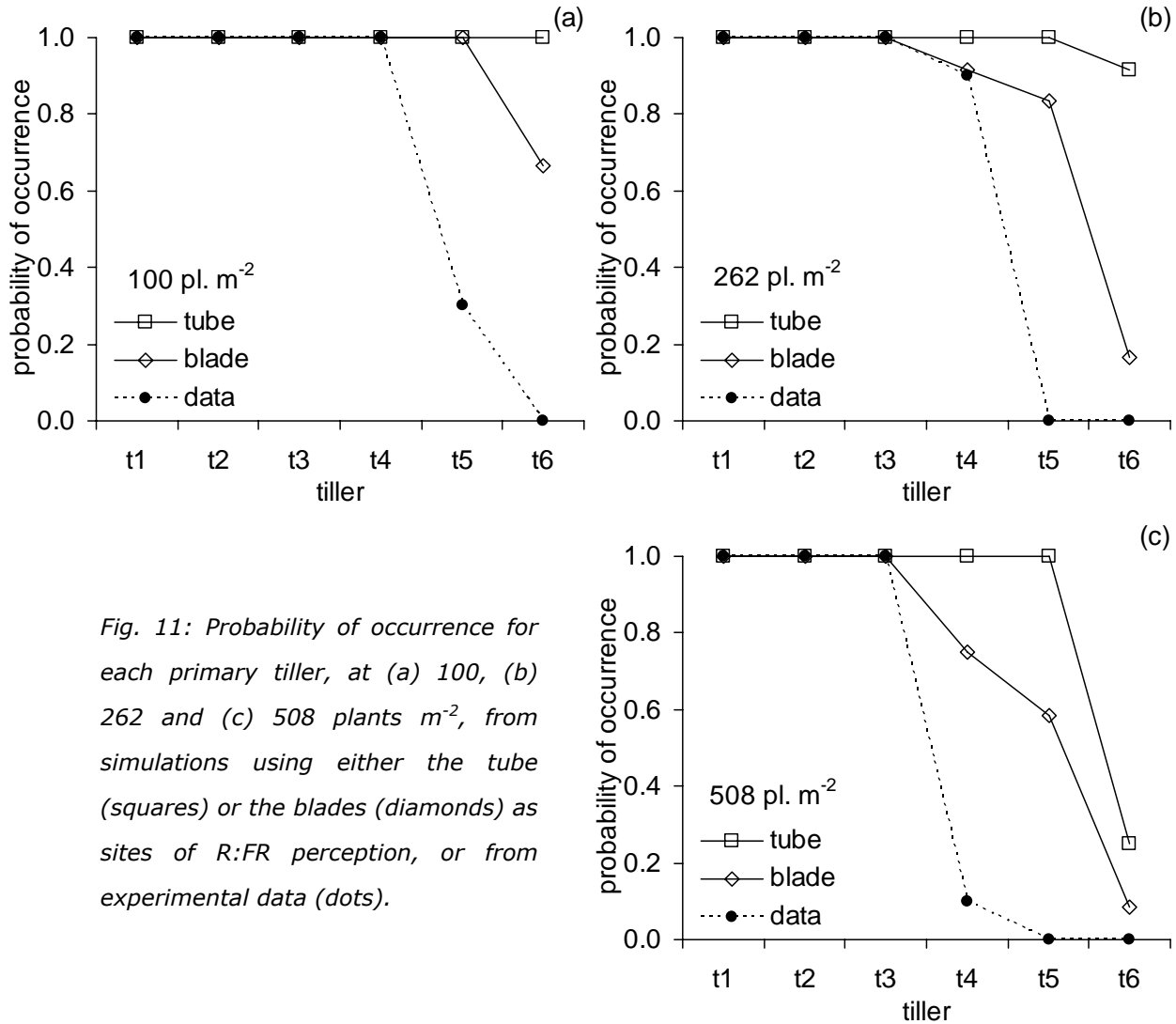
Fig. 11: Probability of occurrence for each primary tiller, at (a) 100, (b) 262 and (c) 508 plants m^{-2}, from simulations using either the tube (squares) or the blades (diamonds) as sites of R:FR perception, or from experimental data (dots).

the R:FR perceived by the tube equally affected every tiller bud on the plant. In the experimental data, higher probability of occurrence for higher-ranked tillers than for preceding tillers was never observed. In real plants t5 tillers sometimes developed but never survived, and t6 tillers never developed due to the lack of a developed tiller bud on the 6th phytomer. Implementation of conditional rules in the model that makes the presence of buds dependent on phytomer number could overcome the development of t6 tillers. However, the absence of a difference between the probabilities of occurrence of tillers of low and high rank in the R_t-tube simulations, supports the perception of R:FR by the tube of sheaths.

Tillering in relation to P_{loc} and R:FR

The divergence between plant population densities in the time course of tillering in the P_t simulations (Fig. 2) was similar to the experimental findings described in chapter 4, and in work reported by Van Oosterom *et al.* (2001) and Lafarge and Hammer (2002) for experiments with pearl millet and sorghum, respectively.

Increasing population density of the simulated plants apparently did not affect P_{loc} of the parent leaf blades during the early stage of development, since there was no effect on average number of tillers per plant during that stage. Indeed, the probability of occurrence (Fig. 7) for the tillers that appeared before a physiological age of 5 phyllochrons was fairly similar for the different population densities. This corroborates findings by Kirby and Faris (1972), who observed in barley that development of the first four tiller buds was not affected by population density (ranging from 50 to 1600 plants m^{-2}). The authors suggested a 'go / no go' type of tiller bud outgrowth as a basis for the observed patterns in tillering, instead of a gradual transition through modulation of early tiller growth. This corresponds to the absence of an effect of plant population density on the delay between the moments of appearance of a leaf and of its axillary tiller (chapter 4). The 'go / no go' suggestion is in line with the views of Williams and Langer (1975) and Williams and Metcalf (1975), who observed an abrupt increase in bud extension rate after a lag period. This transition was ascribed to the physical constraint exerted by sheath tissues that cover the bud, which either could or could not be overcome in time, resulting in 'go / no go' behaviour of tiller bud outgrowth. Such observations support the current implementation of tiller outgrowth in ADELwheat: tiller bud outgrowth either occurs or does not occur, but there is no modulation of growth rate.

The small differences between the P_t simulations (Fig. 8), and also between the R_t-blade and R_t-tube simulations, in the time course of LAI was the result of the relatively small contribution to total leaf area by the tillers that were present in conditions favouring tillers and absent in conditions restricting tillering. These were mainly the higher-ranked tillers, which only had a few leaves. Because of the small differences between the 'virtual treatments' (Fig. 8), the current implementation of bud outgrowth is suitable in case a prediction of LAI is the objective.

Site of R:FR perception

The R_t-tube simulations resulted in more tillers per plant than observed in the experiment, whereas the R_t-blade simulations resulted in fewer tillers per plant than observed in the experiment. Therefore, based on the current study, it cannot be decided which implemented mode of action produces tillering patterns the most closely mimicking reality. However, it is known that sheaths are sites of R:FR perception (Cordukes and Fisher, 1974), whereas fully grown leaf blades are not (Skinner and Simmons, 1993). Since predicted number of tillers in the R_t-tube simulations was higher than in the experimental data, it can be concluded that

tillering was not constrained to such an extent that accurate tiller numbers could be simulated. Apparently, perception by the tube of sheaths alone is not sufficient to model tillering kinetics in the current virtual plant model. Photomorphogenetic effects of R:FR perceived by the tube, combined with effects of shading on resource availability is likely to improve tillering kinetics of ADELwheat. This requires the incorporation of photosynthesis and carbon balance in the model, which is on our research agenda.

Overview and conclusions

Overall, the effects of population density on tillering kinetics agree with the expectations. When population density was increased, less light was intercepted by the parent leaf blades and therefore both P_{loc} and R:FR dropped below the critical thresholds for tillering cessation (P_t and R_t, respectively) earlier in development than at lower population densities, resulting in a reduction of tiller bud outgrowth. Also, in the P_t-simulations, when P_t was increased number of tillers per plant were generally lower as the threshold was exceeded at earlier stages of development.

Usually, photomorphogenetic effects are explained in terms of R:FR or blue light (reviewed in Franklin and Whitelam, 2005). It has been discussed (chapter 4) that the fraction of PAR intercepted by the canopy and R:FR are highly related. Also, it has been shown that reallocation of photosynthetic capacity (a physiological shade avoidance response) can be an effect of the light gradient in canopies, possibly due the increased transport of cytokinins through transpiration (Pons *et al.*, 2001). A similar mechanism may play a role in the effects on the morphological shade avoidance responses, such as reduced tillering. Bud outgrowth is known to be under the control of the auxin-cytokinin ratio (Cline, 1994), and the effect of P_{loc} on the transport of cytokinins may influence this ratio.

The inhibitory effect of a high population density on tiller number per plant in the P_t simulations is a result of both shading and self-shading, which are emergent properties of the model. Such emergent behaviour could also be observed in virtual plant models of trees presented recently (Allen *et al.*, 2005; Eschenbach, 2005; Sterck *et al.*, 2005), in which the effects of shading were due to decreased light intensity per leaf and the consequent reduction in photosynthesis. In contrast to changes in photosynthesis due to shading, photomorphogenetic effects exist to avoid shading instead of to react to it. Until now, these shade-avoidance responses (Aphalo *et al.*, 1999; Franklin and Whitelam, 2005) have only been simulated by Gautier *et al.* (2000) using a

virtual plant model of clover. In their study, petiole length, internode length and branching delay was calculated using empirical relations with local PAR intensity and R:FR. The main difference with the current approach is that in the clover model the responses of the abovementioned light-sensitive variables were continuous functions of both PAR intensity and R:FR, whereas in the current model the sensitive variable (degree of tillering) was basically unconstrained until a certain threshold in P_{loc} or R:FR was reached.

The tillering behaviour of the modelled plants as described in the current study was based on empirical relations derived from experiments. The mechanisms that underlie the relation between PAR intensity, R:FR and bud outgrowth were not included. Much more work needs to be done to explore the boundaries of virtual plant modelling in extending the interpretation, the testing and the extrapolation of plant physiological and ecological concepts. Tiller outgrowth and development requires assimilates, which a young tiller receives from its parent shoot (Rawson and Hofstra, 1969), and which a tiller starts to produce itself when it has developed an adequate amount of leaf area. Therefore, to model tiller outgrowth as a result of carbon partitioning, source activity, sink strength, and source-sink relationships (Heuvelink, 1996; Lacointe, 2000; Minchin and Lacointe, 2005) need to be quantified and included. If the signalling effects of R:FR on tillering (Ballaré *et al.*, 1987) are to be incorporated as well, phytochrome activity (Barnes and Bugbee, 1991) and possibly its relation to the auxin-cytokinin ratio (Tomlinson and O'Connor, 2004) also need to be quantified and included. This is a comprehensive task. Nevertheless, tillering behaviour in the current model displayed sensitivity to population density through the effects on the local light environment. This shows that a model that is based on relatively simple empirical relations can be used to simulate the dynamics of tiller development, without the need of full process integration.

The current study confirms the usability of the virtual plant approach based on L-systems (Měch and Prusinkiewicz, 1996; Měch, 1997) as a suitable platform to model environmental influence at the local level on the development of plants in a canopy, confirming previous studies (Fournier and Andrieu, 1999; Gautier *et al.*, 2000; de Visser *et al.*, 2004; Allen *et al.*, 2005). The NR model (Chelle and Andrieu, 1998) in combination with the CARIBU (Chelle *et al.*, 2004) interface provided a convenient method for calculating complex light properties such as R:FR. The modelling framework provides possibilities for further development, such as the incorporation of photosynthesis and carbon allocation and exploring the consequences of different hypotheses on R:FR effects on the chain of events leading to shade avoidance response.

Chapter 6

General discussion

In this thesis a virtual plant approach for modelling tillering in spring wheat has been presented. All important steps, ranging from model parameterisation to the final simulations, have been covered. This chapter presents and structures the understanding gained on several aspects of the modelled plant, and explores the possibilities and the limitations of the virtual plant modelling approach.

Vegetative development and architecture of wheat

Both the reparameterisation and the validation of ADELwheat have been instrumental in understanding the range of variation that can occur in several phenological and architectural aspects of vegetative wheat development. These aspects, which include the definition of the phytomer, leaf and tiller appearance, the concept of the relative phytomer number (RPN), and geometric features of wheat architecture, are discussed below.

The phytomer – The phytomer, or metamer, is the basic unit of the gramineous plant, giving rise to the modular organisation of plants of Gramineae. There are, however, different views on the sequence of the components a phytomer is composed of. The two most important views mainly differ with respect to the relative position of the leaf and the bud:

1. The 'axillary bud' view, in which the phytomer consists of (from bottom to top) node, leaf, internode with lateral bud at the bottom. Here, the bud resides in the axil of the leaf that belongs to the same phytomer, and therefore gets the same phytomer rank number (e.g. Kirby and Appleyard, 1981; Klepper *et al.*, 1982; Bos, 1999).

2. The 'opposite bud' view, in which the sequence is: node, internode with lateral bud at the bottom, leaf inserted at the top. In this view, the bud resides in the axil of the leaf of the previous phytomer, and is consequently placed opposite to the leaf of the same phytomer (e.g. Briske, 1991; Moore and Moser, 1995). Here the bud, and the tiller that grows from it, do not have the same rank number as the subtending leaf, but one rank higher.

In this thesis, the second view is used (chapter 2, Fig. 1). It has been argued (Fletcher and Dale, 1974) that a tiller bud, once initiated, is not dependent on the subtending leaf in terms of nutrition, but on the leaf above it. This was supported by both anatomical analysis and by an analysis of the relation between photosynthetic activity of the leaf and the growth of the bud below it. The dependency of bud on the leaf above it supports the second view, in which these organs have the same phytomer rank number. Moreover, it has the advantage

that the coleoptile tiller bud receives rank number 1, instead of the awkward but commonly used rank number 0.

Leaf and tiller appearance – In Gramineae the thermal time between the moments of appearance of two successive leaves (the phyllochron) is highly dependent on cultivar and light. Cultivar dependency was evident from the reparameterisation from winter to spring wheat and from literature (Cao and Moss, 1989; Pararajasingham and Hunt, 1995; Hay, 1999), and light dependency was discussed in terms of photoperiod (Volk and Bugbee, 1991; Brooking *et al.*, 1995) and light intensity (chapter 3, Birch *et al.*, 1998; Bos and Neuteboom, 1998a; Bos *et al.*, 2000). The phenomenon that early leaves have a higher rate of appearance than later leaves (as was discussed in chapter 3 appendix B), seems to be a general phenomenon (Jamieson *et al.*, 1995; Abeledo *et al.*, 2004).

As was discussed in chapter 3, plant population density did not have a substantial effect on phyllochron, which was in line with data presented by Casal (1990) and Bos (1999). Population density also did not affect tiller appearance delay, but the number of tillers produced per plant did differ between population densities (chapter 4). In spring wheat, tillers appeared roughly at intervals of one phyllochron (Hay, 1999) and the sequence of appearance within the same order of tillers was always the same (e.g. t4 never appeared before t3 did). Reduced light intensity did delay tiller appearance (chapters 3 and 4), irrespective of modulating effects on the duration of the phyllochron.

Relative phytomer number – The concept of relative phytomer number (RPN), which was introduced for ADELwheat in Fournier *et al.* (2003), appears to be a robust concept to simplify the modelling of tiller organ properties. RPN, i.e. the (fractional) main stem phytomer number from which tiller organ properties are derived, is obtained by adding a specific 'phytomer shift' value to the actual rank number of the phytomer. It has been shown in chapters 2 and 3 that properties of tiller organs such as the lengths of blades, sheaths and internodes can be modelled using one tiller specific phytomer shift value. Not only is the concept general, but also the shift values themselves are quite stable: the winter and spring wheat cultivars used did not show much difference in RPN values (chapter 2 and Fournier *et al.*, 2003), and also the contrasting growth conditions of a growth chamber compared to outdoors hardly affected the RPN values (chapter 3).

A more general approach using the concept of summed phytomer number (SPN) (Bos and Neuteboom, 1998b; Tivet *et al.*, 2001; Buck-Sorlin, 2002; Yan *et*

al., 2004) seems appropriate in case detailed measurements on tiller organ properties are not available, and in case the development of a general Gramineae model is the goal. In this view, a tiller organ gets a rank number which is the sum of all phytomers from the base of the plant to the organ in question. For example, leaf 5 on primary tiller 2 would get rank number 7, and would therefore have the same properties as main stem leaf 7. Note that this system depends on the view on the sequence of organs on a phytomer and the consequent numeration (see above). Concepts like RPN and SPN reflect a similarity in ontogenic pattern between main stem and tiller phytomers with the same RPN or SPN, in spite of the difference in time of initiation. This is an indication of common mechanisms in the determination of that ontogenic pattern.

Geometric features – In the original winter wheat model blade insertion angle and curvature were defined as stochastic elements of the model (i.e. differing each simulation run). This stochasticity was maintained for spring wheat (chapter 2), as the use of angle distributions instead of fixed parameters did justice to the observed variation. The function used for the description of leaf blade angle and curvature (Prévot *et al.*, 1991) was appropriate for spring wheat, winter wheat (Fournier *et al.*, 2003) and maize (Fournier and Andrieu, 1998), and since the function is highly flexible it can be used for probably any Gramineae leaf blade type.

Leaf azimuth, the angle between successive leaves on a stem, was a second stochastic element. In the case of wheat sown in regular grids, as was done in the experiments described in this thesis, a more simplified approach may be used to characterise leaf azimuth: 180º for leaves with RPN values 1 to 3, and uniform distribution for all other leaves. This simplification can be derived from the histograms shown in chapter 2, Fig. 10. However, for maize planted in rows it is observed that leaves can alter their azimuth to minimise self shading, which is mediated by light signals (Maddonni *et al.*, 2002). In that case a fixed parameterisation, i.e. not influenced by light conditions, probably represents a too high degree of simplification.

Tillering and its determinants
The analysis of the effects of plant population density and shading on the tillering pattern of spring wheat has yielded an interesting conclusion: irrespective of the developmental stage of the plants, the population density, the light treatment, or the rank number of the tiller, new tillers cease to appear at a certain fraction of PAR intercepted (P_{int}) by the canopy (chapter 4). A similar conclusion can be

drawn when regarding the red/far-red ratio (R:FR) instead of P_{int}, although here differences could be observed between the full light and shaded plants. There are literature reports indicating that tiller appearance halts at a specific point in canopy (LAI) development, and suggestions were made that this was caused by the decrease in PAR intensity or by photomorphogenetic effects (Simon and Lemaire, 1987; Lafarge and Hammer, 2002). The current study supports the latter suggestion.

However, it has not become fully clear whether the primary determinant is P_{int} or R:FR. Most likely the two are a manifestation of the same mechanism, being the photomorphogenetic response of the plant in the phytochrome photoequilibrium (Pr:Pfr) (Smith, 2000), mediated by the R:FR of the light. The fact that the effect can be observed through P_{int} is caused by the relation between P_{int} and R:FR. This relation is shown in chapter 4 Fig. 1c, and it can be reasoned as well: P_{int} can be regarded as the fraction of foliage and stems 'seen' from the leaf level, in all directions. The remainder is the fraction of sky. Light that is reflected and transmitted by the surrounding foliage and stems has a decreased intensity in the red region of the spectrum compared to far-red (Holmes and Smith, 1977), in contrast to the light directly coming from the sky (R:FR approximately 1.15). Therefore, an increase in P_{int} is likely to be related to a decrease in R:FR. The P_{int} and R:FR data shown in chapter 4 Fig. 1c are in fact highly correlated (Pearson's r = 0.92, P<0.01).

The relation between outgrowth of a tiller bud and LMA (leaf mass per unit leaf area) of the leaf that was associated with it (the parent leaf, sharing phytomer rank number with the tiller bud) was discussed to be caused by photomorphogenetic effects. A reduced R:FR was argued to induce both LMA decrease and reduced tillering, which are typical shade avoidance responses (Franklin and Whitelam, 2005). This was in contrast to an earlier hypothesis (Bos, 1999) stating that a reduction in PAR intensity causes the decrease in LMA of the parent leaves, leading to reduced tiller bud outgrowth. Therefore, it is conceivable that LMA of a leaf reflects the physiological state of the whole plant (affected by photomorphogenetic influences) rather than the local conditions of growth and the functioning of the leaf itself.

The fact that global[1] tiller numbers of plant in a microcanopy could be simulated using local stimuli (chapter 5) supports the view of local responses to the environment. It confirms the usability of virtual plant modelling to simulate global effects of local influences. However, it was clear that tillering constrained

---

[1] In the context of modelling 'global' refers to properties specified at the level of plant or canopy, and 'local' to properties specified at the level of individual organs.

only by thresholds in fraction of PAR intercepted or R:FR was not enough for consistent prediction of tiller production. When constrained by the fraction of PAR intercepted, production of tillers of a high rank was overestimated; when constrained by R:FR, production of all tillers was overestimated. The integration of photosynthesis and carbon allocation throughout the plant is likely to improve the simulation of tillering dynamics.

Extensions of ADELwheat

ADELwheat, in its current state, is adapted to be used for tillering studies in relation to light conditions in spring wheat. However, without any modification, it can be used to study, for example, canopy closure in relation to population density, or PAR interception by leaves in various layers in the canopy. Very small modifications enable the possibility to study, for example, the effect of non-tillering wheat mutants on leaf area development in relation to population density or inter row distance, or the effect of changes in the angle of the solar trajectory on R:FR signals within the wheat canopy.

Furthermore, relatively simple descriptive extensions of the model may already enhance performance and versatility. For example, in the current model the final number of leaves produced on the wheat shoots is a value depending on shoot number, but entirely independent of environmental variables or growing conditions. In chapter 3 (Fig. 4) it has been shown that a high level of shading decreased the final number of produced leaves. Also, it is known that in spring wheat, final leaf number is influenced by environmental factors including temperature and photoperiod (Rawson and Zajac, 1993; Brooking *et al.*, 1995). An empirical relationship between final leaf number and photoperiod has been developed (Jamieson *et al.*, 1998) and can be incorporated into the model as a subroutine for calculation of final leaf number on a shoot.

A considerable step forward can be expected when the empirical (descriptive) relations that currently drive plant development in the model are replaced by mechanisms based on the actual processes that underlie plant growth (Fig. 1). This can be done by adding carbon gain and partitioning ('functionality') to the current model in order to obtain a complete 3D functional-structural model of a canopy of wheat plants. From a given spatial arrangement of plants, the model can then calculate growth and development, size, shape and orientation in space of each organ in relation to temperature and light absorbed by each element of the canopy. In addition to this, the model can be extended with R:FR sensitivity through phytochrome action at the sites of perception, by changing the status of a phytochrome parameter from Pr to Pfr or vice versa. This change in
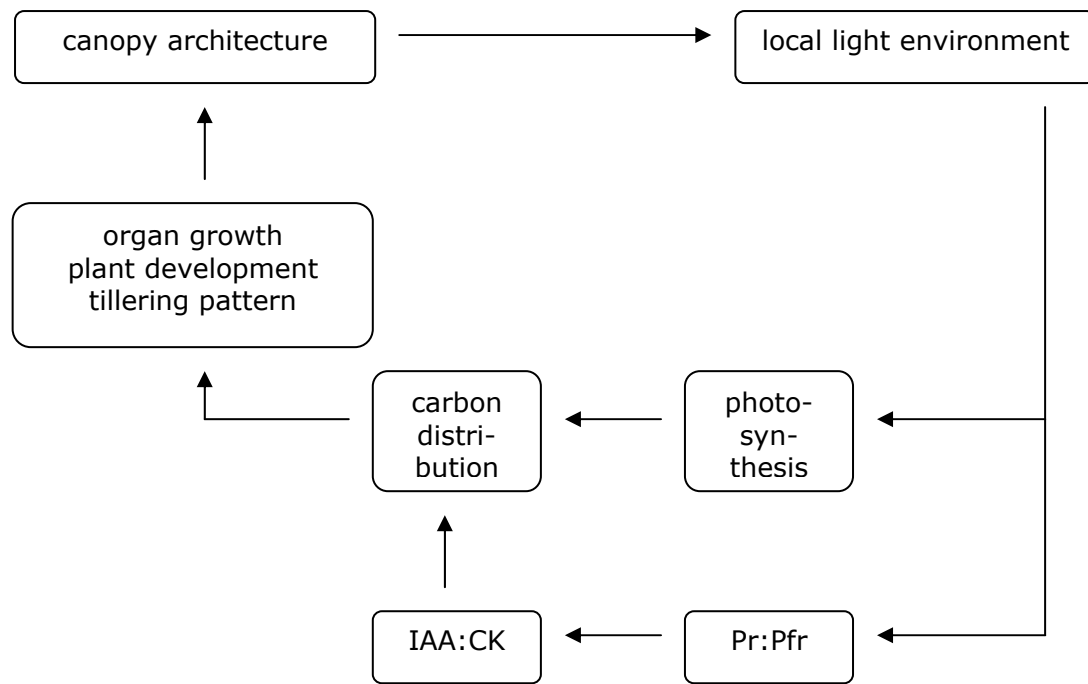
Fig. 1: A process-based feedback mechanism which can be used in a virtual plant modelling approach. The canopy architecture determines the local light environment within the canopy. This affects the photosynthetic rate and the subsequent distribution of carbon through the plant, and also the phytochrome photoequilibrium (Pr:Pfr) and the consequent auxin:cytokinin ratio (IAA:CK). These processes affect organ growth, plant development and the tillering pattern of the wheat plants. This, in turn, determines the canopy architecture, completing the circle.

the phytochrome photoequilibrium (Pr:Pfr) can trigger a change in level of auxin (IAA) production or transport through the plant, and consequently change the auxin/cytokinin ratio (IAA:CK). This ratio changes the degree of bud outgrowth suppression controlled by apical dominance (Cline, 1994).

Emerging properties of these types of process integration can be for example tiller senescence or whole plant death (i.e. self thinning behaviour), and typical shade avoidance responses (Franklin and Whitelam, 2005) such as enhanced leaf and stem elongation, altered leaf angle, and tiller bud outgrowth.

Possibilities for future research using ADELwheat

In the current study, ADELwheat is used to simulate tillering in relation to light conditions. However, the model is suitable or can be made suitable for various other purposes, such as:

- *Crop-weed interaction*. Extending the model with L-system representations of weeds could elucidate some of the components of competition between the wheat crop and the weed. A study of the effects of shading by the weed is

very well feasible; it would require the construction of L-systems for specific weeds, or for example one L-system representing a 'general' broad-leaved weed.

- *Crop-herbivore interactions*. The explicit geometrical description of the wheat plants allows for simulation of insect (or other herbivores) movement and feeding, and the consequent compensatory growth. Examples include Prusinkiewizc *et al.* (1997), Hanan *et al.* (2002) and Skirvin (2004).

- *Belowground competition*. The extension of the model with a spatially explicit 3D root system can make simulation of competition for soil water and nitrogen between the wheat plants possible. 3D roots systems have been modelled by e.g. Shibusawa (1992) and Pagès *et al.* (2004).

- *Remote sensing studies.* The use of the original winter wheat version of ADELwheat (Fournier *et al.*, 2003) for remote sensing studies has been shown by Lewis *et al.* (2004); the current model for spring wheat could be applied in a similar way.

When the focus of the research question lies at a scale level that is higher than the range of levels used in the current research (plant organ, individual plant, and microcanopy), i.e. the field level, the usability of the approach depends on two factors:

1. The necessity of using a virtual plant approach. The high accuracy of estimation of PAR interception due to multiple scattering of light, which is possible with a virtual plant approach, might be appealing, but it is questionable whether the level of detail is necessary when one is interested in, for example, yield prediction. An approach that contains considerably less or no geometric detail (for example a layer approach) may already be more than sufficient and equally accurate. When taking into account the robust mechanisms of photosynthesis and partitioning that are usually part of such models, yield prediction is probably best done using a process-based model designed for this task.

2. The practical feasibility of a virtual plant approach. Simulation at the field level requires simulation of numerous virtual plants, each plant at the same high level of detail. With the current power of regular personal computers, this is hardly feasible. When disregarding light interception and multiple scattering, simulation of entire fields of plants is possible, but this omission will probably be unacceptable for most research questions in the field of agronomy and plant (photo)biology.

Limitations of the approach

Although the applicability of the model to the research questions posed in this thesis has been demonstrated, several limitations of the current approach can be identified:

- The model can be used for a wide range of varieties or growing conditions, but each new application requires moderate to considerable recalibration of at least a part of the parameters and functions. Although several components in the model have been shown to be general for both winter and spring wheat and even other species of Gramineae (chapter 2), features such as number of leaves produced on a stem, the rate of development, and width and curvature of the leaf blades appear to be dependent on conditions during development and/or on species or variety. However, several features, such as the shape of curve describing the blade length along the shoot, can be regarded as generic for wheat (or Gramineae) and therefore only need refitting of the coefficient values that describe the relations.

- As discussed above, the mechanisms incorporated into the model that prevent tiller bud outgrowth based on light conditions inside the canopy, are based on empirical relations and not on the actual physiological processes inside the plant that drive tiller growth (photosynthesis, carbon and nitrogen partitioning, hormone action, etc.). This limits the usability of the model to expand our understanding of the relation between the physiological basis of tillering and its determinants.

- Although the computational power of processors that come with modern personal computers has dramatically increased during the last decades, virtual plant modelling can take up a considerable amount of simulation time. This is especially true in the case of the current model, in which light properties are calculated at the organ level. Speeding up simulation speed is possible in several ways, e.g. by reducing the number of plants in the canopy, the number of triangles used to represent one plant, or the number of light sources in the virtual hemisphere. Fortunately, computational power increases rapidly, thereby constantly providing new possibilities for more comprehensive simulation models.

Main conclusions

The main conclusions that have been drawn in this thesis are:

1. Most of the parameterised functions and coefficients in ADELwheat can be regarded as generic for wheat, or even for Gramineae. Nevertheless, the introduction of more generic components is necessary if a 'template' model for

Gramineae is the objective. An example of this is the introduction of the concept of summed phytomer number, as was explained in chapter 2.

2. ADELwheat (with forced tillering, i.e. not dependent on light conditions) is capable of simulating development of wheat in growth conditions (plant density, light conditions) for which the model was not calibrated; however refitting some key coefficients accounting for the effects of population density and shading yields still better results. As an architectural closed L-system model, it can be used for remote sensing studies or plant-herbivore interactions.

3. At least for the spring wheat cultivar used in this thesis, appearance of new tillers ceases at specific light conditions in the canopy (fraction PAR intercepted, R:FR), irrespective of plant population density in the range of 100 to 508 plants m^{-2}, and to a lesser extent of reduction of light intensity. Based on current results, the previously hypothesised link between outgrowth of a tiller bud and LMA (leaf mass per unit leaf area) of its parent leaf is best explained by photomorphogenetic effects of R:FR, inducing both LMA decrease (leaf area maximisation) and reduced tillering.

4. Virtual plant modelling using open L-systems is a robust approach for modelling the local and global effects of local stimuli on plant development. The effects of plant population density on tiller production could be modelled using simple 'go / no go' rules for tiller bud outgrowth, dependent on fraction PAR intercepted and on the red/far-red ratio.

Overall, this thesis has shown that virtual plant modelling has unique virtues in analysing relevant crop physiological problems. It has also demonstrated that the virtual plant modelling approach can provide insight into the factors that determine the developmental plasticity of wheat in terms of tillering.

References

Abeledo LG, Calderini DF, Slafer GA. 2004. "Leaf appearance, tillering and their coordination in old and modern barleys from Argentina." *Field Crops Research* 86: 23-32.

Allen M, Prusinkiewicz P, DeJong T. 2004. "Using L-systems of modelling the architecture and physiology of growing trees: the L-PEACH model." In Godin C, Hanan JS, Kurth W, Lacointe A, Takenaka A, Prusinkiewicz P, DeJong T, Beveridge C and Andrieu B, eds. *4th International Workshop on Functional-Structural Plant Models*. Montpellier, France: UMR AMAP, 220-225.

Allen MT, Prusinkiewicz P, DeJong TM. 2005. "Using L-systems for modeling source-sink interactions, architecture and physiology of growing trees: the L-PEACH model." *New Phytologist* 166: 869-880.

Andrieu B. 1982. *Evaluation des données fournies par la teledetection aerospatiale pour l'étude multithématique d'un massif forestier.* PhD thesis, University of Paris / INRA Bioclimatologie Versailles, France. 196 pp.

Andrieu B, Allirand JM, Jaggard K. 1997. "Ground cover and leaf area index of maize and sugar beet crops." *Agronomie* 17: 315-321.

Andrieu B, Moulia B, Maddonni GA, Birch CJ, Sonohat G, Sohbi Y, Fournier C, Allirand JM, Chartier M, Hillier J, Drouet J-L, Bonhomme R. 2004. "Plasticity of plant architecture in response to density: using maize as a model." In Godin C, Hanan JS, Kurth W, Lacointe A, Takenaka A, Prusinkiewicz P, DeJong T, Beveridge C and Andrieu B, eds. *4th International Workshop on Functional-Structural Plant Models*. Montpellier, France: UMR AMAP, 141-145.

Aphalo PJ, Ballaré CL, Scopel AL. 1999. "Plant-plant signalling, the shade-avoidance response and competition." *Journal of Experimental Botany* 50: 1629-1634.

Bahmani I, Hazard L, Varlet-Grancher C, Betin M, Lemaire G, Matthew C, Thom ER. 2000. "Differences in tillering of long- and short-leaved perennial ryegrass genetic lines under full light and shade treatments." *Crop Science* 40: 1095-1102.

Baker CK, Gallagher JN. 1983. "The development of winter wheat in the field. 1. Relation between apical development and plant morphology within and between seasons." *Journal of Agricultural Science* 101: 327-335.

Ballaré CL, Sanchez RA, Scopel AL, Casal JJ, Ghersa CM. 1987. "Early detection of neighbour plants by phytochrome perception of spectral changes in reflected sunlight." *Plant, Cell and Environment* 10: 551-557.

Barnes C, Bugbee B. 1991. "Morphological responses of wheat to changes in phytochrome photoequilibrium." *Plant Physiology* 97: 359-365.

Barnes C, Bugbee B. 1992. "Morphological response of wheat to blue light." *Journal of Plant Physiology* 139: 339-342.

Birch CJ, Vos J, Kiniry J, Bos HJ, Elings A. 1998. "Phyllochron responds to acclimation to temperature and irradiance in maize." *Field Crops Research* 59: 187-200.

Birch CJ, Andrieu B, Fournier C. 2002. "Dynamics of internode and stem elongation in three cultivars of maize." *Agronomie* 22: 511-524.

Bos HJ, Neuteboom JH. 1998a. "Morphological analysis and tiller number dynamics of wheat (*Triticum aestivum* L.): responses to temperature and light intenstity." *Annals of Botany* 81: 131-139.

Bos HJ, Neuteboom JH. 1998b. "Growth of individual leaves of spring wheat (*Triticum aestivum* L.) as influenced by temperature and light intensity." *Annals of Botany* 81: 141-149.

Bos HJ. 1999. *Plant morphology, environment, and leaf area growth in wheat and maize.* PhD thesis, Wageningen UR, the Netherlands. 149 pp.

Bos HJ, Tijani-Eniola H, Struik PC. 2000. "Morphological analysis of leaf growth of maize: responses to temperature and light intensity." *Netherlands Journal of Agricultural Science* 48: 181-198.

Briske DD. 1991. "Developmental morphology and physiology of grasses." In: Heitschmidt RK and Stuth JW, eds. *Grazing management: an ecological perspective*. Portland, OR, USA: Timber Press, Inc. 85-108.

Brooking IR, Jamieson PD, Porter JR. 1995. "The influence of daylength on final leaf number in spring wheat." *Field Crops Research* 1995: 155-165.

Brooking IR, Jamieson PD. 2002. "Temperature and photoperiod response of vernalisation in near-isogenic lines of wheat." *Field Crops Research* 79: 21-38.

Buck-Sorlin GH. 2002. "L-system model of the vegetative growth of winter barley." In Polani D, Kim J and Martinez T, eds. *Fifth German Workshop on Artificial Life*. Lübeck, Germany: Akademische Verlagsgesellschaft Aka GmbH, Berlin, 53-64.

Cao W, Moss DN. 1989. "Daylength effect on leaf emergence and phyllochron in wheat and barley." *Crop Science* 29: 1021-1025.

Casal JJ, Deregibus VA, Sanchez RA. 1985. "Variations in tiller dynamics and morphology in *Lolium multiflorum* Lam. Vegetative and reproductive plants as affected by differences in red/far-red irradiation." *Annals of Botany* 56: 553-559.

Casal JJ, Sanchez RA, Deregibus VA. 1986. "The effect of plant density on tillering: the involvement of R/FR ratio and the proportion of radiation intercepted per plant." *Environmental and Experimental Botany* 26: 365-371.

Casal JJ, Sanchez RA, Deregibus VA. 1987a. "Tillering responses of *Lolium multiflorum* plants to changes of red/far-red ratio typical of sparse canopies." *Journal of Experimental Botany* 38: 1432-1439.

Casal JJ, Sanchez RA, Deregibus VA. 1987b. "The effect of light quality on shoot extension growth in three species of grasses." *Annals of Botany* 59: 1-7.

Casal JJ. 1988. "Light quality effects on the appearance of tillers of different order in wheat *(Triticum aestivum)*." *Annals of Applied Biology* 112: 167-173.

Casal JJ, Sanchez RA, Gibson D. 1990. "The significance of changes in the red/far-red ratio, associated with either neighbour plants or twilight, for tillering in *Lolium multiflorum* Lam." *New Phytologist* 116: 565-572.

Cattani DJ, Struik PC, Nowak JN. 2002. "Comparative morphological development of divergent flowering types of annual bluegrass and tillering types of creeping bentgrass." *Crop Science* 42: 1251-1258.

Chelle M, Andrieu B. 1998. "The nested radiosity model for the distribution of light within plant canopies." *Ecological Modelling* 111: 75-91.

Chelle M, Andrieu B, Bouatouch K. 1998. "Nested radiosity for plant canopies." *The Visual Computer* 14: 109-125.

Chelle M, Andrieu B. 1999. "Radiative models for architectural modelling." *Agronomie* 19: 225-240.

Chelle M, Hanan JS, Autret H. 2004. "Lighting virtual crops: the CARIBU solution for open L-systems." In Godin C, Hanan JS, Kurth W, Lacointe A, Takenaka A, Prusinkiewicz P, DeJong T, Beveridge C and Andrieu B, eds. *4th International Workshop on Functional-Structural Plant Models*. Montpellier, France: UMR AMAP, 194.

Cline MG. 1994. "The role of hormones in apical dominance. New approaches to an old problem in plant development." *Physiologia Plantarum* 90: 230-237.

Cordukes WE, Fisher JE. 1974. "Effects of shading of the leaf sheath on the growth and development of the tiller stems of Kentucky bluegrass." *Canadian Journal of Plant Science* 54: 47-53.

Darwinkel A. 1978. "Patterns of tillering and grain production of winter wheat at a wide range of plant densities." *Netherlands Journal of Agricultural Science* 26: 383-398.

Davies A. 1971. "Changes in growth rate and morphology of perennial ryegrass swards at high and low nitrogen levels." *Journal of Agricultural Science* 77: 123-134.

Davies A, Thomas H. 1983. "Rates of leaf and tiller production in young spaced perennial ryegrass plants in relation to soil temperature and solar radiation." *Annals of Botany* 57: 591-597.

Davis MH, Simmons SR. 1994. "Tillering response of barley to shifts in light quality caused by neighbour plants." *Crop Science* 34: 1604-1610.

de Visser PHB, Marcelis LFM, van der Heijden GWAM, Vos J, Struik PC, Evers JB. 2002. "3D modelling of plants: a review". Wageningen: Plant Research International. 38.

de Visser PHB, Marcelis LFM, van der Heijden GWAM, Angenent GC, Evers JB, Struik PC, Vos J. 2004. "Incorporation of 3D plant structures in genetic and physiological models." *Acta Horticulturae* 654: 171-178.

de Wit CT, Goudriaan J, Laar HHv, Penning de Vries FWT, Rabbinge R, van Keulen H, Sibma L, de Jonge C. 1978. *Simulation of assimilation, respiration and transpiration of crops.* Simulation Monographs, Pudoc, Wageningen.141 pp.

Deregibus VA, Sanchez RA, Casal JJ. 1983. "Effects of light quality on tiller production in *Lolium* spp." *Plant Physiology* 72: 900-902.

Drouet J-L. 2003. "MODICA and MODANCA: modelling the three-dimensional shoot structure of gramineous crops from two methods of plant description." *Field Crops Research* 83: 215-222.

Drouet J-L, Pagès L. 2003. "GRAAL: a model of GRowth, Architecture and carbon ALlocation during the vegetative phase of the whole maize plant - model description and parameterisation." *Ecological Modelling* 165: 147-173.

Elings A, Rossing WAH, Van der Werf W. 1999. "Virtual lesion extension: a measure to quantify the effects of bacterial blight in rice leaf CO_2 exchange." *Analytical and Theoretical Plant Pathology* 89: 789-795.

Eschenbach C. 2005. "Emergent properties modelled with the functional structural tree growth model ALMIS: Computer experiments on resource gain and use." *Ecological Modelling* 186: 470.

Fletcher GM, Dale JE. 1974. "Growth of tiller buds in barley: effects of shade treatment and mineral nutrition." *Annals of Botany* 38: 63-76.

Fournier C, Andrieu B. 1998. "A 3D architectural and process-based model of maize development." *Annals of Botany* 81: 233-250.

Fournier C, Andrieu B. 1999. "ADEL-maize: an L-system based model for the integration of growth processes from the organ to the canopy. Application to regulation of morphogenesis by light availability." *Agronomie* 19: 313-327.

Fournier C, Andrieu B. 2000a. "Dynamics of the elongation of the internodes in maize (*Zea mays* L.): analysis of phases of elongation and their relationships to phytomer development." *Annals of Botany* 86: 551-563.

Fournier C, Andrieu B. 2000b. "Dynamics of the elongation of the internodes in maize (*Zea mays* L.). effects of shade treatment on elongation patterns." *Annals of Botany* 86: 1127-1134.

Fournier C, Andrieu B, Ljutovac S, Saint-Jean S. 2003. "ADEL-wheat: a 3D architectural model of wheat development." In Hu BG and Jaeger M, eds. *2003' International Symposium on Plant Growth Modeling, Simulation, Visualization, and their Applications*. Beijing, China PR: Tsinghua University Press / Springer, 54-63.

Fournier C, Durand J-L, Ljutovac S, Schäufele R, Gastal F, Andrieu B. 2004. "A functional-structural model of the elongation of the grass leaf and of its relationships to the phyllochron." In Godin C, Hanan JS, Kurth W, Lacointe A, Takenaka A, Prusinkiewicz P, DeJong T, Beveridge C and Andrieu B, eds. *4th International Workshop on Functional-Structural Plant Models*. Montpellier, France: UMR AMAP, 98-104.

Franklin KA, Whitelam GC. 2005. "Phytochromes and shade-avoidance responses in plants." *Annals of Botany* 96: 169-175.

Gallagher JN. 1979. "Field studies of cereal leaf growth. I. Initiation and expansion in relation to temperature and ontogeny." *Journal of Experimental Botany* 30: 625-636.

Gautier H, Varlet-Grancher C, Hazard L. 1999. "Tillering responses to the light environment and to defoliation in populations of perennial ryegrass (*Lolium perenne* L.) selected for contrasting leaf length." *Annals of Botany* 83: 423-429.

Gautier H, Měch R, Prusinkiewicz P, Varlet-Grancher C. 2000. "3D Architectural modelling of aerial photomorphogenesis in white clover (*Trifolium repens* L.) using L-systems." *Annals of Botany* 85: 359-370.

Godin C. 2000. "Representing and encoding plant architecture: a review." *Annals of Forest Science* 57: 413-438.

Godin C, Sinoquet H. 2005. "Functional-structural plant modelling." *New Phytologist* 166: 705-708.

Gomez-Macpherson H, Richards RA, Masle J. 1998. "Growth of near-isogenic wheat lines differing in development - plants in a simulated canopy." *Annals of Botany* 82: 323-330.

Goral CM, Torrance KE, Greenberg DP, Battaile B. 1984. "Modeling the interaction of light between diffuse surfaces." *Computer Graphics* 18: 213-222.

Goudriaan J. 1988. "The bare bones of leaf-angle distribution in radiation models for canopy photosynthesis and energy exchange." *Agricultural and Forest Meteorology* 43: 155-169.

Hanan JS, Prusinkiewicz P, Zalucki M, Skirvin D. 2002. "Simulation of insect movement with respect to plant architecture and morphogenesis." *Computers and Electronics in Agriculture* 35: 255-269.

Hanan JS, Hearn AB. 2003. "Linking physiological and architectural models of cotton." *Agricultural Systems* 75: 47-77.

Haun JR. 1973. "Visual quantification of wheat development." *Agronomy Journal* 65: 116-119.

Hay RKM, Kirby EJM. 1991. "Convergence and synchrony - a review of the coordination of development in wheat." *Australian Journal of Agricultural Research* 42: 661-700.

Hay RKM. 1999. "Physiological control of growth and yield in wheat: analysis and synthesis." In: Smith DL and Hamel C, eds. *Crop Yield, Physiology and Processes*. New York: Springer-Verlag. 1-33.

Heuvelink E. 1996. "Dry matter partitioning in tomato: validation of a dynamic simulation model." *Annals of Botany* 77: 71-80.

Holmes MG, Smith H. 1977. "The function of phytochrome in the natural environment. 2. Influence of vegetation canopies on spectral energy-distribution of natural daylight." *Photochemistry and Photobiology* 25: 539-545.

Hotsonyame GK, Hunt LA. 1997. "Effects of sowing date, photoperiod and nitrogen on variation in main culm leaf dimensions in field-grown wheat." *Canadian Journal of Plant Science* 78: 35-49.

Jacquemoud S, Baret F. 1990. "PROSPECT: A model of leaf optical properties spectra." *Remote Sensing of Environment* 34: 75-91.

Jaffuel S, Dauzat J. 2005. "Synchronism of Leaf and Tiller Emergence Relative to Position and to Main Stem Development Stage in a Rice Cultivar." *Annals of Botany* 95: 401-412.

Jamieson PD, Brooking IR, Porter CH, Wilson DA. 1995. "Prediction of leaf appearance in wheat: a question of temperature." *Field Crops Research* 41: 35-44.

Jamieson PD, Semenov MA, Brooking IR, Francis GS. 1998. "Sirius: a mechanistic model of wheat reponse to environmental variation." *European Journal of Agronomy* 8: 161-179.

Kaitaniemi P, Hanan JS, Room PM. 1999. "Architecture and morphogenesis of grain sorghum, *Sorghum bicolor* (L.) Moench." *Field Crops Research* 61: 51-60.

Kasperbauer MJ, Karlen DL. 1986. "Light-mediated bioregulation of tillering and photosynthate partitioning in wheat." *Physiologia Plantarum* 66: 159-163.

Kirby EJM, Faris DG. 1972. "The effect of plant density on tiller growth and morphology in barley." *Journal of Agricultural Science* 78: 281-288.

Kirby EJM, Riggs TJ. 1978. "Developmental consequences of two-row and six-row ear type in spring barley. 2. Shoot apex, leaf and tiller development." *Journal of Agricultural Science* 91: 207-216.

Kirby EJM, Appleyard M. 1981. *Cereal Development Guide*. Cereal Unit, National Agricultural Centre, Stoneleigh, Warwickshire, UK,pp.

Kirby EJM, Appleyard M, Fellowes G. 1985. "Leaf emergence and tillering in barley and wheat." *Agronomie* 5: 193-200.

Kirby EJM. 1990. "Co-ordination of leaf emergence and leaf and spikelet primordium initiation in wheat." *Field Crops Research* 25: 253-264.

Klepper B, Rickman RW, Peterson CM. 1982. "Quantitative characterization of vegetative development in small cereal grains." *Agronomy Journal* 74: 789-792.

Klepper B, Belford RK, Rickman RW. 1984. "Root and shoot development in winter wheat." *Agronomy Journal* 76: 117-122.

Lacointe A. 2000. "Carbon allocation among tree organs: a review of basic processes and representation in functional-structural tree models." *Annals of Forest Science* 57: 521-533.

Lafarge TA, Broad IJ, Hammer GL. 2002. "Tillering in grain Sorghum over a wide range of population densities. Identification of a common hierarchy for tiller emergence, leaf area development and fertility." *Annals of Botany* 90: 87-98.

Lafarge TA, Hammer GL. 2002. "Tillering in grain Sorghum over a wide range of population densities. Modelling dynamics of tiller fertility." *Annals of Botany* 90: 99-110.

Lewis P, Saich P, Disney M, Andrieu B, Fournier C, Macklin T, Bodley J. 2004. "Calibration of an L-system model of winter Wheat for remote sensing modelling and inversion." In Godin C, Hanan JS, Kurth W, Lacointe A, Takenaka A, Prusinkiewicz P, DeJong T, Beveridge C and Andrieu B, eds. *4th*

International Workshop on Functional-Structural Plant Models. Montpellier, France: UMR AMAP, 257-261.

Lindenmayer A. 1968. "Mathematical models for cellular interaction in development, part I and II." *Journal of Theoretical Biology* 18: 280-315.

Ljutovac S. 2002. *Coordination dans l'extension des organes aériens et conséquences pour les relations entre les dimensions finales des organes chez le blé.* PhD thesis, Institut National Agronomique Paris-Grignon. 128 pp.

Longnecker N, Kirby EJM, Robson A. 1993. "Leaf emergence, tiller growth, and apical development of nitrogen-deficient spring wheat." *Crop Science* 33: 154-160.

Longnecker N, Robson A. 1994. "Leaf emergence of spring wheat receiving varying nitrogen supply at different stages of development." *Annals of Botany* 74: 1-7.

Maddonni GA, Otegui ME, Andrieu B, Chelle M, Casal JJ. 2002. "Maize leaves turn away from neighbors." *Plant Physiology* 130: 1181-1189.

Matthew C, Yang JZ, Potter JF. 1998. "Determination of tiller and root appearance in perennial ryegrass (Lolium perenne) swards by observation of the tiller axis, and potential application in mechanistic modelling." *New Zealand Journal Of Agricultural Research* 41: 1-10.

Měch R, Prusinkiewicz P. 1996. "Visual models of plants interacting with their environments. *SIGGRAPH '96*. New York: ACM SIGGRAPH, 397-410.

Měch R. 1997. *Modeling and simulation of the interaction of plants with the environment using L-systems and their extensions.* PhD thesis, University of Calgary. pp.

Měch R. 2004. *CPFG Version 4.0 User's Manual.*129 pp.

Minchin PEH, Lacointe A. 2005. "New understanding on phloem physiology and possible consequences for modelling long-distance carbon transport." *New Phytologist* 166: 771-779.

Moore KJ, Moser LE. 1995. "Quantifying developmental morphology of perennial grasses." *Crop Science* 35: 37-43.

Morgan DC, O'Brien T, Smith H. 1980. "Rapid photomodulation of stem extension in light-grown *Sinapis alba* L." *Planta* 150: 95-101.

Motulsky HJ, Christopoulos A. 2003. *Fitting models to biological data using linear and nonlinear regression. A practical guide to curve fitting.* GraphPad Software Inc., San Diego CA.351 pp.

Oguchi R, Hikosaka K, Hirose T. 2003. "Does the photosynthetic light-acclimation need change in leaf anatomy?" *Plant, Cell and Environment* 26: 505-512.

Pagès L, Vercambre G, Drouet J-L, Lecompte F, Collet C, Le Bot J. 2004. "Root Typ: a generic model to depict and analyse the root system architecture." *Plant and Soil* 258: 103-119.

Pararajasingham S, Hunt LA. 1995. "Effects of photoperiod on leaf appearance rate and leaf dimensions in winter and spring wheats." *Canadian Journal of Plant Science* 76: 43-50.

Pons TL, Jordi W, Kuiper D. 2001. "Acclimation of plants to light gradients in leaf canopies: evidence for a possible role for cytokinins transported in the transpiration stream." *Journal of Experimental Botany* 52: 1563-1574.

Prévot L, Aries F, Monestiez P. 1991. "Modélisation de la structure géométrique du mais." *Agronomie* 11: 491-503.

Prusinkiewicz P, Hanan JS. 1990. "Visualization of botanical structures and processes using parametric L-systems." In: Thalmann D, ed. *Scientific Visualization and Graphics Simulation*: J. Wiley & Sons. 183-201.

Prusinkiewicz P, Lindenmayer A. 1990. *The Algorithmic Beauty of Plants*. Springer-Verlag, New York.228 pp.

Prusinkiewicz P, Hammel M, Hanan JS, Měch R. 1997. "Visual models of plant development." In: Rozenberg G and Salomaa A, eds. *Handbook of Formal Languages*. Berlin: Springer. 535-597.

Prusinkiewicz P. 1999. "A look at the visual modelling of plants using L-systems." *Agronomie* 19: 211-224.

Prusinkiewicz P, Karwowski R, Měch R, Hanan JS. 2000. "L-studio/CPFG: a software system for modeling plants." In: Nagl M, Schürr A and Münch M, eds. *Applications of Graph Transformations with Industrial Relevance. Lecture notes in Computer Science 1779.* Berlin, Germany: Springer. 457-464.

R Development Core Team. 2003. "R: a language and environment for statistical computing." Vienna, Austria: R Foundation for statistical computing.

Rajapakse NC, Kelly JW. 1992. "Regulation of Chrysanthemum growth by spectral filters." *Journal of the American Society for Horticultural Science* 117: 481-485.

Rajcan I, AghaAlikhani M, Swanton CJ, Tollenaar M. 2002. "Development of redroot pigweed is influenced by light spectral quality and quantity." *Crop Science* 42: 1930-1936.

Rawson HM, Hofstra G. 1969. "Translocation and remobilization of 14C assimilated at different stages by each leaf of the wheat plant." *Australian Journal of Biological Science* 22: 321-331.

Rawson HM, Zajac M. 1993. "Effects of higher temperatures, photoperiod and seed vernalisation on development in two spring wheats." *Australian Journal of Plant Physiology* 20: 211-222.

Room PM, Hanan JS, Prusinkiewicz P. 1996. "Virtual plants: new perspectives for ecologists, pathologists and agricultural scientists." *Trends in Plant Science* 1: 33-38.

Sanderson JB, Daynard TB, Tollenaar M. 1981. "A mathematical model of the shape of corn leaves." *Canadian Journal of Plant Science* 61: 1009-1011.

Scanlon M, Freeling M. 1997. "Clonal sectors reveal that a specific meristematic domain is not utilized in the maize mutant *narrow sheath*." *Developmental Biology* 182: 52-66.

Shibusawa S. 1992. "Hierachical modelling of a branching growth root system based on L-system." *Acta Horticulturae* 319: 649-664.

Sievänen R, Nikinmaa E, Nygren P, Ozier-Lafontaine H, Perttunen J, Hakula H. 2000. "Components of functional-structural tree models." *Annals of Forest Science* 57: 399-412.

Silsbury JH. 1971. "The effects of temperature and light energy on dry weight and leaf area changes in seedling plants of *Lolium perenne* L." *Australian Journal of Agricultural Research* 22: 177-187.

Simon J-C, Lemaire G. 1987. "Tillering and leaf area index in grasses in the vegetative phase." *Grass and Forage Science* 42: 373-380.

Skinner RH, Simmons SR. 1993. "Modulation of leaf elongation, tiller appearance and tiller senescence in spring barley by far-red light." *Plant, Cell and Environment* 16: 555-562.

Skirvin DJ. 2004. "Virtual plants of predatory mite movement in complex plant canopies." *Ecological Modelling* 171: 301-313.

Smith H. 1982. "Light quality, photoperception and plant strategy." *Annual Review of Plant Physiology* 33: 481-518.

Smith H, Whitelam GC. 1997. "The shade avoidance syndrome: multiple responses mediated by multiple phytochromes." *Plant, Cell and Environment* 20: 840-844.

Smith H. 2000. "Phytochromes and light signal perception by plants - an emerging synthesis." *Nature* 407: 585-591.

Sterck FJ, Schieving F, Lemmens A, Pons TL. 2005. "Performance of trees in forest canopies: explorations with a bottom-up functional-structural plant growth model." *New Phytologist* 166: 827-843.

Streit C. 1992. *Graphtal user manual*. University of Bern: SIG computer graphics, Bern, Switzerland,pp.

Tivet F, da Silveiro Pinheiro B, de Raissac M, Dingkuhn M. 2001. "Leaf blade dimensions of rice (*Oryza sativa* L. and *Oryza glaberrima* Steud.). Relationships between tillers and the main stem." *Annals of Botany* 88: 507-511.

Tomlinson KW, O'Connor TG. 2004. "Control of tiller recruitment in bunchgrasses: uniting physiology and ecology." *Functional Ecology* 18: 489-496.

van Ittersum MK, Leffelaar PA, van Keulen H, Kropff MJ, Bastiaans L, Goudriaan J. 2003. "On approaches and applications of the Wageningen crop models." *European Journal of Agronomy* 18: 201-234.

van Loo EN. 1993. *On the relation between tillering, leaf area dynamics and growth of perennial ryegrass (Lolium perenne L.)* PhD thesis, Wageningen UR, the Netherlands. 169 pp.

van Oosterom EJ, Carberry PS, O'Leary GJ. 2001. "Simulating growth, development, and yield of tillering pearl millet. II. Simulation of canopy development." *Field Crops Research* 72: 67-91.

Volk T, Bugbee B. 1991. "Modeling light and temperature effects on leaf emergence in wheat and barley." *Crop Science* 31: 1218-1224.

Vos J. 1995. "The effects of nitrogen supply and stem density on leaf attributes and stem branching in potato (*Solanum tuberosum* L.)." *Potato Research* 38: 271-279.

Vos J, van der Putten PEL. 1998. "Effect of nitrogen supply on leaf growth, leaf nitrogen economy and photosynthetic capacity in potato." *Field Crops Research* 59: 63-72.

Wan C, Sosebee RE. 1998. "Tillering responses to red:far-red light ratio during different phenological stages in Eragrostis curvula." *Environmental and Experimental Botany* 40: 247-254.

Watanabe T, Hanan JS, Room PM, Hasegawa T, Nakagawa H, Takahashi W. 2005. "Rice morphogenesis and plant architecture: measurement, specification and the reconstruction of structural development by 3D architectural modelling." *Annals of Botany* 95: 1131-1143.

Wherley BG, Gardner DS, Metzger JD. 2005. "Tall fescue photomorphogenesis as influenced by changes in the spectral composition and light intensity." *Crop Science* 45: 562-568.

Williams RF, Langer RHM. 1975. "Growth and development of the wheat tiller bud. II. The dynamics of tiller growth." *Australian Journal of Botany* 23: 745-759.

Williams RF, Metcalf RA. 1975. "Physical constraints and tiller growth in wheat." *Australian Journal of Botany* 23: 213-223.

Yan H-P, Kang MZ, de Reffye P, Dingkuhn M. 2004. "A dynamic, architectural plant model simulating resource-dependent growth." *Annals of Botany* 93: 591-602.

Yin X, Goudriaan J, Lantinga EA, Vos J, Spiertz HJ. 2003. "A flexible sigmoid function of determinate growth." *Annals of Botany* 91: 361-371.

Summary

This thesis presents a 3D virtual plant modelling study of tillering in spring wheat. A virtual plant is a three-dimensional representation of the development of a plant or crop, i.e. the geometrical and topological properties of the plant are taken into account. The advantage of this approach is that the level of detail is much higher than in traditional crop growth models. Therefore, in cases in which the research question benefits from analysis at the level of the individual organ, the virtual plant approach has an advantage over less detailed modelling methods. The subject of research chosen to be analysed using this modelling approach is the phenomenon of tillering (analogous to branching in dicotyledons) in spring wheat, and its determinants. Next to nitrogen availability, which was not taken into account in this thesis, light properties greatly influence the pattern of tillering in wheat and other Gramineae. Two properties of light are especially important: (a) the intensity of Photosynthetically Active Radiation (PAR), and (b) the ratio between the respective intensities of red and far-red light (red/far-red ratio, R:FR).

a) It had been hypothesised before, that for tiller bud outgrowth, the PAR intensity at the parent leaf of the bud (which is the leaf on the same phytomer as the bud) is an important determinant of bud outgrowth, through its effect on the assimilate production of the parent leaf.

b) It had been shown that a reduction in R:FR resulting from the differential scattering properties of plant tissues for red and far-red light, severely reduces tillering in Gramineae. Changes in R:FR are perceived by vertically oriented organs such as sheaths and elongating leaves; in general the base of the plant is a site of R:FR perception, especially at early stages of development.

The local nature of the responses to the two determinants of tillering (at the parent leaf and at the base of the plant, respectively) made this problem an ideal candidate to be analysed using a virtual plant modelling approach.

Model construction and parameterisation (chapter 2)
The first objective was to design an architectural model of spring wheat, which would be able to produce a 3D description of a wheat canopy, for the cultivar and growing conditions as prevalent in spring wheat cropping seasons in the Netherlands. In the initial model, the occurrence of tillers was not dependent on light conditions, as this was a feature to be implemented after the correct functioning and performance of the wheat model had been evaluated. The model

was based on an existing architectural model of wheat, called ADELwheat. This model, based on the L-system formalism, contained explicit descriptions of rates of extension of organs and final organ dimensions, leaf geometrical properties (base angle, curvature, azimuth), and tillering kinetics. The model was initially parameterised for winter wheat. Reparameterisation therefore provided the opportunity to compare parameters and functions for winter and spring wheat. The reparameterisation was based on an outdoor experiment using spring wheat cultivar Minaret, grown in a regular grid in containers of 70 × 90 cm, at a low plant population density (100 plants m^{-2}) to allow for extensive tillering. The following components of ADELwheat were reparameterised:

- *Leaf appearance*: The thermal time between appearance of two consecutive leaves (the phyllochron), was found to differ between main stem and tillers, and therefore in the model two values were used: one value for main stem leaves, and one for tiller leaves. Later, after re-examination of the dataset, this was changed to one value for main stem leaves one to four, and one value for the remaining main stem leaves and tiller leaves together (appendix B in chapter 3).

- *Tiller appearance*: Tiller appearance was parameterised through the use of a tiller-specific parameter (tiller appearance delay, TAD), which defines the difference between the appearance of leaf one of a tiller and leaf one of the preceding tiller on the same shoot (or the parent shoot in case of tiller one).

- *Relative phytomer number* (RPN): In the original winter wheat parameterisation, several properties of tillers could be directly derived from those of the main stem (leaf blade and sheath dimensions, internode length, final leaf number; see below for their specific parameterisation) using the RPN concept. The RPN of a phytomer is the sum of the rank number of the phytomer on the shoot it is part of and a shift value. The latter is specific for a particular tiller type. Phytomers with similar RPN share similar properties, equal to those of the main stem with similar rank number as the value of RPN. The RPN concept appeared applicable for our spring wheat cultivar as well, the shift values differing only slightly between the spring and winter varieties.

- *Leaf dimensions*: Final length and width of the leaf blade, and final length of the leaf sheath were parameterised by coefficient fitting appropriate functions. For blade length, the Lorentz Peak Distribution function was used; for blade width, a linear relation on sheath length data appeared appropriate. For sheath length, a logistic function was used. The functions were all slightly different from the ones used for winter wheat, and were discussed to be applicable for Gramineae in general.

- *Internode length*: A linear relation between relative phytomer number and internode length proved appropriate; the values of the parameters differed between spring and winter varieties, which was due to higher total number of phytomers in the winter variety.

- *Final leaf number*: For the main stem, the final number of leaves produced was fixed at nine; final numbers of leaves of tillers were calculated by subtracting respective phytomer shift value of the tillers from nine.

- *Leaf geometry*: To parameterise the geometrical properties of leaf blades, a magnetic digitisation method was used. This method records the co-ordinates (x, y, z) of a point in space relative to a reference point. For each leaf blade, several points along the midrib were digitised. From this data, the base angle and the curvature of the leaf blades were derived, as well as the azimuth of the leaves (the angle between consecutive leaves, when viewed from the top). These were all stochastic components in the model: during a simulation, for each individual leaf the coefficients defining its base angle, curvature and azimuth were drawn from distributions derived from the digitisation data. This stochasticity reflected the variation as experimentally observed.

Model evaluation (chapter 3)

To evaluate the parameterisation and the performance of ADELwheat, a second outdoor experiment was performed, in which the plants were grown in both contrasting and similar conditions compared to the parameterisation experiment. Three plant population densities were used (100, 262 and 508 plants m^{-2}), and the plants were subjected to two light regimes (0% and 75% shading). To obtain additional data, an indoor (growth chamber) experiment was conducted with plants grown at 100 plants m^{-2}.

Various components of the model parameterisation were evaluated. Generally, phyllochron, tiller appearance delay, and the final number of produced leaves were not significantly affected by population density in the full light treatments. Shade generally reduced phyllochron and final number of leaves. The distribution of final blade length and width, sheath length, and internode length was comparable to the parameterisation, but the coefficient values of the used parameterisation functions depended on the light regimes and the plant population density. The phytomer shift values were similar to those obtained from the parameterisation experiment.

The performance of ADELwheat was evaluated using the time courses of both ground cover and gLAI (gross leaf area index) as test variables. Both are global characteristics of the change over time of leaf production and their values

integrate effects of several important model parameters and functions such as phyllochron and blade dimensions. ADELwheat appeared capable of simulating development of wheat in growth conditions for which the model was not calibrated; however refitting some key coefficients accounting for the effects of population density and shading yielded still better results. A sensitivity analysis of changes in blade length, width, phyllochron and tiller appearance delay showed that phyllochron needs to be parameterised accurately as small changes can have significant effects on the model output.

Analysis of tillering behaviour (chapter 4)

The experiment that was used for the model evaluation was also used to analyse the mechanisms that determine the tillering pattern of spring wheat. To this end, data were gathered on the tillering dynamics of the plants grown in the different treatments; simultaneously changes over time were measured in fraction PAR interception and R:FR (both measured at soil surface).

Both population density and shading affected the time course of the number of tillers per plant: a higher population density resulted in fewer tillers per plant than a lower population density, and shading dramatically decreased the number of tillers per plant. The timing of appearance of tillers was hardly affected by population density, but shading delayed tiller appearance. The maximum number of tillers produced per plant differed between treatments, as was the stage of development at which this maximum number was reached (i.e. cessation of tiller appearance). However, it appeared that the fraction of PAR intercepted by the canopy at the moment of cessation of tiller appearance was identical in five out of six treatments, independent of the rank number of the tiller, the population density or the shading treatment. Also R:FR at soil level at the moment of tillering cessation was independent of the rank number of the tiller and the population density, but differed between light regimes. The probability of a bud to grow out was shown to be related to the LMA (leaf mass per unit leaf area, in mg cm^{-2}) of its parent leaf: a low LMA was related to bud dormancy, and a high LMA to bud outgrowth.

From the data, it was concluded that cessation of tiller appearance was primarily regulated by the fraction of PAR intercepted, and/or R:FR (taking into account that these two are highly correlated), rather than the absolute amount of intercepted light; only the appearance of the first primary tiller (the coleoptile tiller) seemed related to absolute PAR. A threshold value of fraction PAR intercepted (0.40) or R:FR (0.32 in full light situations and 0.51 in shade) was considered to be the determinant of tiller bud outgrowth. It was hypothesised

that the relation between bud dormancy and LMA was caused by the photomorphogenetic effects R:FR has on both bud outgrowth and LMA of the parent leaves.

Simulation of tillering pattern under the influence of light properties (chapter 5)
The light conditions for suppression of tiller bud outgrowth, described above, were adopted for use in the virtual plant model. ADELwheat was interfaced with a light model (Nested Radiosity), using the L-systems communication module ?E. The Nested Radiosity model is capable of calculating PAR interception and R:FR perception at the level of the individual organ, and was therefore highly suitable for our purpose. ADELwheat was modified to make tiller bud outgrowth dependent on the fraction of PAR intercepted by the buds parent leaf blade, and on the R:FR perceived by either the tube of sheaths (the pseudostem) or the buds parent leaf blade; sheaths are known to act as an R:FR sensor, fully grown leaf blades are not. Simulations were done using a threshold of fraction PAR intercepted for tillering cessation of 0.2, 0.4, 0.6 and 0.8, or using a R:FR threshold of 0.32 with either the sheaths or the parent leaf blades as the sites of R:FR perception.

Plant population density affected the degree of tillering in accordance with expectations: a higher population density resulted in fewer tillers produced per plant. A higher threshold value for PAR interception resulted in reduced tillering and a lower production of leaf area. When comparing to experimental data, the fraction of PAR intercepted at the parent leaf blade appeared to be a good indicator for outgrowth of tillers of a low rank, but outgrowth of tillers of a high rank was overestimated. Perception of R:FR by the tube resulted in an overestimation of tiller production. These overestimations suggested that photomorphogenetic effects alone may not be sufficient to predict tiller production; introduction of photosynthesis and carbon distribution through the plant may enhance model performance in terms of tiller production. Nevertheless, the study showed that the L-system approach is a powerful tool to analyse crop morphological/ecological research questions in which the determinants act on the level of the individual plant organ.

Overall, this thesis has shown that (a) most of the spring wheat parameterisation functions in ADELwheat can be regarded as generic for Gramineae, (b) the model is capable of simulating leaf area for situations it was not calibrated for, (c) in our experiment, cessation of tiller appearance occurred at fixed light conditions within

the canopy, and (d) hypotheses on local stimuli affecting global characteristics of crop development can be modelled using a 3D virtual plant modelling approach.

Samenvatting

Dit proefschrift presenteert een methode voor het modelleren van uitstoeling in zomertarwe, gebruikmakend van 'virtuele planten'. Een virtuele plant is een driedimensionale beschrijving van (de ontwikkeling van) een plant of een gewas, waarbij de geometrische en topologische eigenschappen van de plant in beschouwing worden genomen. Het voordeel van deze benadering is dat de mate van detail veel hoger is dan in traditionele gewasgroeimodellen. Voor analyses waarbij het functioneren van organen wordt bestudeerd in relatie tot het functioneren van het gewas als totaal bieden virtuele planten meer mogelijkheden dan minder gedetailleerde modelleermethoden. Het onderwerp van onderzoek dat is gekozen om bestudeerd te worden met deze modelleermethode is het fenomeen 'uitstoeling' in zomertarwe (analoog aan vertakking in dicotylen) en de determinanten hiervan. Naast de beschikbaarheid van stikstof, die buiten beschouwing is gelaten in dit proefschrift, hebben lichteigenschappen een grote invloed op het patroon van uitstoeling (uitlopen van okselknoppen) in tarwe en andere Gramineae. Twee lichteigenschappen zijn vooral belangrijk: (a) de intensiteit van fotosynthetisch actieve straling (afgekort tot PAR voor 'photosynthetically active radiation',) en (b) de verhouding tussen de intensiteiten van rood en ver-rood licht (afgekort tot R:FR voor 'red/far-red ratio').

a) In het verleden is de hypothese opgesteld dat de intensiteit van PAR op het blad van hetzelfde fytomeer als de okselknop (het 'moederblad') een belangrijke determinant is van de uitloop van een okselknop via de licht-gerelateerde productie van assimilaten van het moederblad.

b) Het is aangetoond dat een reductie van R:FR, als resultaat van de verschillende verstrooiingseigenschappen van plantweefsels voor rood en voor ver-rood licht, uitstoeling in Gramineae in hoge mate reduceert. Veranderingen in R:FR worden waargenomen door verticaal georiënteerde organen zoals bladscheden (de 'schijnstengel') en groeiende bladeren; in het algemeen is de basis van de plant de plaats van waarneming van R:FR, vooral tijdens de vroege ontwikkelingsstadia.

Het lokale karakter van de respons op de twee determinanten van uitstoeling (respectievelijk op het moederblad, en aan de basis van de plant) maken dit probleem een ideale kandidaat om geanalyseerd te worden met behulp van de virtuele plant modelleermethode.

Modelconstructie en parameterisatie (hoofdstuk 2)

De eerste doelstelling was het ontwerpen van een architectuurmodel van zomertarwe dat een 3D beschrijving zou moeten geven van een tarwebladerdek voor het gekozen ras en groeicondities zoals gangbaar in groeiseizoenen in Nederland. In het initiële model was de mate van uitlopen van zijassen niet afhankelijk van lichtcondities, daar dit een modelfunctie was die pas werd geïmplementeerd nadat zou zijn nagegaan of het functioneren en de prestaties van het tarwemodel kloppen met de werkelijkheid. Het model was gebaseerd op een bestaand architectuurmodel van tarwe, ADELwheat. Dit model, gebaseerd op L-systemen, bevatte de expliciete omschrijvingen van de snelheden van orgaangroei, de geometrische eigenschappen van bladeren (bladhoek, kromming, azimut) en de uitstoelingsdynamiek. Het model was in eerste instantie geparameteriseerd voor wintertarwe. Herparameterisatie bood daarom de mogelijkheid om parameterwaarden en functies van winter- en zomertarwe onderling te vergelijken. De herparameterisatie was gebaseerd op een experiment in de open lucht, gebruik makend van het zomertarweras Minaret, gekweekt in een vierkant plantverband in containers van 70 bij 90 cm, bij een lage populatiedichtheid (100 planten m^{-2}) waarbij de plant wordt aangezet tot flinke uitstoeling (productie van veel zijassen). De volgende componenten van ADELwheat zijn geparameteriseerd:

- *Verschijning van bladeren:* De periode tussen het verschijnen van twee opeenvolgende bladeren (het zgn. phyllochron) bleek te verschillen tussen hoofdas en de zijassen. Daarom werden in het model twee waarden voor het phyllochron gebruikt: één waarde voor bladeren aan de hoofdas en één waarde voor bladeren aan de zijassen. Na nadere inspectie van de dataset werd dit later veranderd in één waarde voor bladeren één tot vier van de hoofdas en één waarde voor alle overige bladeren (appendix B in hoofdstuk 3).

- *Verschijning van zijassen:* Het verschijnen van zijassen werd geparameteriseerd gebruik makend van een zijas-specifieke parameter ('tiller appearance delay', TAD, voor zijasverschijningsuitstel), welke het verschil definieert tussen het verschijnen van blad één van een zijas en blad één van de vorige zijas op dezelfde as (of de hoofdas in het geval van zijas nummer één).

- *Relatief fytomeer nummer ('relative phytomer number', RPN):* In de originele parameterisatie voor wintertarwe konden diverse eigenschappen van zijassen direct worden afgeleid van de overeenkomende eigenschappen van het hoofdasfytomeer met het RPN concept (afmetingen van bladschijf en –schede,

internodiumlengte, het maximale aantal bladeren op een zijas; zie hieronder voor hun afzonderlijke parameterisatie). Het RPN van een fytomeer is de som van het rangnummer van het fytomeer op de as waar het deel van uitmaakt, en een 'verschuivingswaarde'. Deze laatste is specifiek voor elk type zijas. Fytomeren met overeenkomende RPN delen overeenkomende eigenschappen, gelijk aan die op de hoofdas met hetzelfde rangnummer als de waarde van het RPN. Het RPN concept bleek ook toepasbaar voor ons zomertarweras, met 'verschuivingswaarden' die slechts marginaal verschilden van het wintertarweras (aanvankelijke parameterisatie).

- *Afmetingen van bladeren:* De uiteindelijke lengte en breedte van de bladschijf en de uiteindelijke lengte van de bladschede werden geparameteriseerd door het fitten van geschikte functies. Voor bladlengte werd de Lorentz Peak Distribution functie gebruikt; voor bladbreedte bleek een lineaire relatie met de lengte van de bladschede geschikt. Voor de lengte van de bladschede werd een logistische functie gebruikt. De functies verschilden allemaal enigszins van degene die werden gebruikt voor wintertarwe en het werd bediscussieerd dat ze geschikt waren voor Gramineae in het algemeen.

- *Lengte van het internodium:* Een lineaire relatie tussen RPN en internodiumlengte bleek geschikt; de waarden verschilden tussen het winter- en het zomertarweras doordat de hoofdas van wintertarwe een groter aantal fytomeren omvat dan de hoofdas van zomertarwe.

- *Maximum aantal bladeren:* Voor de hoofdas werd het maximum aantal bladeren vastgezet op negen; het maximum aantal bladeren op zijassen werd berekend door de fytomeer 'verschuivingswaarden' van de zijassen af te trekken van negen.

- *Bladgeometrie:* Om de geometrische eigenschappen van de bladeren te parameteriseren werd een magnetische digitalisatiemethode gebruikt. Deze methode slaat de coördinaten (x, y, z) van een punt in de ruimte op ten opzichte van een referentiepunt. Voor iedere bladschijf werden meerdere punten langs de middennerf gedigitaliseerd. Uit deze data werd de bladhoek en de kromming van de bladschijven, en het azimut van de bladeren (de hoek tussen opeenvolgende bladeren, van bovenaf bekeken) berekend. Dit werden allemaal stochastische elementen in het model: gedurende een simulatie werd voor elk afzonderlijk blad de coëfficiënten die de bladhoek, kromming en azimut definiëren getrokken uit een distributie die gebaseerd was op de digitalisatiedata. Deze stochasticiteit reflecteerde de variatie zoals die experimenteel was waargenomen.

Modelevaluatie (hoofdstuk 3)

Om de parameterisatie en de prestaties van ADELwheat te kunnen evalueren werd een tweede experiment in de open lucht uitgevoerd, waarin de planten in vergelijking met het parameterisatie-experiment zowel in overeenkomende als contrasterende omstandigheden werden gekweekt. Drie populatiedichtheden werden gebruikt (100, 262 en 508 planten m^{-2}) en de planten werden onderworpen aan twee lichtregimes (0% en 75% beschaduwing). Daarnaast werd nog een experiment in een fytotroncel uitgevoerd, om extra data te vergaren, met planten opgekweekt bij een populatiedichtheid van 100 planten m^{-2}.

Diverse componenten van de modelparameterisatie werden geëvalueerd. In het algemeen werden phyllochron, TAD, en het maximale aantal bladeren niet significant beïnvloed door populatiedichtheid in de behandeling in vol licht. Schaduw reduceerde in het algemeen phyllochron en het maximale aantal bladeren. De distributie van uiteindelijke lengte en breedte van de bladschijf, lengte van de bladschede en de lengte van het internodium bleken vergelijkbaar met de oorspronkelijke parameterisatie, maar de waarden van de coëfficiënten van de gebruikte functies hingen af van de lichtregimes en de populatiedichtheid. De waarden voor de 'fytomeerverschuiving' kwamen overeen met die welke in het parameterisatie-experiment werden gevonden.

De prestaties van ADELwheat werden geëvalueerd gebruik makend van het tijdsverloop van de bedekkingsgraad van de grond en van de gLAI ('gross leaf area index', de verhouding tussen het totale bruto bladoppervlak en grondoppervlak) als testvariabelen. Beide variabelen weerspiegelen de verandering in de tijd van de productie van bladeren en hun waarden integreren effecten van een aantal belangrijke modelparameters en –functies zoals het phyllochron en afmetingen van de bladschijf. ADELwheat bleek in staat de ontwikkeling van tarwe te simuleren in groeicondities waarvoor het model niet was geparameteriseerd; echter, het opnieuw fitten van enkele sleutelcoëfficiënten, rekening houdend met de effecten van populatiedichtheid en beschaduwing, leverde betere resultaten op. Een analyse van de gevoeligheid voor veranderingen in lengte en breedte van de bladschijf, phyllochron, en verschijning van zijassen liet zien dat het phyllochron nauwkeurig moet worden geparameteriseerd, omdat kleine wijzigingen significante effecten kunnen hebben op de uitkomsten van het model.

Analyse van de uitstoelingsdynamiek (hoofdstuk 4)

Gegevens voorvloeiend uit het experiment dat was gebruikt voor de evaluatie van het model, werden ook ingezet met het doel de mechanismen die het

uitstoelingspatroon van zomertarwe bepalen te analyseren. Hiervoor werden gegevens verzameld over de uitstoelingsdynamiek van de planten, gekweekt in de verschillende omstandigheden; tegelijkertijd werden de veranderingen in fractie onderschepte PAR en in R:FR gemeten (beide op het niveau van het grondoppervlak).

Zowel populatiedichtheid als beschaduwing beïnvloedde het tijdsverloop van het aantal zijassen per plant: een hoge populatiedichtheid resulteerde in minder zijassen per plant dan een lage populatiedichtheid en beschaduwing reduceerde het aantal zijassen per plant drastisch. Het moment van verschijning van zijassen werd nauwelijks beïnvloed door de populatiedichtheid, maar beschaduwing vertraagde het verschijnen van zijassen wel. Het maximum aantal zijassen dat per plant werd geproduceerd verschilde tussen de behandelingen; dit gold ook voor de ontwikkelingsstadia van de hoofdas waarin dit maximum aantal werd bereikt (m.a.w. de beëindiging van het verschijnen van zijassen). Niettemin bleek dat de fractie door het bladerdek onderschepte PAR op het moment van de beëindiging van het verschijnen van zijassen identiek was in vijf van de zes behandelingen, onafhankelijk van het rangnummer van de zijas, de populatiedichtheid, of beschaduwing. Op het moment van de beëindiging van het verschijnen van zijassen was R:FR op het niveau van het grondoppervlak hetzelfde, onafhankelijk van rangnummer van de zijas en van populatiedichtheid, maar de waarde van R:FR op het moment van de beëindiging van het verschijnen van zijassen was hoger in de schaduw dan in vol licht. De kans op uitloop van een okselknop bleek gerelateerd aan de LMA (voor 'leaf mass per unit leaf area', het bladgewicht per eenheid bladoppervlak) van het moederblad van de knop: een lage LMA was gerelateerd aan inactiviteit van de knop en een hoge LMA aan uitloop van de knop.

Op basis van de proefgegevens werd de conclusie getrokken dat de beëindiging van het verschijnen van zijassen eerder werd gereguleerd door de fractie onderschepte straling en/of de R:FR (rekeninghoudend met het feit dat deze twee nauw zijn gecorreleerd) dan door de absolute hoeveelheid onderschept licht; alleen het verschijnen van de eerste zijas van de eerste orde (de coleoptielas) leek verband te houden met de absolute hoeveelheid PAR. Een grenswaarde van de fractie onderschepte PAR (0.40) of R:FR (0.32 in vol licht en 0.51 in schaduw) werd beschouwd als grenswaarde voor de uitloop van okselknoppen tot zijassen. De hypothese werd opgesteld dat de relatie tussen inactiviteit van een tillerknop en LMA veroorzaakt werd door de fotomorfogenetische effecten die R:FR had op zowel uitloop van knoppen als op de LMA van moederbladeren.

De simulatie van het patroon van uitstoeling onder invloed van lichteigenschappen (hoofdstuk 5)

De hypothesen over de lichtcondities benodigd voor het onderdrukken van de uitloop van okselknoppen, zoals hierboven beschreven, werden gebruikt in het virtuele plantmodel. ADELwheat werd gekoppeld aan een lichtmodel ('Nested Radiosity'), gebruik makend van de L-systeem communicatiemodule '?E'. Het Nested Radiosity model kan PAR onderschepping en R:FR waarneming berekenen op het niveau van het individuele orgaan en was daarom zeer geschikt voor ons doel. In ADELwheat werd de afhankelijkheid van knopuitloop voor de fractie onderschepte PAR door de bladschijf van het moederblad ingebouwd, alsmede voor R:FR waarneming door de 'bundel van bladscheden' of door de bladschijf van het moederblad. Het is bekend dat de 'bundel van bladscheden' een plaats van perceptie van R:FR is; volgroeide bladschijven kunnen dat niet. Simulaties werden gedaan met een grenswaarde voor onderschepte PAR van 0.2, 0.4, 0.6 en 0.8, of met een R:FR grenswaarde van 0.32 voor van de bladscheden of de bladschijven van de moederbladeren als locaties van waarneming van R:FR.

Populatiedichtheid beïnvloedde de mate van uitstoeling naar verwachting: een hogere populatiedichtheid resulteerde in minder zijassen per plant. Een hogere grenswaarde voor PAR onderschepping resulteerde in een reductie van het aantal zijassen en een lagere productie van bladoppervlak. Wanneer deze effecten werden vergeleken met de experimentele gegevens, dan bleek de fractie van onderschepte PAR door het moederblad een goede indicator voor de uitloop van zijassen met een laag rangnummer, maar de uitloop van zijassen met een hoog rangnummer werd door het model overschat. De aanname dat de schijnstengel de plaats van waarneming van R:FR is resulteerde in een overschatting van het aantal zijassen. Deze overschattingen suggereerden dat fotomorfogenetische effecten alleen waarschijnlijk niet voldoende zijn om productie van zijassen te voorspellen; de introductie van fotosynthese en koolstofdistributie door de plant zou de prestaties van het model kunnen verbeteren in termen van betere simulatie van het aantal zijassen. Niettemin heeft deze studie laten zien dat L-systemen een krachtig gereedschap zijn om gewasmorfologische en –ecologische vraagstukken te analyseren waarbinnen de determinanten opereren op het niveau van het individuele plantenorgaan.

Dit proefschrift heeft laten zien dat (a) de meeste functies voor de morfologische beschrijving van zomertarwe in ADELwheat kunnen worden beschouwd als algemeen voor Gramineae (met soortspecifieke parameterwaarden), (b) het model in staat is om de productie van bladoppervlak te simuleren voor situaties

waarvoor het niet is gecalibreerd, (c) in ons experiment de beëindiging van het verschijnen van zijassen plaats vond bij specifieke lichtcondities binnen het bladerdek en (d) hypothesen aangaande de invloed van lokale stimuli op globale karakteristieken van gewasontwikkeling kunnen worden gesimuleerd met een 3D model.

Acknowledgements

The thesis of which you are now reading the acknowledgements – I am excited to see you actually made it to page 151! – is the result of over four years of reading literature, conducting experiments, modelling, analysing data, and finally writing it all down. If I would have had to do this all by myself, I would probably still be in the reading phase now. Fortunately, there have been many people during those years that have helped me, answered my questions, facilitated the work, and made me feel at home at Haarweg 333.

In the first place, I would like to thank my supervision team: my daily supervisor and co-promotor Jan Vos, my promotor Paul Struik, and my INRA co-promotor Bruno Andrieu. Jan, I could not have wished for anything more in a supervisor. You always made time for me in case I needed any help, were always interested to hear how (whether) I was progressing, but – fortunately – were not looking over my shoulder all the time. I think you found an excellent balance there, making working under your supervision an absolute pleasure. Paul, I am amazed by the speed and accuracy you displayed when commenting on papers and other texts, which was very pleasant when trying to finish a paper in time. I liked to talk to you about the progress within the project; the interest and enthusiasm you displayed and the suggestions you made were always encouraging. Bruno, I very much enjoyed our stimulating discussions on various topics, both face-to-face and through e-mail. Also, I would like to thank you for your valuable input in the manuscripts, and for facilitating my stays in Grignon.

Christian Fournier and Michaël Chelle, you have been invaluable in the completion of the work. Therefore I would like to thank you Christian, for devoting all your time to me when I was in Grignon, discussing and helping me with the model code; and Michaël, for helping me in using and fine-tuning the light model, and for incorporating new features that I needed.

Also I would like to express my gratitude to the other members (next to Jan and Paul) of the Wageningen 'Virtual Plant' group: Leo Marcelis, Gerie van der Heijden, Ep Heuvelink, Fokke Buwalda, Frank Sterck, and especially Pieter de Visser with whom I shared the experience of learning the first lines of L-system code, at the CPAI in Brisbane. Furthermore, the following people have been very helpful in various areas of the project: Peter van der Putten has been indispensable in my experimental work by showing me the tricks of the trade and helping with the measurements; Ans Hofman and Henriëtte Drenth did several measurements and assisted me during the digitisation sessions in a scorching hot glasshouse; many people from PPW (Plantkundig Proefcentrum Wageningen)

Funding

Publication List

Evers JB, Vos J, Andrieu B, Struik, PC. 2006. "Cessation of tillering in spring wheat in relation to light interception and red/far-red ratio." *Annals of Botany* (in press).

Evers JB, Vos J, Fournier C, Andrieu B, Chelle M, Struik PC. 2005. "Towards a generic architectural model of tillering in Gramineae, as exemplified by spring wheat (*Triticum aestivum*)." *New Phytologist* 166: 801-812.

de Visser PHB, Marcelis LFM, van der Heijden GWAM, Angenent GC, Evers JB, Struik PC, Vos J. 2004. "Incorporation of 3D plant structures in genetic and physiological models." *Acta Horticulturae* 654: 171-178.

Evers JB, Vos J, Fournier C, Andrieu B, Chelle M, Struik PC. 2004. "A 3D approach for modelling tillering in wheat (*Triticum aestivum* L.)." In Godin C, Hanan JS, Kurth W, Lacointe A, Takenaka A, Prusinkiewicz P, DeJong T, Beveridge C and Andrieu B, eds. *4th International Workshop on Functional-Structural Plant Models*. Montpellier, France: UMR AMAP, 210-215.

Evers JB, Vos J, Fournier C, Chelle M, Andrieu B. 2003. "Modeling tillering in wheat (*Triticum aestivum*) using L-systems." In Hu BG and Jaeger M, eds. *2003' International Symposium on Plant Growth Modeling, Simulation, Visualization, and their Applications*. Beijing China PR: Tsinghua University Press / Springer, 329-337.

de Visser PHB, Marcelis LFM, van der Heijden GWAM, Evers JB, Vos J, Struik PC. 2002. "Virtual plants in research, education and marketing. *VIAS*. Wageningen, 107-115.

de Visser PHB, Marcelis LFM, van der Heijden GWAM, Vos J, Struik PC, Evers JB. 2002. "3D modelling of plants: a review". Wageningen: Plant Research International. 38p.

Curriculum Vitae

Jochem Bas Evers was born on 10 February 1977 in Schiedam, the Netherlands. He attended the 'Erasmiaans Gymnasium' in Rotterdam, from which he graduated in 1995. In the same year he started to study biology at Utrecht University. For his first thesis, he conducted research together with two fellow students at the Utrecht University branch of the 'Nationaal Herbarium Nederland', within the 'Flora of the Guianas' framework. This resulted in a thesis entitled 'Revision of the genus *Guatteria* of the Guianas'. After finishing this work, he paused his studies for a year, within which he took place on the board of student association B.I.T.O.N. in Utrecht. He resumed his studies at the Netherlands Institute for Ecological research, Centre for Terrestrial Ecology, Department of Plant Population Biology in Heteren, where he wrote a thesis entitled 'The influence of a heterogeneous environment on genetic variation' together with a fellow student. After this he did a literature study at the same group, resulting in a thesis entitled 'Theoretical studies on the maintenance of male-sterility in plant populations: A review on several aspects of the modelling of gynodioecy'. This concluded his biology studies, and he obtained his MSc in 2001. That year he started his PhD research at Wageningen University, Plant Sciences Group, Crop and Weed Ecology in Wageningen, which is described in this PhD thesis. Currently, he is appointed as a PostDoc researcher at the Crop and Weed Ecology group, continuing and extending his PhD work.

PE&RC PhD Education Statement Form

With the educational activities listed below the PhD candidate has complied with the educational requirements set by the C.T. de Wit Graduate School for Production Ecology and Resource Conservation (PE&RC) which comprises of a minimum total of 22 credits (= 32 ECTS = 22 weeks of activities)
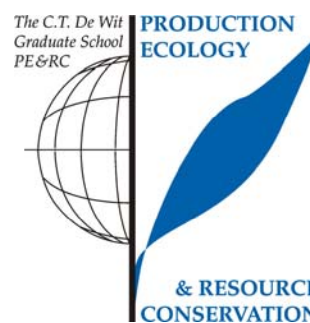
Review of Literature (3 credits)
- 3D modelling of plant development (2002)

Post-Graduate Courses (3 credits)
- Spatial modelling in ecology (2002)
- Basic Statistics (2002)
- Advanced Statistics (2003)

Deficiency, Refresh, Brush-up and General Courses (6 credits)
- Simulation of ecological processes (2002)
- Simulation of crop growth (2002)

PhD Discussion Groups (5 credits)
- Plant and crop ecology (2001-2005)
- Statistics, mathematics and modelling (2001-2003)

PE&RC Annual Meetings, Seminars and Introduction Days (0.75 credits)
- PE&RC weekend (2003)
- PE&RC annual meeting: "Biological disasters" (2004)

International Symposia, Workshops and Conferences (3 credits)
- 2003 International symposium on plant growth, modeling, simulation, and their applications, LIAMA-CIRAD, Beijing, China P.R. (2003)
- International workshop "Virtual plants/crops", IAC/Martin Luther University, Halle, Germany (2004)
- 4th International workshop on functional-structural plant models, INRA/CIRAD, Montpellier, France (2004)

Laboratory Training and Working Visits (3 credits)
- Plant digitizing and L-systems. CPAI, Brisbane, Australia (2001)
- Architectural modelling of wheat. INRA, Grignon, France (2002)